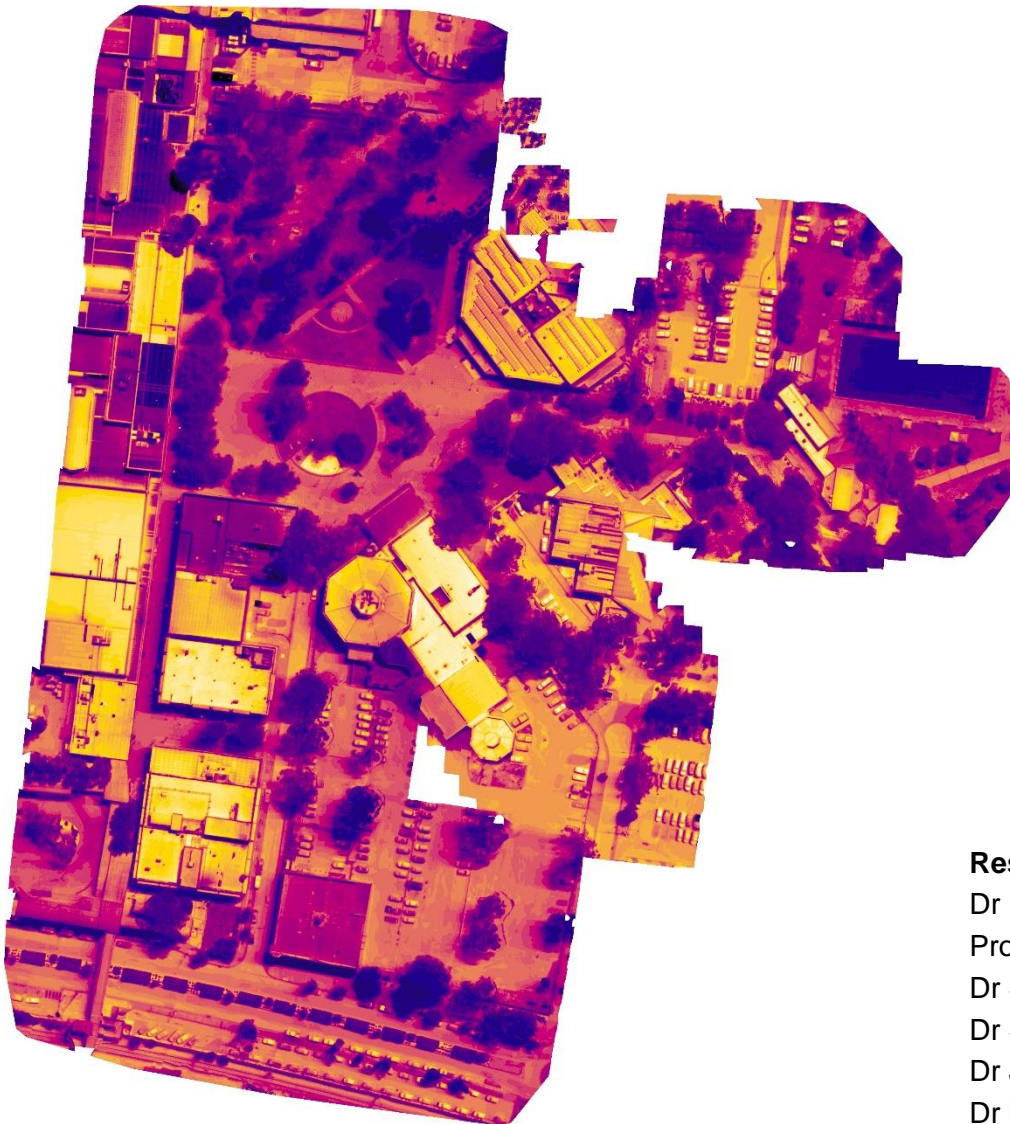




LG NSW Increasing Resilience to Climate Change

Evidence based interventions for urban cooling

Mt Druitt, Blacktown, NSW



Research group

Dr Riccardo Paolini
Prof Mattheos Santamouris
Dr Shamila Haddad
Dr Samira Garshasbi
Dr Jie Feng
Dr Kai Gao

This report is submitted by the University of New South Wales

Research group. High Performance Architecture research cluster. School of Built Environment, UNSW

<https://www.be.unsw.edu.au/research/research-clusters-and-groups/high-performance-architecture-research-cluster>

Dr Riccardo Paolini

Prof Mattheos Santamouris

Dr Shamila Haddad

Dr Samira Garshasbi

Dr Jie Feng

Dr Kai Gao

Thermographer, UAV pilot, and aerial images postprocessing

Bill Apostolidis, National Drones.

Project contacts: Riccardo Paolini – r.paolini@unsw.edu.au

The legal entity for the contract is the University of New South Wales

ABN: 57 195 873 179

UNSW is a GST-registered organisation. CRICOS Provider Code 00098G

Image on the cover page: infrared aerial orthophoto of Mt Druitt.

Contents

Executive Summary	5
1. Introduction and Project Objectives	7
2. Case Study Area: Mt Druitt	8
3. Methods	9
3.1 Preliminary fieldwork.....	9
3.2 Weather stations and temperature sensors for long-term monitoring	9
3.2.1 Existing networks of sensors	9
3.2.2 Temperature and humidity sensors in Mount Druitt.....	10
3.2.3 Weather station in Mount Druitt	14
3.2.4 Weather data treatment	15
3.3 Fieldwork campaign	16
3.3.1 Terrestrial and aerial campaign	16
3.3.2 Albedo measurements.....	18
3.4 Microclimate simulations.....	19
3.4.1 Microclimate model.....	19
3.5 Assessment of impacts.....	20
3.5.1 Weather data inputs for the assessment of impacts.....	20
3.5.2 Building Performance Simulations.....	21
3.5.3 Electricity demand calculation	21
3.5.4 Mortality Risk	23
4. Design Scenarios.....	25
5. Results and Discussion.....	27
5.1 Temperature and humidity records.....	27
5.2 Fieldwork.....	30
5.2.1 Terrestrial and aerial survey	30
5.2.2 Albedo measurements.....	32
5.3 Microclimate simulation model validation	33
5.4 Results of the mitigation scenarios	35
5.5 Results of Building Performance Simulations.....	40
5.6 Influence of microclimate on electricity demand.....	41
5.7 Influence of microclimate on the risk of heat-related mortality	43
6. Conclusions and Recommendations	46
Annex A – Building parameters for energy simulations	48
Annex B – Maps output of microclimate simulations	50

Air temperature distribution.....	50
Surface temperature distribution.....	55
Wind speed distribution.....	60
References	65

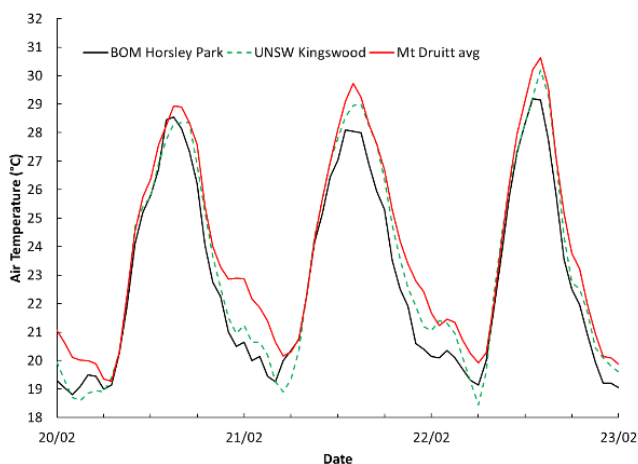
Executive Summary

The context. The combination of global climate change and urban overheating are leading to an increase in peak summer temperatures and intensity of heatwaves, especially in Western Sydney. Urban overheating has consequences for human thermal comfort, health, building cooling energy needs, and even the ability to live outdoors in the public space during significant fractions of summertime, especially for the vulnerable population.

Here, we studied heat-mitigation and its benefits on ambient temperature, building energy needs, electricity demand and risk of heat-related mortality in Mount Druiitt, which is a socio-economically disadvantaged area. We focused on increasing the resilience to climate change of Dawson Mall. This is a popular open-air shopping mall where Blacktown City Council may soon consider designs for urban revitalisation.



Unmitigated climate in Mt Druiitt. With a network of six temperature and humidity sensors, we monitored the local conditions for more than one year and observed that in Mt Druiitt in peak conditions is 1.2-1.7 °C hotter than the values recorded at the Bureau of Meteorology's station in Horsley Park, which is approximately 10 km south of Mt Druiitt, in a non-urban area at the same distance from the coast. Especially, the air temperature in Mt Druiitt is even 2.5 °C hotter than in Horsley Park in the evening and night. Then, we performed detailed measurements on a clear sky hot day at 23 locations in Mt Druiitt, with mobile weather stations and a drone equipped with a thermal camera. Thus, we used the collected data to validate a microclimate simulation model.

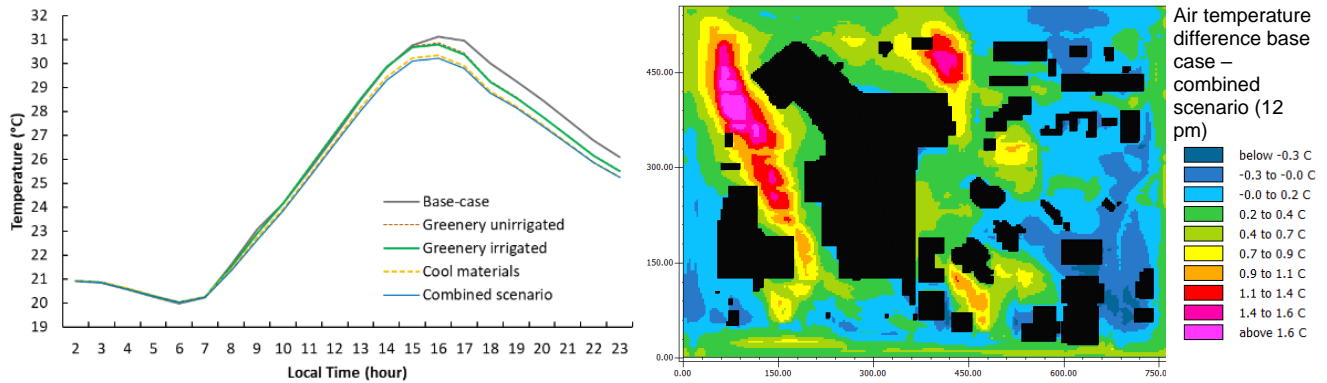


Mitigation scenarios and air temperature reductions. Upon consultation with Blacktown City Council, with the measured data, we calibrated a microclimate model to assess five design scenarios:

- Base case – unmitigated
- Unirrigated greenery – 10 unirrigated trees on Dawson Mall and 337 additional trees in other locations
- Irrigated greenery – 10 passively irrigated trees on Dawson Mall and 337 additional trees in other locations
- Cool materials – Albedo of roofs increased to 0.75 and albedo of car parks and pedestrian areas increased to 0.40
- Combined – Combination of all the above mitigation strategies plus shading of car parks.

The maximum reductions are achieved in the combined scenario and equal a peak air temperature reduction of 1.24 °C, followed by the cool materials scenario with a peak reduction of 1.17 °C, and then irrigated and unirrigated greenery scenarios with reductions of 0.76 °C and 0.71 °C. These temperature reductions are in line with results previously achieved with heat mitigation on a small area, while peak air temperature reductions of 2.2-2.9 °C are

possible only with a Sydney-wide application of heat mitigation, including the irrigation of greenery, which can be allowed by the synergy of green and blue infrastructure.



Trees or other urban shading improve human thermal comfort by reducing the solar radiation directly reaching people and street pavements, and thus reducing their surface temperature. Along Dawson Mall trees can reduce the pavement temperature by more than 15 °C.

Benefits of heat mitigation on energy and health. The cooling energy needs for all simulated buildings is 20-40% higher in Mt Druitt (urban area) than at Horsley Park (non-urban), depending on insulation level and internal heat loads, showing an energy penalty for all urban buildings in Mt Druitt. A reflective roof (albedo = 0.75) instead of a conventional roof (albedo = 0.15) can deliver cooling energy savings in all situations, with the greatest advantage for poorly insulated low-rise buildings (e.g., existing office buildings). Here, we computed cooling energy savings up to 18% for an uninsulated low-rise office building. High levels of roof insulation (as per current building code levels) are not beneficial in buildings with high internal heat gains, such as a shopping mall, because they reduce heat dissipation and increase cooling energy needs. Cooling energy savings in the range between 10% and 24% can be achieved with the combination of cool roofing and urban heat mitigation. The electricity demand over the hot period (November-March) for all uses can be reduced by 1.5% with urban heat mitigation. It is to be noted that the modelled electricity demand includes transport and all other uses. Finally, heat mitigation can reduce the risk of heat-related mortality, which remains high in Western Sydney, and significantly higher than on the coast.

Recommendations. The project findings lead to the following recommendations:

- Heat mitigation should be implemented in the most comprehensive way, with a combination of heat mitigation technologies, as in the combined scenario.
- Heat mitigation of a single hot spot is helpful to improve the local thermal comfort, but in the case of Dawson Mall an advective inflow of hot air due to the north-south axis of the pedestrian mall reduces the air temperature reductions.
- Heat mitigation should be implemented at the regional scale, i.e., Sydney-wide, to achieve reductions in the ambient temperature exceeding 2 °C, thus contrasting the effects of urbanization. A single council cannot alone achieve this level of urban heat mitigation.
- In addition to urban heat mitigation, an improvement of the building performance is also necessary to reduce the cooling energy demand of buildings in the context of global and regional warming.
- Hyper insulation is not the most appropriate strategy, and performance solutions – in compliance with the National Construction Code – should be pursued to reduce the cooling energy needs of buildings in Mt Druitt.
- Reflective roofing is an effective intervention that can deliver benefits at building and urban scale, acting in synergy with other heat-mitigation strategies.
- Reflective roofs and cool pavements are the single most effective strategy for reducing air temperature, and can work in positive synergy with greenery, which provides the greatest improvements on-site improvements in local thermal comfort.

Further research and monitoring should consider:

- Monitoring the effectiveness and performance of interventions in Mt Druitt, also exploiting the network of sensors established in this project.
- The development of synergies between heat-mitigation strategies.

1. Introduction and Project Objectives

Climate change and rapid urbanization are causing air temperature increases across Greater Sydney. Blacktown City is expected to experience an additional 5-10 hot days (>35 °C) by 2030 and a further 10-20 hot days by 2070. Council's climate change risk assessment and adaptation plan identifies extreme temperatures and heatwaves resulting in premature deaths as a high priority and likely risk with a catastrophic consequence.

This report documents a project carried out by Blacktown City Council in collaboration with the University of New South Wales to identify the most effective cooling strategies to build adaptive capacity to reduce vulnerability to increasing temperatures and heat waves of longer duration.

The project focused on microclimate elements of Dawson Mall in Mount Druitt, a popular open-air shopping mall. The project findings provide an evidence base for upgrading the mall to be a demonstration site of interventions that improve thermal comfort. Dawson Mall is located near the Mount Druitt Railway Station and the heart of the central business district for the local area. The 11 suburbs within the Mount Druitt precinct are the most disadvantaged in Blacktown City, as measured by the Socio-Economic Indexes for Areas (SEIFA). This project will help improve the thermal comfort for those with the least ability to shelter in air-conditioned homes and who rely more on public spaces.

The project has three declared objectives:

- Objective 1. To analyse the microclimatic conditions of the site and consider the summer cooling impacts that could be achieved through various interventions.
- Objective 2. To determine the most effective interventions and combination of intervention methods for reducing ambient temperatures, improving thermal comfort and reducing the need for energy to cool adjacent buildings.
- Objective 3. To promote people-focused design in Blacktown City, grow the city's capacity to apply and drive innovation on smart climatic solutions and accelerate the use of advanced adaptive interventions.

More in detail, this project specifically aims to analyse and recommend opportunities that will:

- Decrease the peak local ambient temperature, improve comfort, reducing heat vulnerability levels, and increasing the resilience of the community
- Reduce energy consumption, carbon emissions pollution in the specific location and contribute to improved wellbeing and health of the local population
- Demonstrate the efficiency and the performance of advanced mitigation, technologies to further replicate and use in other parts of Blacktown City and in other council areas
- Enhance Blacktown City Council staff capacity to conceive, design and implement climatic solutions in public assets.
- Accelerate changes, assist in overcoming gaps in science and technology, markets, policy and society and will create new game-changing operational conditions in the municipality
- Support leadership with vision with objectives based on the city needs.

The main methodology to investigate the potential for urban cooling in Mt Druitt includes:

- Reviewing available heat mapping for the area
- Site analysis to determine the main contributors to heat in the site's microclimate, e.g. site characteristics, current materials used, prevailing wind.
- Locations where cooling interventions will provide the best results
- Analysis and comparison of a range of cooling interventions for the site, including infrared reflecting pavements ('cool' pavements), cool asphalt, cool roofs, vertical greening and use of water features, and identify opportunities for onsite water sensitive urban design
- Recommendations for the most effective interventions for the site.

This report documents the activity conducted in Mt Druitt and the achieved results, delivering recommendations for the implementation phase.

2. Case Study Area: Mt Druitt

The case study area is the precinct of Mount Druitt, delimited by the railway on the south, Mount St on the east, and Carlisle Ave and Luxford Rd on the west and north, respectively (Figure 1).

The project focused on microclimate elements of Dawson Mall in Mount Druitt. This is a popular open-air shopping mall where Blacktown City Council may soon consider designs for urban revitalisation. The project findings provide an evidence base for upgrading the mall to be a demonstration site of interventions that improve thermal comfort. Dawson Mall is located near the Mount Druitt Railway Station and the heart of the central business district for the local area. The 11 suburbs within the Mount Druitt precinct are the most disadvantaged in Blacktown City, as measured by the Socio-Economic Indexes for Areas (SEIFA). This project will help improve the thermal comfort for those with the least ability to shelter in air-conditioned homes and who rely more on public spaces.



Figure 1. Satellite view of the case study area. Source: NSW Map Six (<https://maps.six.nsw.gov.au/>).

3. Methods

3.1 Preliminary fieldwork

To identify the locations where to position temperature and weather stations and where to collect data, several site inspections and preliminary fieldwork activities have been conducted. A preliminary thermographic survey had identified several hotspots, including the playground within the Mount Druiitt Swimming Centre area, whose surface can reach very high temperatures on a sunny afternoon since its high solar absorbance (Figure 2). Furthermore, a first set of temperature sensors (TRIX16 by Logtag enclosed in a radiation shield) have been deployed for six months, collecting temperature data every 30 min from March 2020 until May 2020 to investigate the representativity of tentative areas to be surveyed.

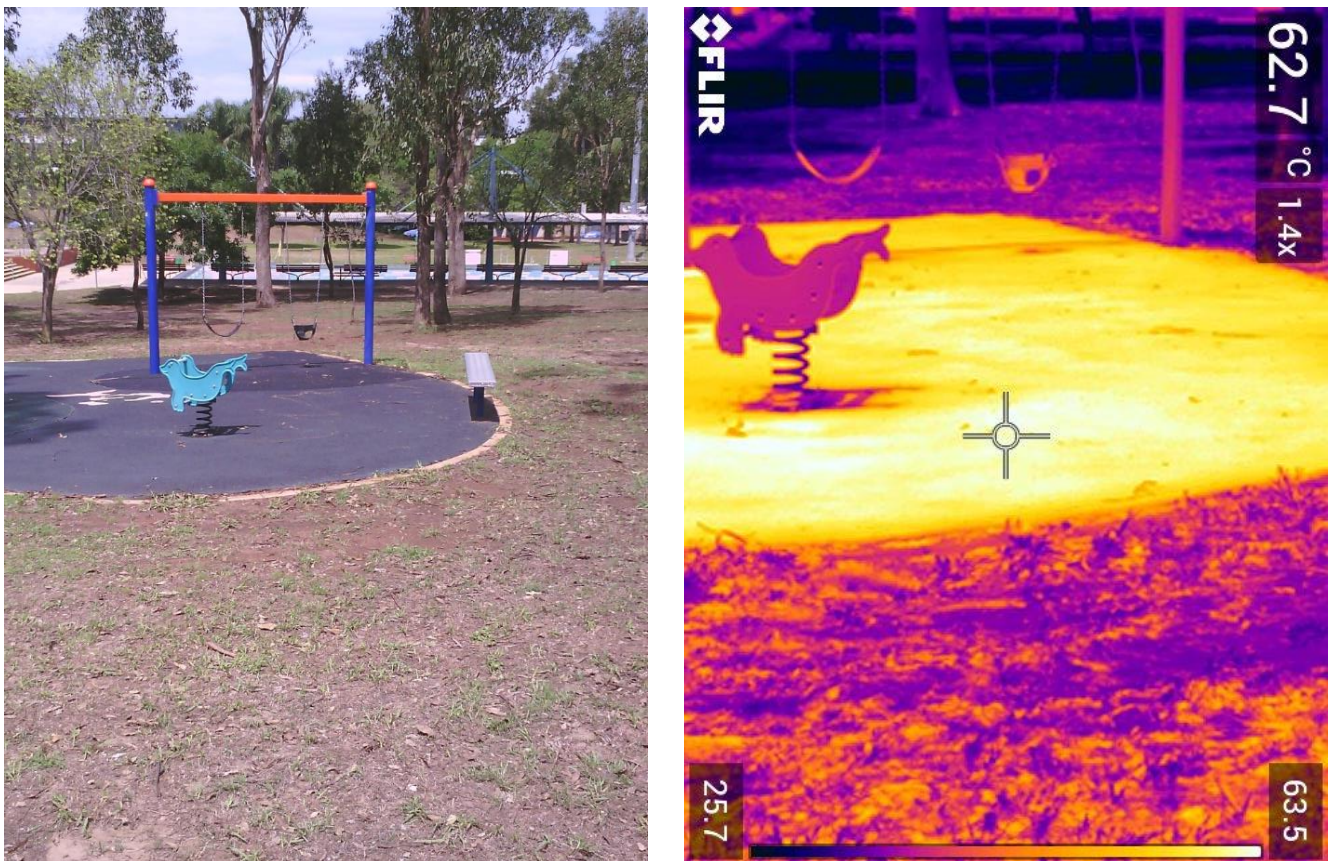


Figure 2. Visible and infrared view of the playground and surrounding grass within the Mount Druiitt Swimming Centre area.

3.2 Weather stations and temperature sensors for long-term monitoring

3.2.1 Existing networks of sensors

There is no established set of climate sensors in Mount Druiitt, with the closest station of the Bureau of Meteorology [1] being at the Horsley Park Equestrian Centre, approximately 9.5 km from Mount Druiitt (Figure 3). Other stations in the proximity are Penrith Lakes (at 14 km) and Badgerys Creek (16 km). An additional weather station was established by UNSW in Kingswood in late 2019 and is also 9.5 km from the Mount Druiitt study area. The station established by UNSW at Western Sydney University Kingswood campus (in collaboration with WSU) is a Vaisala WXT 536, a state-of-the-art automatic weather station. The only other station in the area is an air quality station managed by DPIE south of St Marys, approximately 6 km from Mt Druiitt.

Given the absence of weather stations in the immediate proximity of Mount Druiitt, there was the need for the establishment of sensors to monitor the local climate in the area before considering potential mitigation interventions.

The data collected by the BOM station in Horsley Park and the UNSW station in Kingswood have been used to provide the boundary conditions out of the urban texture, as both sites can be classified as Class 1 according to the World Meteorological Organization, thus describing the regional climate, free from the influence of nearby buildings.

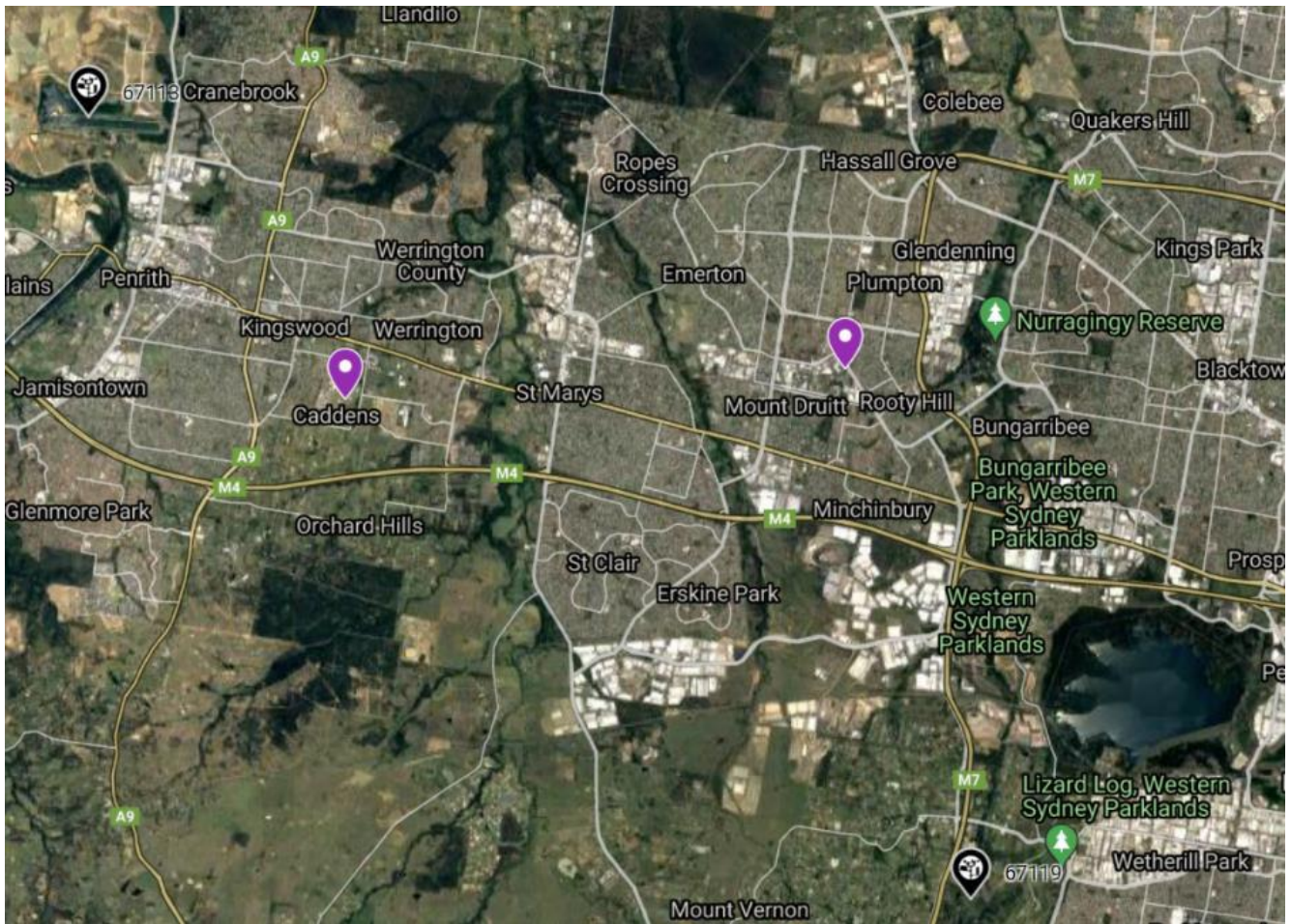


Figure 3. Automated weather stations in the area. The closest BOM stations (black pinpoints) are Horsley Park (station code 67119, west of Wetherill Park) and Penrith Lakes (station code 67113, west of Penrith). There is an additional automatic weather station established by UNSW in 2019 in Kingswood (indicated by the purple pinpoint).

3.2.2 Temperature and humidity sensors in Mount Druit

Once suitable sites had been identified and approval granted (some poles are property of Endeavour Energy), a network of 5 temperature and humidity sensors was established on 14th May 2020 (Figure 4 & Table 1), as soon as the hard lockdown restrictions related to the first wave of COVID-19 eased, and the sensors were procured.

The location of the sensors is also given in Figure 5. As previously mentioned, temporary sensors have been placed in the preceding two months to characterise the sites.

The sensors installed are HOBO 2301A dataloggers that measure air temperature and humidity with an external sensor, placed in an RS1 radiation shield, to prevent the sunlight from influencing the reading (both the sensor and radiation shield are manufactured by HOBO). The sensors have been installed on light poles identified by UNSW and BCC at 3.5 m from pedestrian level to prevent vandalization. Data can be retrieved via Bluetooth, which removes the need for a cherry picker (used for the installation) to remove the sensors, collect data, and reinstall the sensors. All these sensors are still in place, collect data every 10 minutes, and have capacity for more than 6 months. The last data collection was performed at the beginning of March 2021. The following data collection was scheduled in June, but it was prevented by the COVID-19 outbreak, and it will be performed in October 2021.

A set of additional 3 temperature sensors (Logtag temperature dataloggers inside an RS1 radiation shield) was installed on 10th February 2021 in preparation of the fieldwork campaign (and later retrieved on 01/03/2021), to collect data in additional points. These sensors have been installed at 3.1 m at three locations:

- Jirrang CI
- Caltex
- Westfield, in front of Target, before traffic lights. Carlisle Ave on Luxford Rd

These sensors were installed without the aid of a cherry picker, and therefore the maximum installation height was 3.1 m. The difference of 0.4 m in installation height between the main and this second set of sensors has negligible influence on temperature, as temperature decreases rapidly with height within the first 1.5 m from the ground, while after it varies less rapidly.

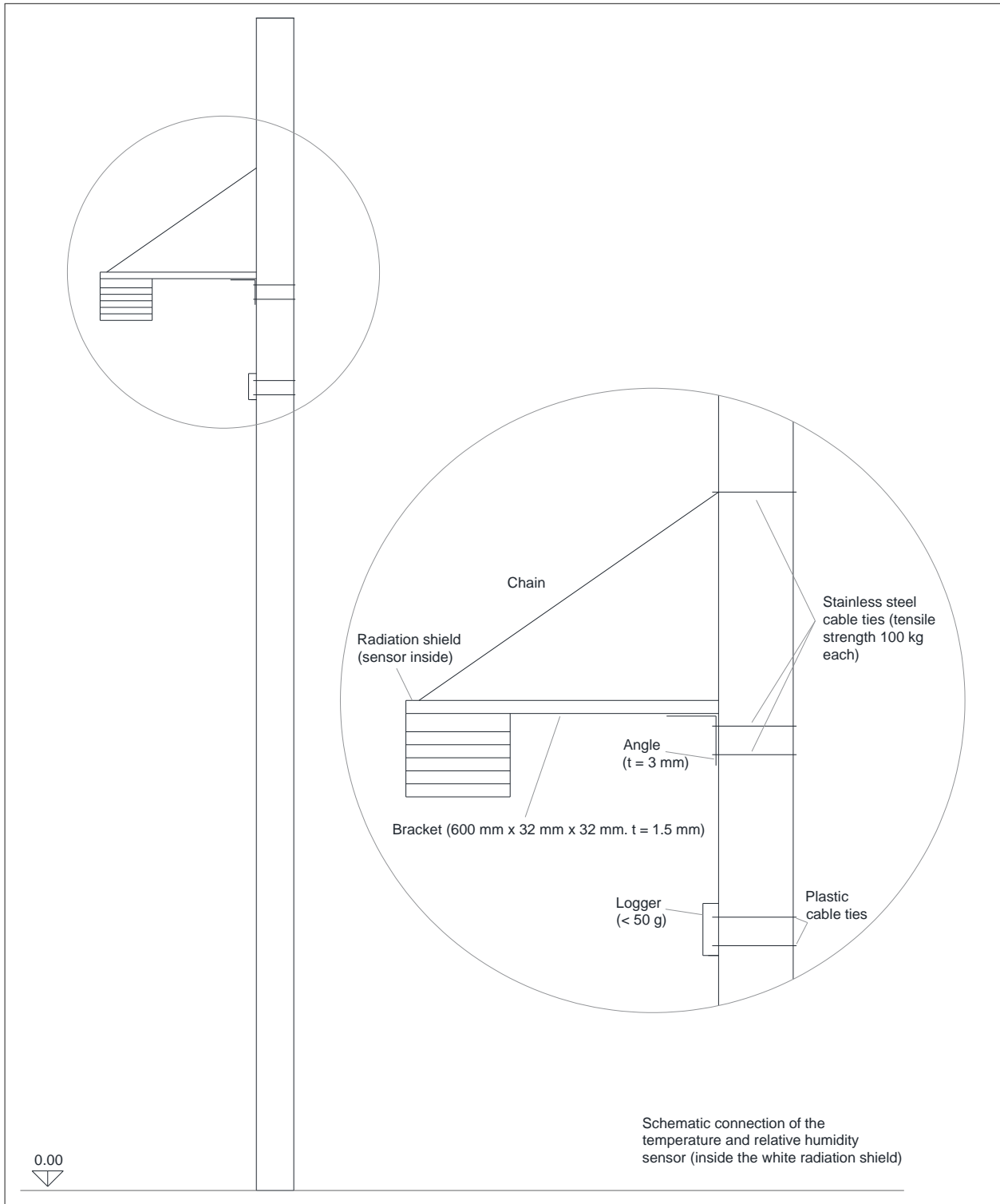








Figure 4. Schematic drawing of the installation of the temperature and humidity datalogger on light poles.

Table 1. Installed temperature and humidity sensors.

Code	Hobo S/N & coordinates	Position and description	Image
T1	20816318 Black_T1_20816318 Lat: -33.76696 Long: 150.82355	In front of the playground (swimming pool area)	
T2	20745988 Black_T2_20745988 Lat: -33.76692 Long: 150.82226	Central pole carpark swimming pool / The Hub	
T3	20745990 Black_T3_20745990 Lat: -33.76743 Long: 150.82124	Black pole in front of flag poles & library	

Continues

Code	Hobo S/N and coordinates	Position and description	Image
T4	20816316 Black_T4_20816316 Lat: -33.76805 Long: 150.82044	Dawson Mall - Black pole in front of Hot Price (opposite pole with CCTV)	
T5	20816317 Black_T5_20816317 Lat: -33.76861 Long: 150.82034	Black pole in front of Asian Food Market & 7 eleven (close to the station)	
T0	20739090 Black_T0_20739090 Lat: -33.76601 Long: 150.83114	Fire & Rescue station	

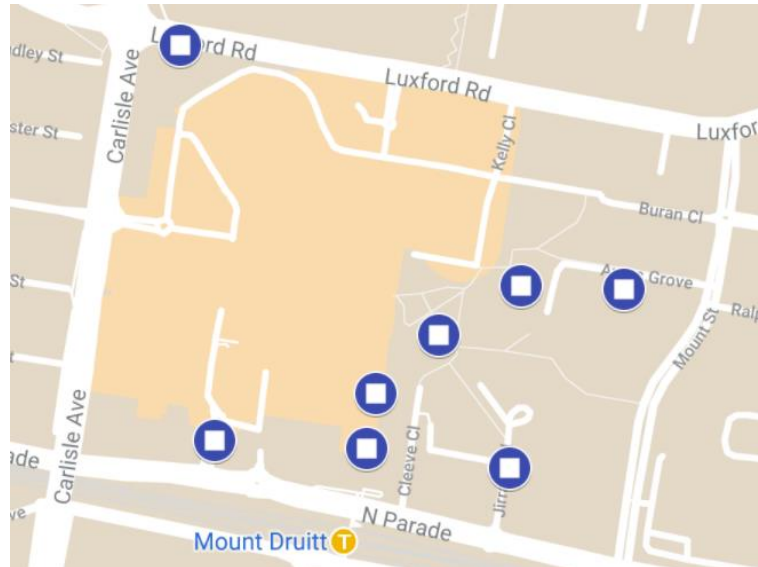


Figure 5. Position of the temperature and humidity sensors.

3.2.3 Weather station in Mount Druiitt

A weather station has been established in Mount Druiitt and hosted on the NSW Fire and Rescue site. Blacktown City Council has arranged for the agreement with NSW Fire and Rescue and carried out the installation with UNSW on 22/01/2021 (Figure 6-8). The delivery of the station from Observer (based in Victoria) has been delayed by the COVID-19 impacts in the Melbourne area.



Figure 6. Weather station at Mt Druiitt Fire & Rescue station.

The station is a GMX500 by Gill, and records air temperature, humidity, and pressure, as well as wind speed and direction. The station is installed at 1.6 m above grass and can transmit data remotely. Unfortunately, the weather station has been affected by a fabrication issue resulting in faulty data transmission, whose resolution has been delayed by the pandemic since the supplier (Observer) was unable to come on-site and the supply lines have been impacted. Once the issue is resolved, the station will continue to collect data. In the meantime, a temperature and humidity sensor like those installed in Mount Druiitt (i.e., HOBO 2301A in an RS1 radiation shield) has been installed on the same weather pole, collecting data since May 2020 (Figure 6).

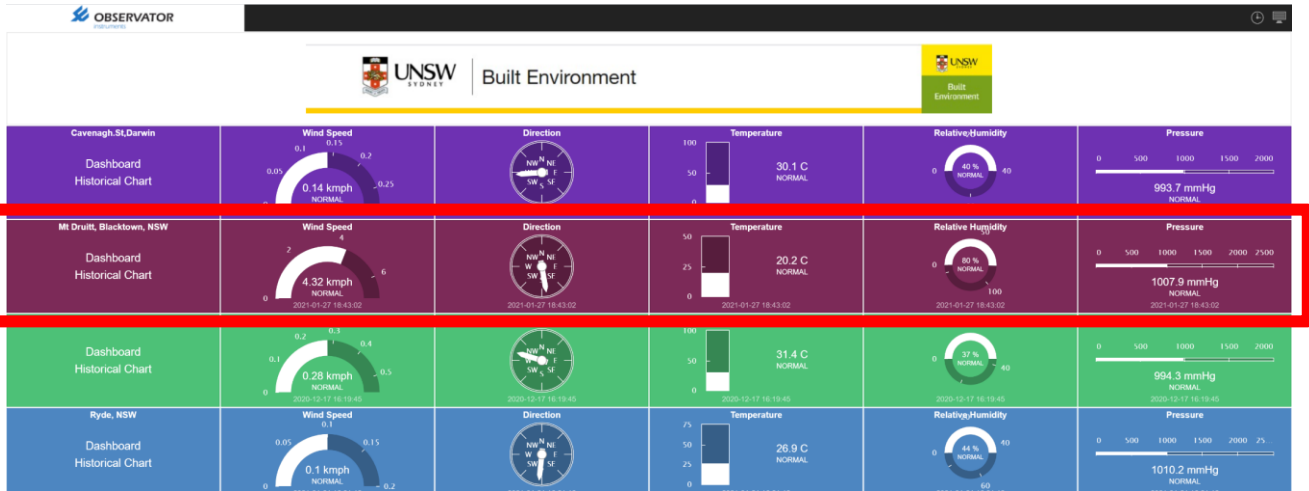


Figure 7. Example of the dashboard view.

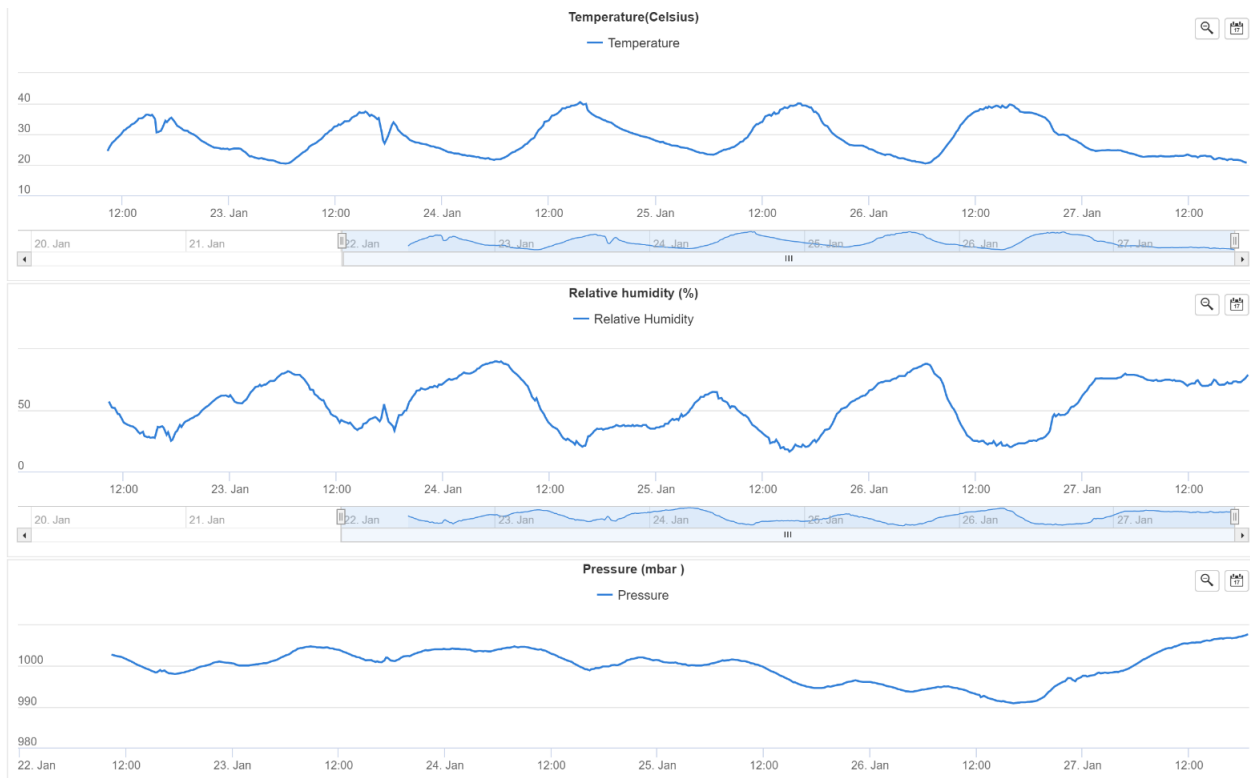


Figure 8. Example of collected data.

3.2.4 Weather data treatment

For the measured weather data, unrealistic values (i.e., wrong readings) were filtered performing the validation procedures detailed by Estevez et al. [2], performing the following tests:

- Range tests (e.g., relative humidity comprised between 5 and 100%);
- Step tests (e.g., air temperature change of less than 10 °C in one hour, or relative humidity variation not exceeding 45% in one hour);
- Persistence tests (e.g., steady values for long periods are filtered as equipment failure);
- Relational tests (i.e., if the wind speed is null, then the wind direction cannot be different from 0°).

In addition to invalid readings, when using raw data measured by weather stations, encountering missing values is inevitable [3]. Similarly to Paolini et al. [4], who used a Back-Propagated Neural Network, to infill the gaps in the data series, we linearly interpolated between values if the gaps accounted for a maximum of three hours. For longer interruption in the continuity of the weather data series, we found an analytical relation between a quantity (e.g., air temperature) at one station and the same quantity measured by the three closest stations triangulating the target station.

3.3 Fieldwork campaign

The fieldwork activities include terrestrial and aerial surveys, with the primary purpose of collecting input data and data for the validation of the microclimate model, then used to assess different design scenarios. The aerial and terrestrial surveys have been conducted simultaneously on a clear sky day on the 22nd February 2021. Albedo measurements were performed on 1st March 2021, completing the campaign.

3.3.1 Terrestrial and aerial campaign

The terrestrial survey has been carried out by means of the UNSW Energy Bus, a vehicle equipped with a foldable telescopic mast, to which weather stations and other sensors can be connected. The vehicle serves the purpose of driving a weather station to a location where one is not available. The mast has been extended to a maximum height of 10 m (Figure 9), with the vehicle parked in a temporarily restricted area of the parking lot of the Vegas Hotel Mount Druitt, between North Parade, Cleeve Cl and Jirrang Cl.

The position of the Energy Bus has been selected to capture the wind inflow from the southern portion of the simulation domain and to provide a vertical profile of temperature and wind speed to calibrate the simulations captured in a relatively open area in the built environment of Mount Druitt, while still within the urban texture.

Two weather stations (MetPak Pro by Gill Instruments, Table 2) has been used to measure air temperature, humidity, and air pressure, as well as wind speed at 10 m (top of the mast) and 1.5 m (on a tripod), in the proximity of the Energy Bus. Moreover, a pyranometer and a pyrgeometer measured the incoming solar (shortwave) and thermal (longwave) radiation (NR01 by Hukseflux). Data were logged every 15s by a DT85 Datataker (by Lontek) to which they were connected.

In parallel with the measurements logged by the Energy Bus, two carts equipped with GMX500 weather stations (by Gill Instruments), measured the same quantities (i.e., air temperature, humidity, air pressure and wind speed) at 1.1 m, which is the conventional height of the centre of mass of an adult (Figure 9). These two carts performed measurement sessions of 10 min at each of the 22 locations identified during the planning phase of the campaign (Figure 10). One of the two carts was equipped with a pyranometer measuring incoming solar radiation (SMP11 by Kipp Zonen), and both carts were equipped with a DT80 datataker (by Lontek) to record measurements, logging data every 15 s. The first 5 min of each session were discarded, retaining the last 5 min to allow for signal stabilisation. The two carts started at opposite sides, pursuing one another so that the same point was measured twice, within 3 hours. Together with the carts, a thermal camera FLIR T540 collected pictures in the infrared wavelength range at ground level.

The UNSW weather station in Kingswood (synoptic station 10 km from Mount Druitt), the main weather station in Mt Druitt (at the NSW Fire & Rescue site) as well as the eight temperature sensors on poles also collected data during the fieldwork activity.

Table 2. Specifications of the measurement equipment.

MetPak Pro meteorological station (short-term ground-based measurements)					
<ul style="list-style-type: none"> - On-board high accuracy barometric pressure sensor - Rotronic Hygroclip HC2-S3 temperature/humidity probe housed in a naturally aspirated radiation shield - ultrasonic wind detector 					
Parameter	Temperature	Relative humidity	Wind speed	Wind direction	Barometric Pressure
Range	-50 to +100 °C	0-100%	0-60 m/s	0 to 359 °	600-1100 hPa
Accuracy	±0.1 °C	±0.8% @ 23 °C	±2% @12 m/s	±3 ° @12 m/s	±0.5 hPa
Resolution	0.1 °C	0.10%	0.01m/s	1 °	0.1 hPa
Net radiometer:					
<ul style="list-style-type: none"> - Two identical ISO 9060 second class pyranometer; - Two identical pyrgeometer with 150 ° field of view 					
Parameter	Net radiation				
Range	-300 to +300 W/m ² (measurement range) 285 to 3000 x 10 ⁻⁹ m (spectral range solar); 4.5 to 40 x 10 ⁻⁶ m (spectral range longwave)				
Accuracy	6.2% (summer), 9.9% (winter), daily, mid-latitude				
Resolution	10 W/m ²				



Figure 9. Energy Bus and drone (left) and cart with pyranometer and weather station (right).

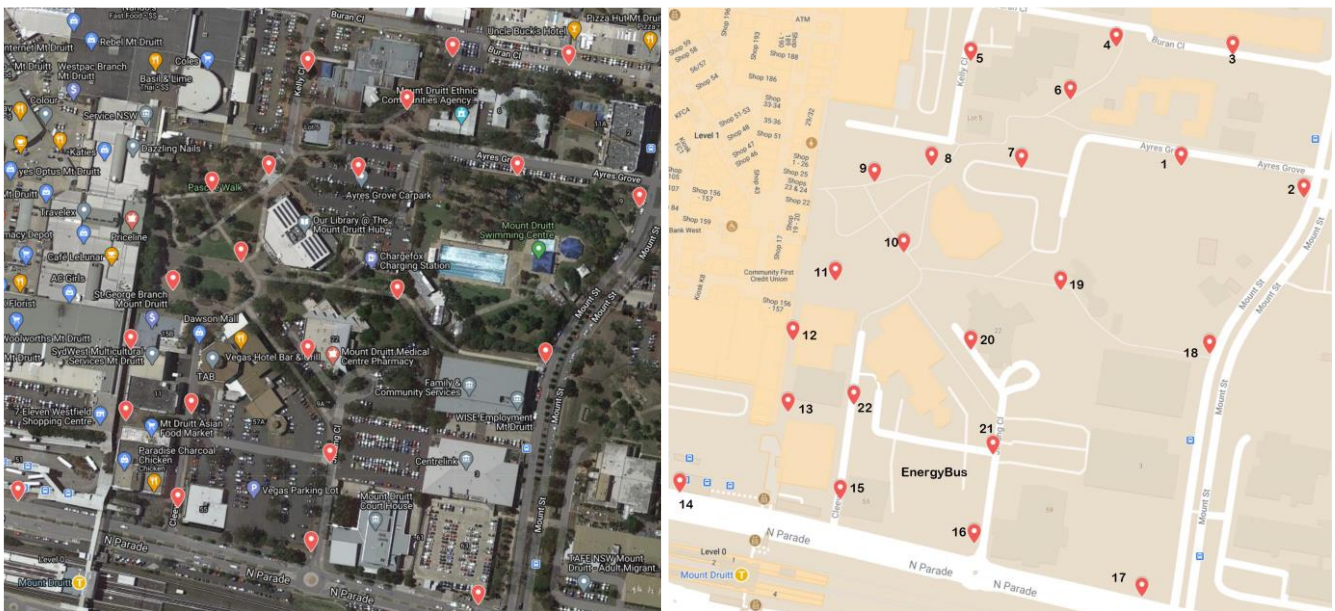


Figure 10. Data collection points.

An Unmanned Aerial Vehicle (UAV) equipped with a FLIR thermal camera collected surface temperature images of the area, operated by National Drones, after take off from a restricted area nearby the Energy Bus (Figure 11). The drone collected 805 thermal and visible images, later post-processed and composed in a single orthophoto of Dawson Mall. The drone used for the campaign is a DJI Matrice 210V2, equipped with a Zenmuse XT2 thermal sensor, combining the FLIR Tau 2 thermal sensor and 4K visual camera. The sensor has a scene range (high gain) of 640 x 512.



Figure 11. Drone takeoff location.

3.3.2 Albedo measurements

After the main fieldwork activity, the albedo of the street pavements at different locations was measured with two back-to-back pyranometers (part of an NR01 net radiometer, by Hukseflux) on 1st March 2021. The albedo, or solar reflectance, is the ratio of reflected to incident solar radiation and indicates the portion of sunlight that is not absorbed by urban surfaces such as streets, grass, sidewalks, etc. The albedo measurements do not need to be performed simultaneously with the other fieldwork activities. It is sufficient to carry out the measurements on a clear sky day with solar elevation of more than 45°. The instrument was positioned at 50 cm above the ground, which is a standard compromise to minimise the surface area seen by the instrument (so that only an area of approximately 4 m² is captured at one time) while containing the influence of the shadow of the instrument itself (Figure 12). For this reason, the instrument is always facing the sun. The albedo was measured at 23 different locations in the area of interest, covering every main type of urban surface and material displayed in Mount Drutt, later used as an input for microclimate simulations (Figure 13).



Figure 12. Cart equipped with a net radiometer, shown while performing measurements along Dawson Mall.

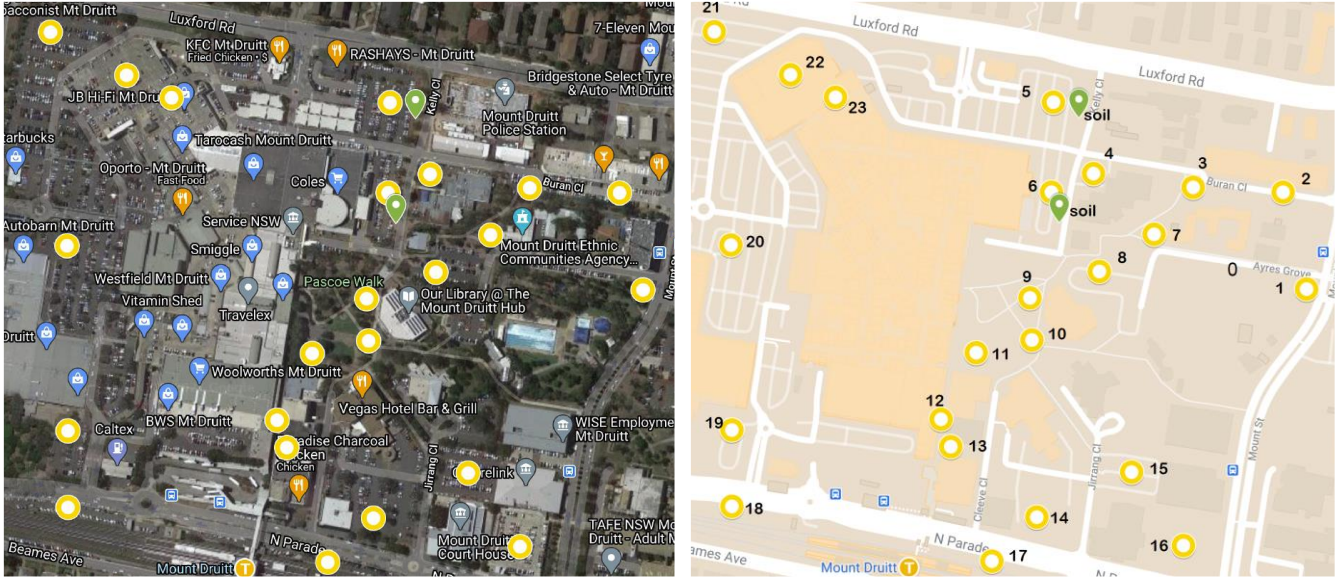


Figure 13. Location of the albedo measurements.

3.4 Microclimate simulations

3.4.1 Microclimate model

The local microclimate Mt Druitt has been simulated using ENVI-met V4.4.6, which is a three-dimensional microclimate model based on computational fluid dynamics and thermodynamics [5,6]. It is designed to simulate the influence of buildings, the surface characteristics, plant, soil and climate interactions in an urban environment, and it is widely used in the scientific community to assess urban heat mitigation at the microscale [7–9].

The simulated area in Mt Druitt is approximately 700 m x 530 m (Figure 14), rendered with a mesh having a resolution of 3 m (dx) × 3 m (dy) × 0.25 m (dz, base). The grid at the z-axis is telescopic with a thicker cell near the ground, allowing a better accuracy for edge effects. The simulation domain comprises the funded and unfunded projects indicated by Blacktown City Council.

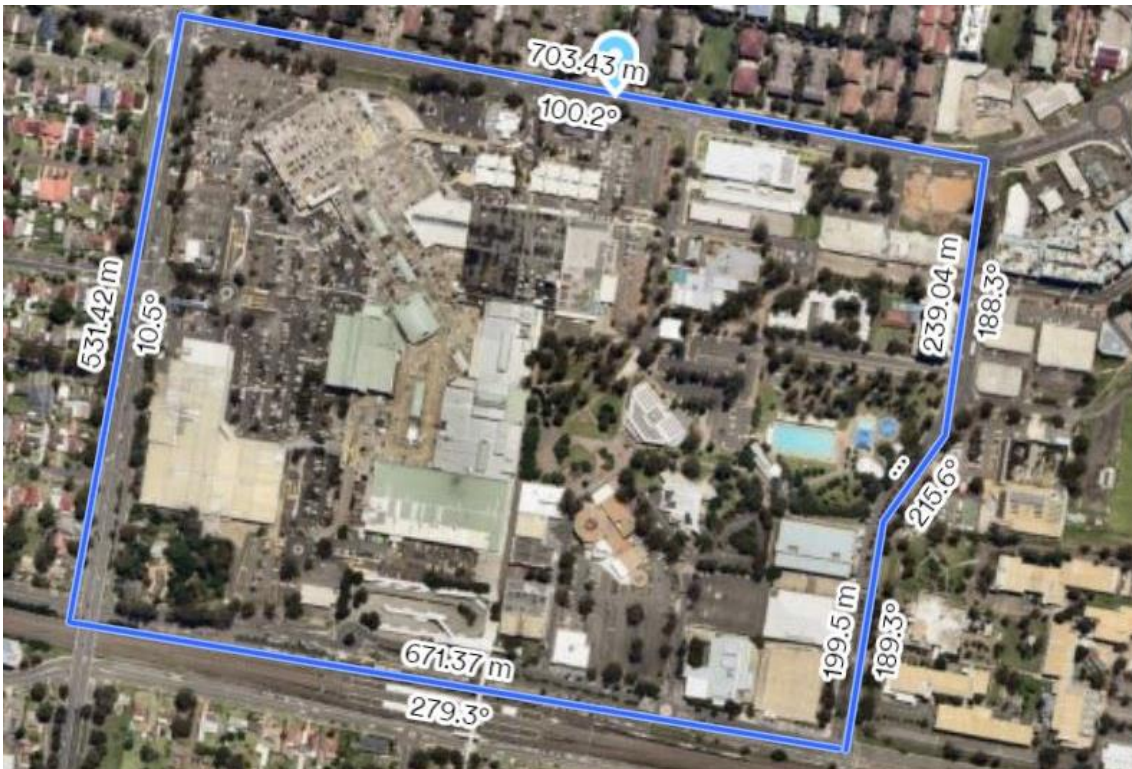


Figure 14. Simulation domain.

The building heights and geometries were communicated by Blacktown City Council and the position of trees has been derived with the survey (Figure 15). Also, the albedo of urban materials has been directly measured where possible (see the previous section) and estimated with values measured during previous campaigns in NSW for similar materials for inaccessible rooftops. The day simulated is the 22nd of February 2021, when the fieldwork has been performed. The boundary conditions to the simulations (air temperature, humidity and wind speed and direction) have been provided by the synoptic weather station in Kingswood (~ 10 km south of Mt Druitt), which measured an undisturbed condition.

The simulations were performed with the simple input model, with a constant wind speed of 2 m/s and direction from south to north, as taken from the Kingswood site, which was consistent with the measurements at 10 m performed by the Energy Bus. The semi-hourly values of ambient temperature and humidity – also from the UNSW station at Kingswood – are inputted in the model, while the incoming solar and longwave radiation are simulated by ENVI-met. We decided to use the simple input model instead of the full forcing model (which allows for semi-hourly input of all quantities) because of the instability of the latter resolution method in ENVI-met, which appears to be under development. The same issue was confirmed by colleagues in the USA and Europe who also use the same simulation tool, who reported good performance with the model with the simple forcing and issues with the full forcing.

ENVI-met was run for a 24-hour period, starting at 2 a.m., with constant time steps (2 s) and model output every 30 min, with the first four hours as a spin-up time.



Figure 15. Axonometric view of the simulation domain.

3.5 Assessment of impacts

3.5.1 Weather data inputs for the assessment of impacts

The semi-hourly air temperature and absolute humidity data in Mt Druitt have been computed over long periods and out of the monitoring period with the correlation between air temperature and absolute humidity measured in Mt Druitt and the values observed at Horsley Park (BOM station). The relative humidity has been then computed from the temperature and absolute humidity with the well-known psychrometric equations given in ISO standards or any heat and moisture transport handbook [10]. In the combined mitigated scenario, the ambient temperature

has been computed by multiplying the mitigation coefficients derived from the simulations (ratio of mitigated to unmitigated ambient temperature) times the ambient temperature in Mt Druitt for the unmitigated scenario. Then, the relative humidity has been computed with the mitigated temperature and the absolute humidity in the unmitigated condition. A relation between the mitigated and unmitigated absolute humidity was not established from the simulations since no moisture storage properties from building materials have been surveyed, and supplementary data would be required to calibrate the simulations with this respect.

The undisturbed wind speed, instead, was not recalibrated, as the observations later revealed that at 10 m the wind speed is approximately the same as in Horsley Park, which is representative of the conditions of the upper portion of buildings and rooftops. Moreover, existing building energy simulation models do not allow to run simulations with different wind speeds depending on the height of a façade portion, for instance. Thus, this is considered an acceptable approximation.

3.5.2 Building Performance Simulations

To assess the potential benefits of urban heat mitigation on building energy performance, we performed building energy simulations by means of EnergyPlus 9.5 [11], a state of the art software tool initially developed by Lawrence Berkeley National Laboratory (Berkeley, CA) under contract for the US Department of Energy, and later contributed by the National Renewable Energy Laboratory and many other institutions. It is an open-source and freely available tool that has been widely validated in scientific studies and is commonly regarded as the benchmark simulation tool.

Weather data inputs. The weather data used as input for the simulations were the weather data for the year 2016-2017 for the BOM station of Horsley Park, with BOM estimated solar and infrared radiation. The year 2016-2017 (May to April) has been selected as it includes a relatively hot but not extreme summer. Furthermore, solar radiation data after 2018 are not released by BOM. Then, temperature and humidity for Mount Druitt have been computed with a correlation established between the data measured in Mount Druitt in 2020-2021 and Horsley Park. The mitigated weather data have been computed by multiplying the unmitigated temperatures times the ratio between the mitigated and unmitigated temperature resulting from the microclimate simulations.

Simulated buildings. The buildings selected for the simulations are archetypical buildings whose typologies can be considered representative for the context in Mount Druitt. More in detail, the buildings include

- Low-rise office buildings (existing and new)
- Low-rise shopping mall (existing and new)
- A low-rise (3 stories) apartment building (new)
- A school (new).

For existing buildings, the thermal properties of the building envelope have been assumed as for pre-code buildings, while for new buildings, the Deemed to Satisfy R-values given by the National Construction Code (NCC 2019) have been used [12].

All buildings have been simulated with a conventional non-reflective roof (albedo = 0.15 and thermal emittance = 0.9) and with a reflective roof (albedo = 0.75 and thermal emittance = 0.9). All other building inputs and simulation parameters are given in the annex.

The building energy simulations have been performed for the period from the 15th of October to the 15th April, thus covering only the cooling season (and part of the intermediate season). The buildings have been simulated with an ideal air conditioning system, thus computing the cooling energy needs (or cooling loads), namely the energy to be provided to the indoor space to maintain the setpoint temperatures.

3.5.3 Electricity demand calculation

To assess the electricity demand as a function of temperature, we used a model previously developed. We selected this approach to avoid the high uncertainty related to the construction of electricity demand models in small areas – due to the uncertainty in population – and since a long enough data series to develop the model was not sourced (since changes in the grid structure determined by new connections lead to discontinuity in the data series).

In Sydney, semi-hourly weather data were collected by nine weather stations managed by the Bureau of Meteorology [1] for the period 2013-2017 (Table 3). Lacking long term records of global horizontal solar radiation free of gaps, the extraterrestrial global horizontal radiation from satellite measurements [13] was used to compute

the solar position with a high-accuracy algorithm [14]. The simulated environmental conditions in the precincts showed a very good agreement with the BoM stations that were directly used. Population weighted average temperatures and statistical data on the population [15] were also used.

Table 3. Specifications of the measurement equipment.

BoM Station code	Station name	Latitude	Longitude	Location
66137	Bankstown	-33.918	150.986	
68257	Campbelltown	-34.062	150.774	
66194	Canterbury	-33.906	151.113	Western Sydney, 20-30 km from the coast
66161	Holsworthy	-33.993	150.949	
67119	Horsley Park	-33.851	150.857	
66212	Olympic Park	-33.834	151.072	
66062	Observatory Hill	-33.859	151.202	Coastal, NSW
67113	Penrith	-33.720	150.678	NSW, 50 km from the coast
67105	Richmond	-33.600	150.776	coast

These data are representative of an area of Sydney (~ 4,500 km²) with approximately 4.2 million residents. Electricity data were obtained from AEMO. The electricity demand plotted versus the ambient temperature shows the typical U shape, with an inflection point at approximately 18 °C (Figure 16). The correlation for the semi-hourly electricity demand (ELDem) expressed in MW is a function of the population-weighted average temperature (T) for the areas and the extraterrestrial horizontal irradiance (G).

$$\text{ELDem} = 6157.6 + 73.9 \cdot \text{sma}(T, 113) + 0.136 \cdot T \cdot \text{sma}(T, 10) \cdot \text{sma}(T, 26) - 4.335 \cdot \max(\text{smm}(G, 191), 0.024 \cdot \text{delay}(G, 29) \cdot \text{sma}(T, 10)) \quad (1)$$

Where sma (x, n) is the simple moving average of the previous n records of the quantity x. Similarly, smm is the simple moving median. Delay (x, n) indicates a delayed variable, namely for the time step t, it considers the value quantity n time steps before. A ceiling and a floor were applied to the computed results, corresponding to the 0.1th and 99.9th percentile of the demanded power. The mean absolute error was 513 MW, symmetrically distributed, with differences between observed and modelled total demand equal to 0.1 TWh (~ 0.6 % of 17.4 TWh over the average summer period), and to 0.5 % of the peak demand. This model was developed during the Cooling Western Sydney project [16].

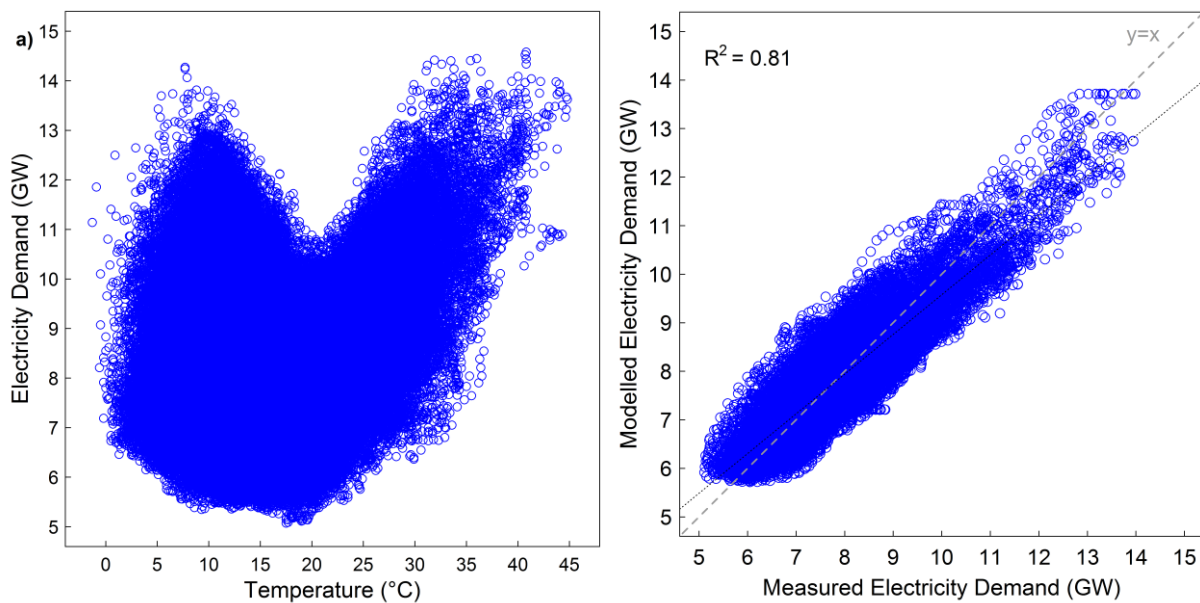


Figure 16. Electricity demand against air temperature and performance of the model against electricity demand in NSW.

The model can predict the general trend of the electricity demand but does not capture the fuzziness, likely due to other factors that were not considered, such as other climate parameters and social variables such as population and holiday/working-day [17]. Incorporating these aspects with fuzzy algorithms could provide a further

improvement of the model [18]. Moreover, further improvements can come from apportioned data for energy uses and relative to the specific local government areas.

For ambient temperatures below 18 °C, the peak values were not reached for the lowest temperatures, but at approximately 10 °C. This might indicate the impact of poor weather on the electricity uses as well as on the generation off-the-grid (e.g., building integrated photovoltaic or solar collectors for domestic hot water), since the rainfalls were prevalent in the intermediate season. The ambient humidity did not show a dominant impact on the electricity demand, although several occurrences of high demand with high absolute humidity were noted.

This model was used to compute the electricity demand in Mount Druitt, computing the electricity demand for the whole New South Wales and dividing it by the NSW population of 2013-2017. In NSW the peak demand per capita (state average) was approximately 2 kW. The output of the model reflected the current electricity demand profile, with the existing technology and efficiency of the grid and appliances of the period 2013-2017. The model did not predict the future electricity demand that could result from a variety of factors. These include but are not limited to:

- Improved efficiency of refrigerators and other domestic appliances imposed by legislation or market-driven;
- Reduced building electricity demand for heating, ventilation and cooling due to improved building quality or use of more efficient controllers in combination with a building management system;
- Increased use of air conditioning by increased market penetration (i.e., people who did not have air conditioning at home purchase it and start using it);
- Modified thermal comfort expectations by the population and other social changes.

Market penetration and available income are two major drivers that will dramatically increase the electricity demand for cooling [19].

Weather data inputs. As for the building performance simulations, also for the calculation of the electricity demand, three datasets were used:

- Horsley Park (out of the urban area)
- Mount Druitt unmitigated
- Mount Druitt mitigated (combined scenario)

In this case, the temperature data for the last 20 years have been used, to provide an appraisal of the interannual variability. It is to be noted that the electricity consumption relates to 2013-2017 levels (which the model represents), so the only variable is the ambient temperature.

3.5.4 Mortality Risk

To define the relation between ambient temperature and heat-related mortality, we used the relation found by Gosling et al. for Sydney [20]. They analysed the daily maximum temperatures for the period 1988-2003 for the Observatory Hill station of the Bureau of Meteorology, and they considered the daily mortality. Therefore, by means of multiple regression techniques, they found an exponential relation between the maximum outdoor air temperature (T_{max} , in °C) and the heat-related daily mortality rate MR per 100,000 people:

$$MR = e^{4.898 - 241.2 / T_{max}} \quad (1)$$

The model by Gosling et al., for Sydney, has a squared correlation coefficient of 0.917. Gosling et al. also noted that the threshold at which heat-related deaths occur tends to be lower in the cities with a lower mean summer maximum ambient temperature, likely related to acclimatisation. Finally, for Sydney, the time lag between peak temperature and mortality tends to zero; namely, no time shift was observed between extra-mortality and peak environmental conditions.

Here, we applied this parametrization to data of both mitigated and mitigated scenarios. We highlight that the correlation has been developed based on the epidemiologic data of the population in the Greater Sydney Area for the period 1988-2003. Now, also post COVID-19, the demographics could be very different in terms of age distribution, general health conditions, country of origin and tolerance to extreme heat, socio-economic status. Moreover, the building stock quality and consequent response to heathwaves, market penetration of air conditioning, health infrastructure, medical and emergency procedures can also be different. Therefore, this analysis is only representative of the risk of heat-related mortality, while it cannot include the other important scenario variations. In other words, important co-factors for heat-related mortality are [21,22]:

- Personal: age, chronic diseases, etc.

- Context: no access to air conditioning, top floor, not leaving home, etc.

Under the same climate conditions, different areas may show higher or lower actual mortality rates depending on the spatial distribution of:

- Vulnerable population (and its composition)
- Air-conditioned dwellings, social exclusion, etc.

As mentioned, the daily mortality rates and the cumulative heat-related deaths shall not be interpreted as a forecast but as a risk indicator.

Weather data inputs. As for the building performance simulations, also for the calculation of the electricity demand, three datasets were used:

- Horsley Park (BOM station 67119, out of the urban area, 10 km from Mount Druitt)
- Mount Druitt unmitigated
- Mount Druitt mitigated (combined scenario)
- Penrith Lakes (BOM station 67113, out of the urban area, 10 km from Mount Druitt)
- Terrey Hills (BOM station 66059, established in 2008, out of the urban area)

In this case, the data for the last 20 years have been used. The stations in Terrey Hills and Penrith have been considered to provide a reference for the conditions in a coastal area cooled by the sea breeze (Northern Beaches, for Terrey Hills) and at the westmost boundary of the Greater Sydney area (Penrith Lakes), where typically the highest peak summer temperatures are recorded.

4. Design Scenarios

The consideration of the design scenarios started from the plan of funded projects for the revitalisation of Mount Druitt (Figure 17), and the consideration of the hotspots identified with the fieldwork, as well as the state-of-the-art heat mitigation technologies applied in Australia [23] and overseas [24], as the research experience previously gathered in Western Sydney [25,26].

Furthermore, the heat mitigation technologies have been discussed between Blacktown City Council and UNSW. Therefore, the design scenarios modelled with the microclimate simulations are:

1. Base case. The current situation in Mount Druitt captured by the fieldwork without mitigation.
2. Greenery – unirrigated. 10 unirrigated mature trees on Dawson Mall and 337 unirrigated trees in the rest of the domain, added to the already available trees in the area.
3. Greenery – irrigated. 10 passively irrigated trees are added on Dawson Mall. All the other additional 337 trees are unirrigated.
4. Cool Materials – The albedo of car parks and street pavements is increased from the measured value (~0.09 for aged asphalt) to 0.40, and the albedo of rooftops is increased from the current values to 0.75. Rooftop car parks are treated like car parks, increasing the albedo to 0.40. In all cases, the thermal emittance is set to 0.90.
5. Combined scenario – Irrigated greenery, in combination with cool materials and shading of the main car parks (Figure 18).

All scenarios are assessed with the microclimate simulations, while the impacts are assessed only for the base case and combined scenario.

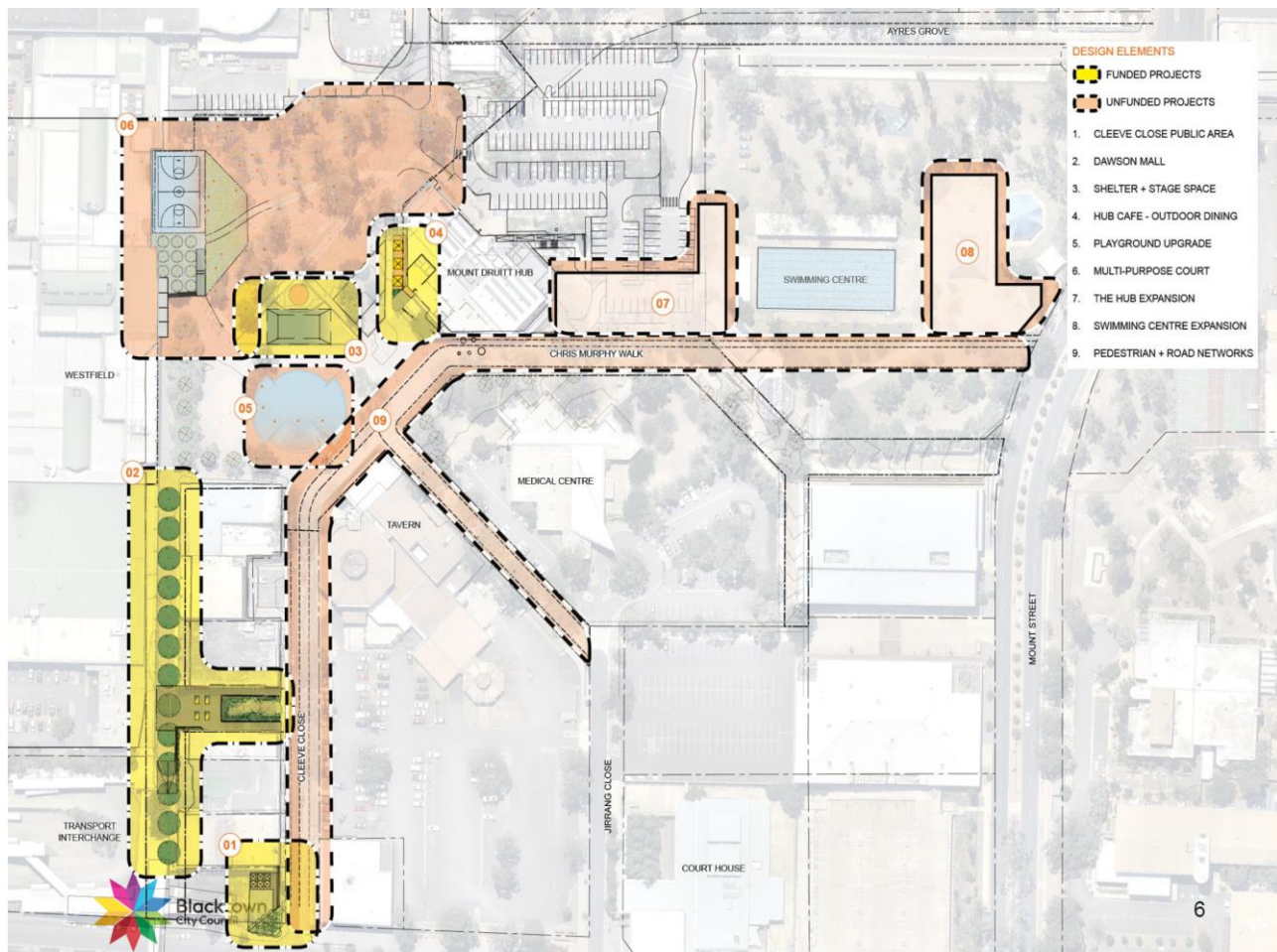


Figure 17. Funded and unfunded projects for the revitalisation of Mount Druitt.



Figure 18. Combined mitigation scenario.

An albedo of 0.40 for a car park or pedestrian area can be achieved with a red or grey cool coloured pavement [27], which reflects most in the near infrared than in the visible wavelength range, thus not affecting visual comfort [28]. The red bus lanes can be a visual reference for the type of brightness that can be expected from a similar technology.

An albedo of 0.75 for roofing materials is representative of an aged white roof (metal roofing or a roofing membrane) in a non-heavily polluted area [29].

The shading over the car parks is similar in concept to the tents that are already present over some car parks in the Westfield area, in the north part of the simulation domain. Canopy shading serves multiple purposes:

- Minimising the thermal discomfort of pedestrians [30];
- Reflecting more sunlight before it enters the urban fabric and gets absorbed after multiple reflections and absorptions;
- Reduce the overheating of parked vehicles, which then emit more pollutants when switching on air conditioning at maximum power [31].

5. Results and Discussion

5.1 Temperature and humidity records

The first use of the data recorded by the temperature and humidity sensors deployed in Mt Druitt was to compute an average value for the sensors on Dawson Mall, behind the community centre, and at the NSW Fire & Rescue station (thus excluding the sensor at the Swimming Centre, as part of a park and exposed to increased humidity). Then, we computed a simple moving average over 2.5 hours for the data measured in Horsley Park and the average of the sensors in Mt Druitt (Sensors T0, T2, T3, and T4). With this approach, we capture the trend in temperature and humidity, ignoring temporal differences due to the time a perturbation or air front takes to move from Horsley Park to Mt Druitt. Therefore, the developed correlations show a very good goodness of fit (r^2), exceeding 0.98 for the air temperature and 0.99 for the absolute humidity (Figure 19). These regressions allow us to compute the temperature and humidity in Mt Druitt starting from the data measured in Horsley Park for a prolonged period or a period different from that of the project monitoring.

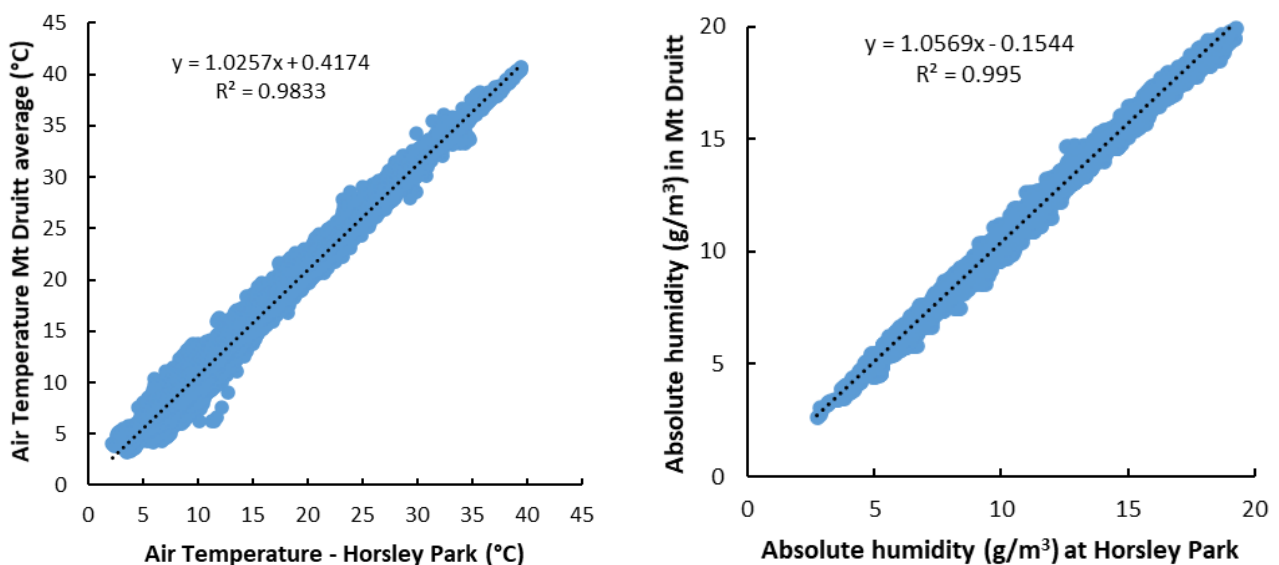


Figure 19. Relations between the ambient conditions in Horsley Park and the measured average values in Mt Druitt.

Moreover, it helps us to consider the systematic differences between Mt Druitt and the site of Horsley Park, which is at approximately 10 km south of Mt Druitt and roughly the same distance from the coast (Mt Druitt is 42 km from the coast, while Horsley Park is 38 km). Here we observe that the average of the four sensors in Mt Druitt was systematically warmer than Horsley Park, as well as more humid. For instance, when the air temperature in Horsley Park exceeds 30 °C, in Mt Druitt is on average 1.2 °C warmer. These values are typical of a medium to low-density urban area [32]. These figures have been computed considering the period from 14/05/2020 and 01/03/2021, when the sensors in Mt Druitt collected data. Therefore, they capture the complete range of temperatures and climate conditions that can be observed during the cold, intermediate and hot season.

By considering the evolution of temperature over a period of a few days, we can better appraise the differences. In this case, we focus on the three-day period of the fieldwork day and the preceding two days (from 20 Feb to 22 Feb 2021), which offered a sequence of hot and clear sky days (Figure 20). The average of the measurements in Mt Druitt in peak conditions is 1.2-1.7 °C hotter than the values recorded at Horsley Park and approximately 0.7-0.8 °C hotter than Kingswood (which is closer to the urban fabric of Penrith). Also, the air temperature in Mt Druitt is higher during the evening and first part of the night than out of the urban area, as it is typical of urban climates [33,34]. Importantly, the number of hours above the set point temperature for cooling (conventionally equal to 25 °C for residential buildings) is larger in Mt Druitt than out of the city, which may result in an energy penalty.

Among all locations in Mt Druitt, the sensor at NSW Fire & Rescue recorded the lowest temperature, while the hottest portion is Dawson Mall, where the urban canopy contributes to entrapping heat (Figure 21), with all stations within 0.5 °C during the central part of the day and the maximum difference occurring over the night when Dawson

Mall remains about 1 °C warmer than the less built-up area north of the hospital. All these trends are consistent with what is widely documented in the literature.

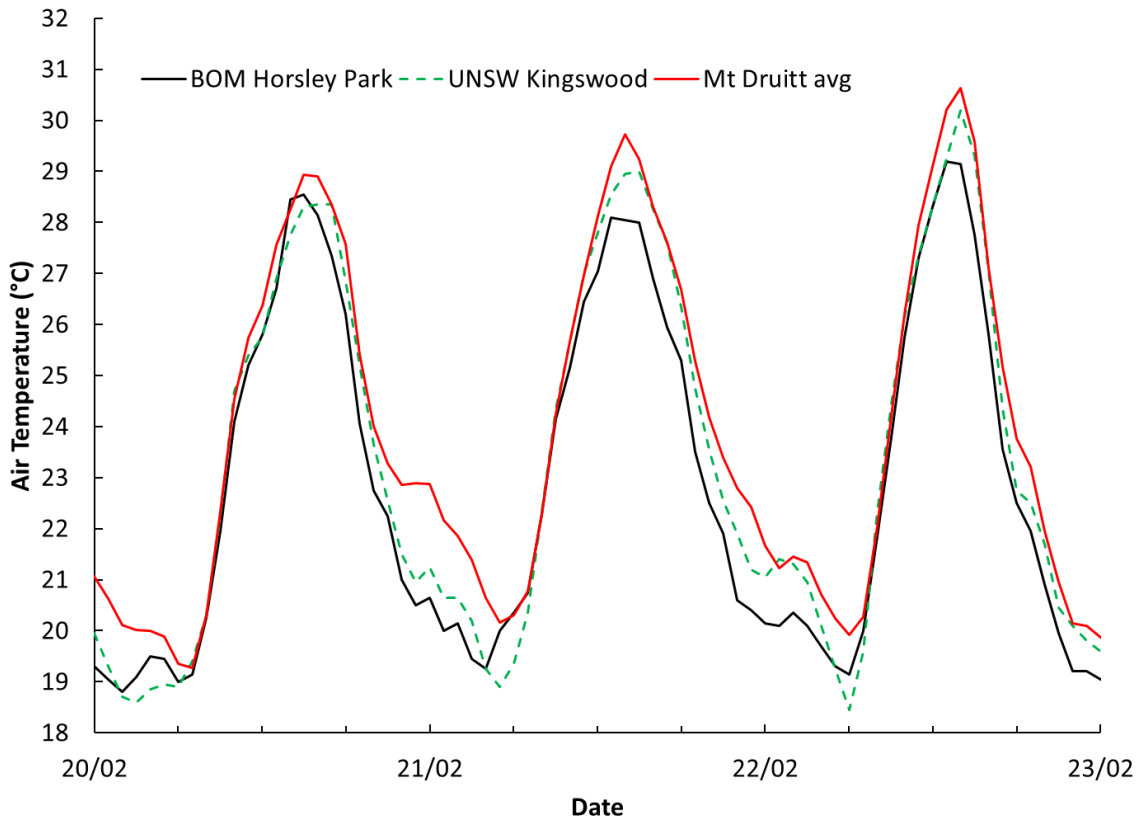


Figure 20. Ambient air temperature measured at Kingswood (UNSW station), Horsley Park (BOM station) and average of the temperature recordings in Mt Druiit.

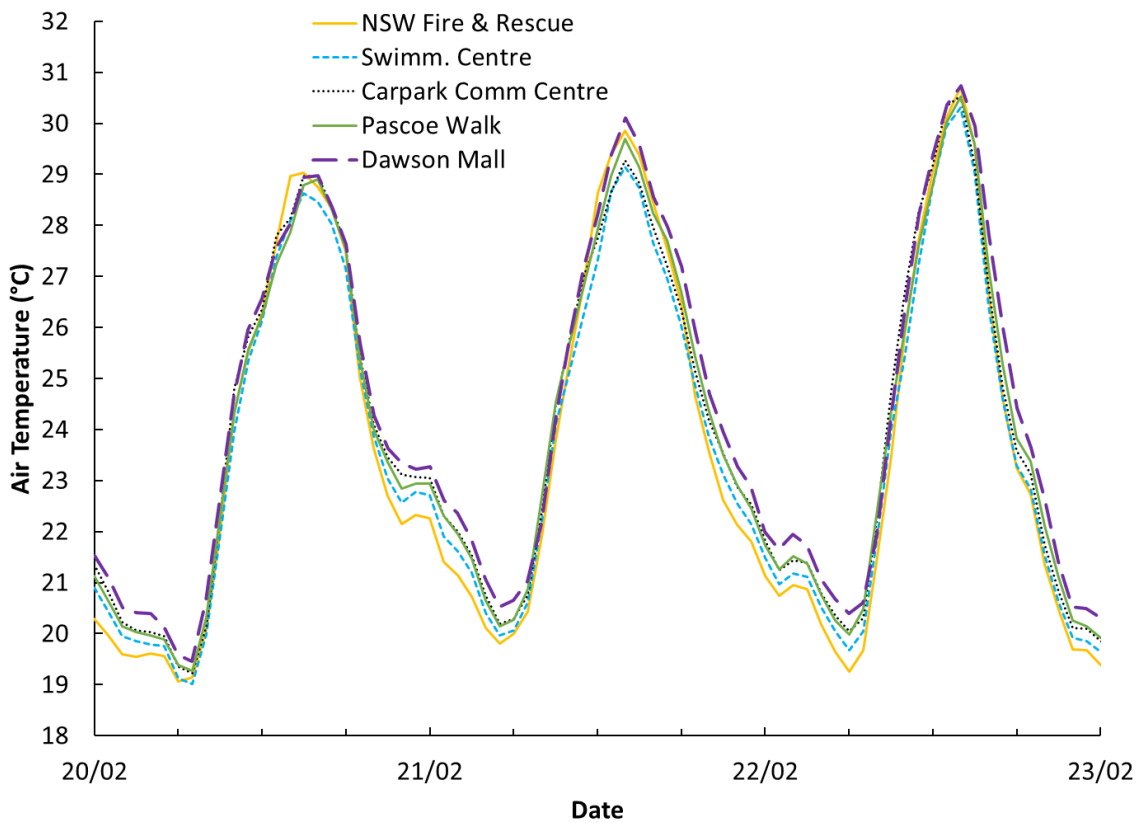


Figure 21. Ambient air temperature measured by the different sensors in Mt Druiit.

The site in Mt Druiit is also relatively more humid than Horsley Park or Kingswood, which is instead less common. In fact, typically, urban areas are drier than adjacent rural or otherwise non-urban areas [35]. This might be

explained by the presence of the creeks in the area of Mt Drutt or simply by the advective flows. Since the locations are at different ambient temperatures, the comparison must be carried out considering the absolute humidity (Figure 22) and not the relative humidity (Figure 23, displayed for the immediacy of representation).

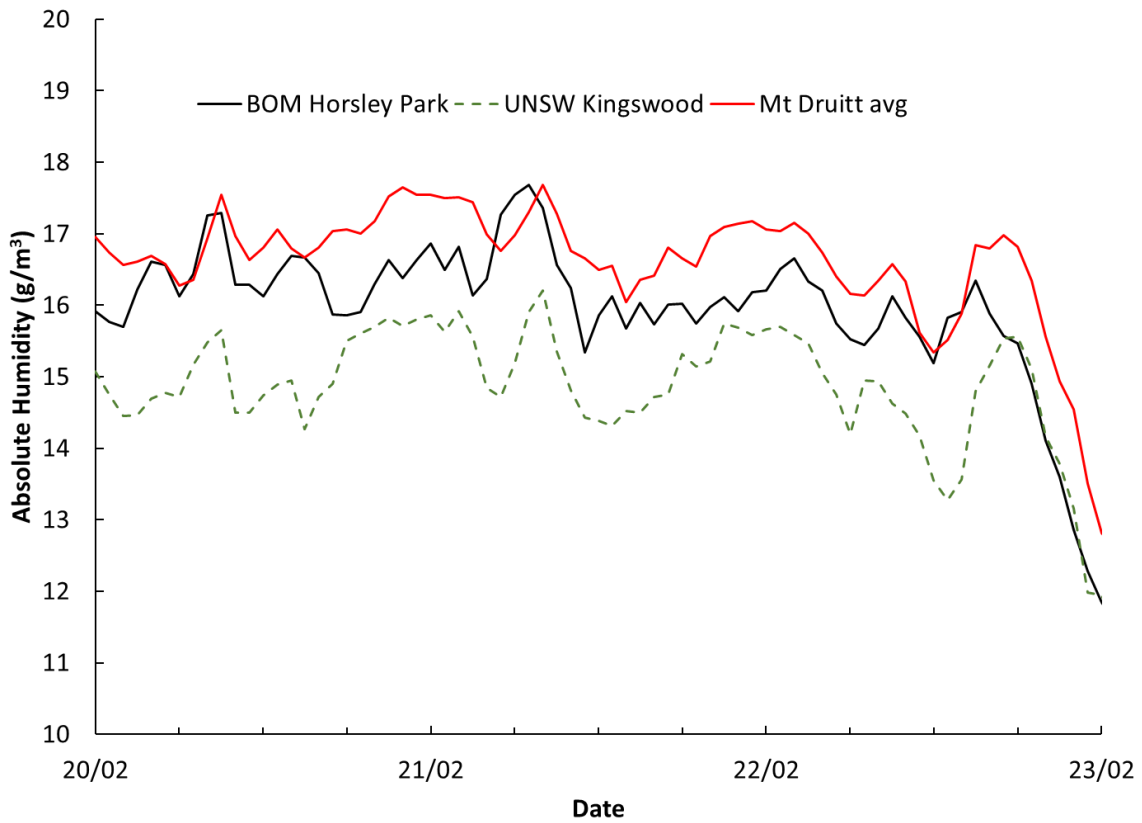


Figure 22. Absolute humidity measured at Kingswood (UNSW station), Horsley Park (BOM station) and average of the temperature recordings in Mt Drutt.

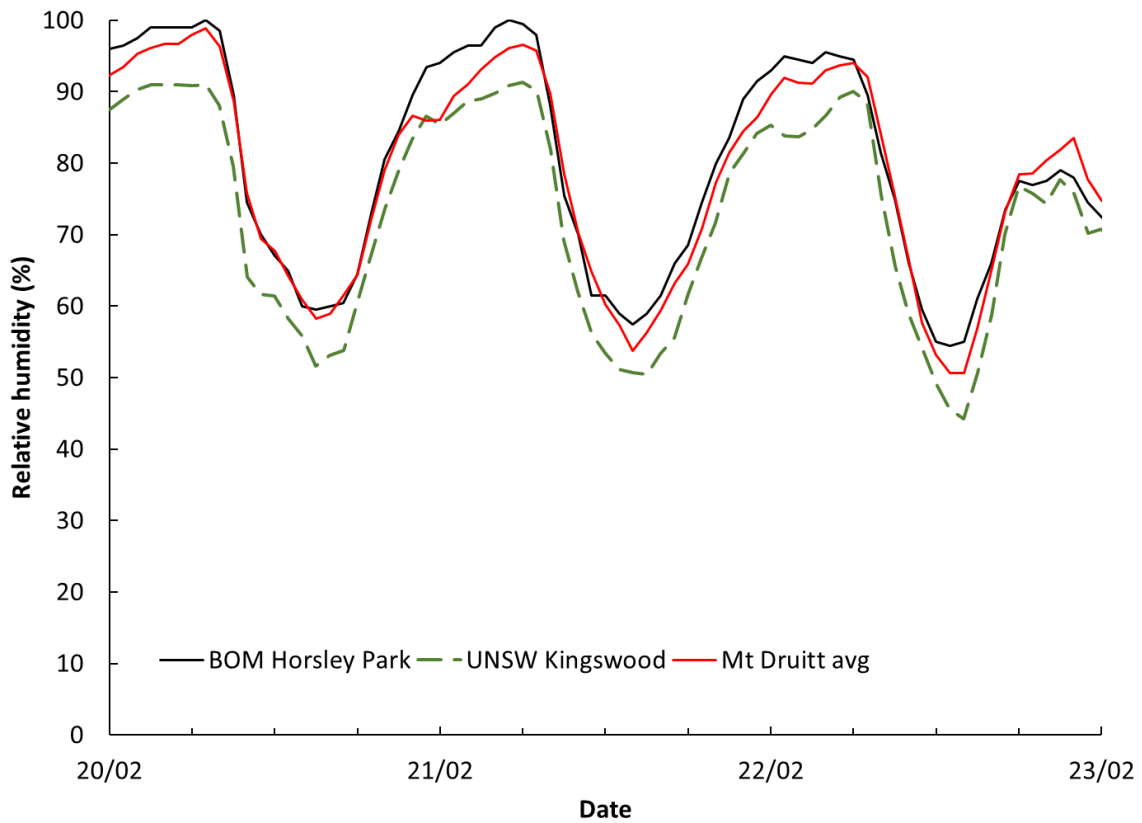


Figure 23. Relative humidity measured at Kingswood (UNSW station), Horsley Park (BOM station) and average of the temperature recordings in Mt Drutt.

5.2 Fieldwork

The fieldwork was completed on the first available date with clear sky following the period affected by a COVID-19 outbreak in Mt Druiitt. The EnergyBus was set up on-site on the morning of the 22nd of February 2021 with all the main activity performed during the central hours of the day.

5.2.1 Terrestrial and aerial survey

The conditions during the fieldwork day were measured within the area of interest with the EnergyBus, documenting a clear sky day with occasional passing clouds. Figure 24 shows the incoming shortwave radiation (solar) and incoming infrared radiation (thermal radiation from the sky). After 2.30 pm, with increasing wind speed and decreasing air pressure (Figure 25), and the campaign was concluded at 3 pm. Then, the sky became overcast, and the temperature started to drop. The figures present 5-min averages of all collected data (sampling each 15s). The results of the measurements performed with the carts are presented together with the simulation validation for the sake of conciseness. The wind speed measured by the EnergyBus at 10 m is approximately the same as the wind speed measured in Kingswood (synoptic station), with differences between the hourly averages not exceeding 0.3 m/s, while it is slightly higher at Horsley Park.

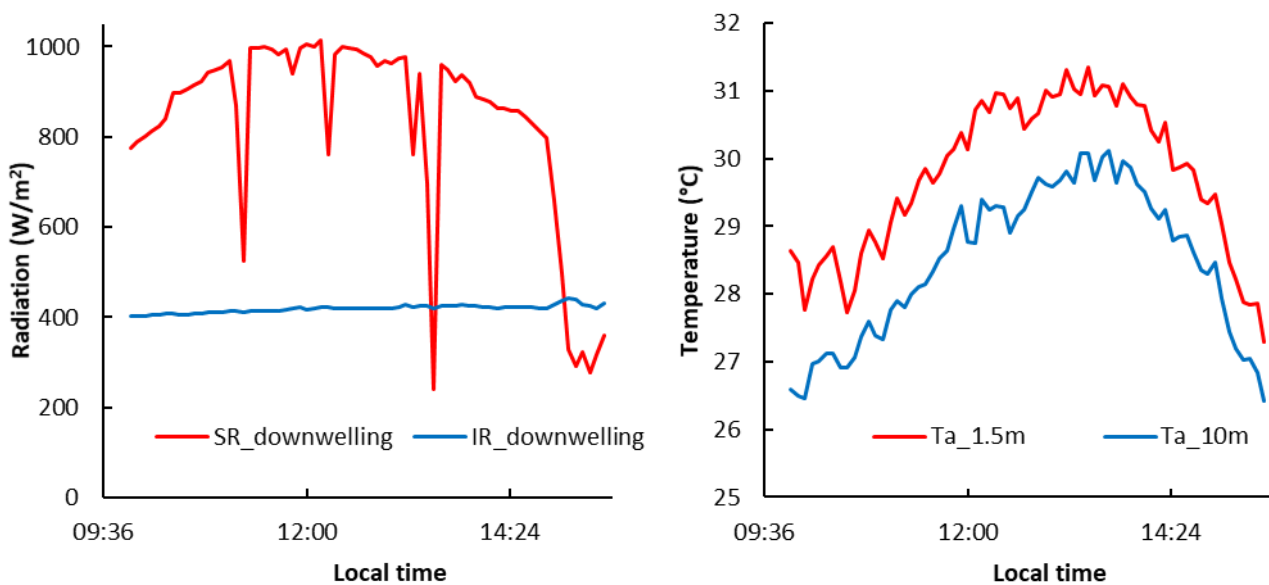


Figure 24. Incoming solar and infrared radiation measured by the Energy Bus, and temperature at 1.5 m and 10 m height.

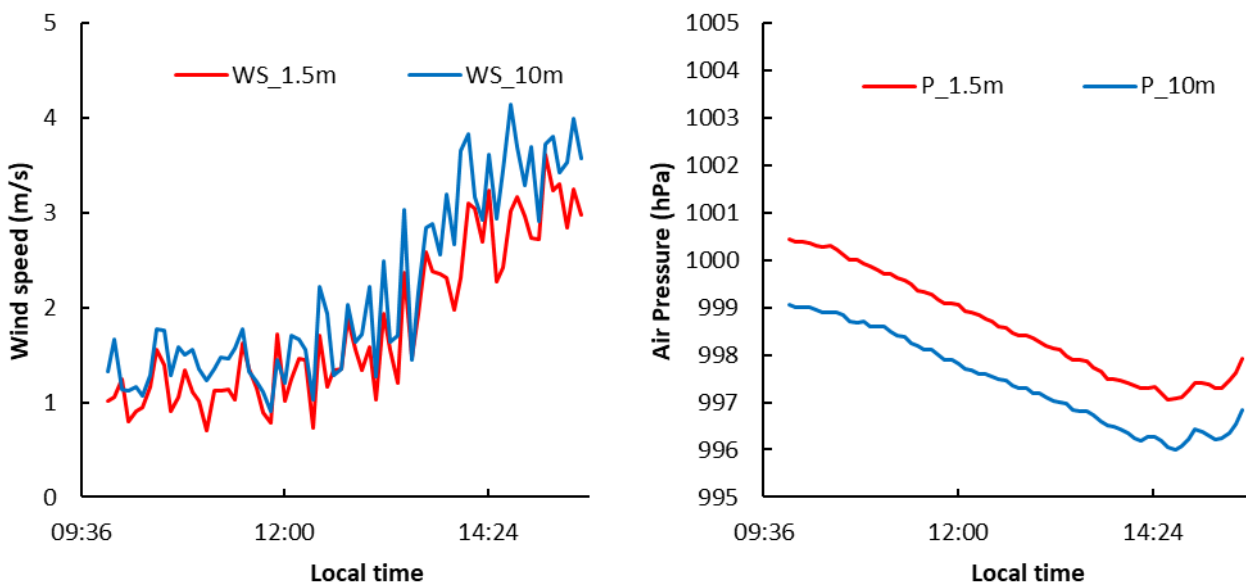


Figure 25. Incoming solar and infrared radiation measured by the Energy Bus, and temperature at 1.5 m and 10 m height.

Then, the aerial survey was completed with two flights covering the east and west portion of the area of interest, where a drone flight was permissible. The two portions have been later recomposed in a single orthophoto (Figure 26). The infrared aerial images display the darkest roofs achieving a surface temperature of almost 70 °C and street pavements having surface temperatures between 45 °C and 50 °C. The same values were measured with the handheld thermal camera taking pictures together with the cart measurements (Figure 27). However, the hottest surfaces at the pedestrian level are landscaping or dry grass (Figure 28), since they do not conduct heat through the ground as efficiently as a street pavement. The car parks with the newest asphalt (and therefore more absorptive) displayed surface temperature exceeding 55 °C (Figure 29).

The drone images in the visible range provided high resolution information for the microclimate model generation both concerning position and type of trees.

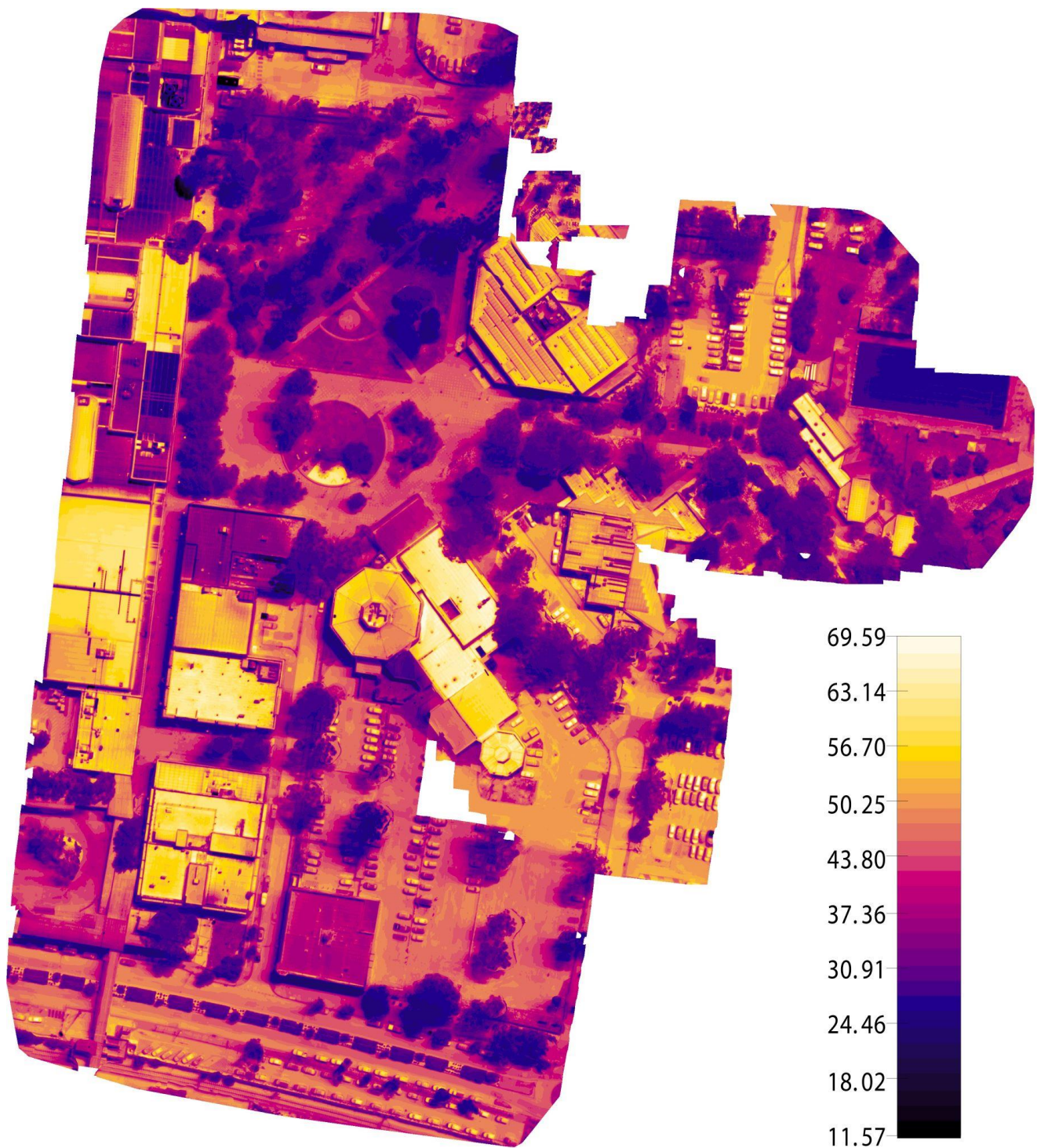


Figure 26. Orthophoto displaying the aerial infrared survey over Mt Druitt.



Figure 27. Infrared and visible images of Ayres Grove.

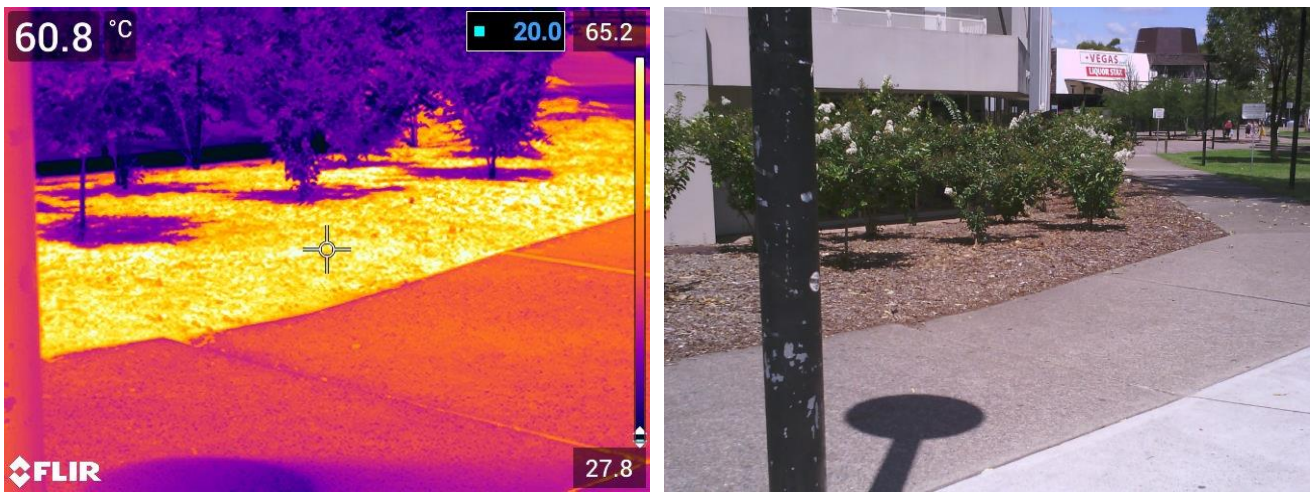


Figure 28. Infrared and visible images of landscaping at the entry of Pascoe Walk.



Figure 29. Infrared and visible images of a carpark behind the community centre.

5.2.2 Albedo measurements

The albedo measurements were performed on 1st March 2021 on a clear sky day, collecting data at 23 different locations identified with a previous inspection (Table 4). The measurements show the lowest solar reflectances measured for asphalt car parks, for which only 9% of sunlight gets reflected while the rest is absorbed. Also, some pedestrian areas and the pavers with a darker pattern on Dawson Mall display very low solar reflectance, not exceeding 10%. Cement concrete rooftop car park displayed an albedo of approximately 20-24%, instead. The collected values have been used as inputs for the microclimate simulation model.

Table 4. Albedo measurements.

<i>Point</i>	<i>Albedo</i>	<i>Location</i>	<i>Material description</i>
0	0.185	Ayres grove – sidewalk between swimming centre and car parking	Concrete sidewalk
1	0.176	Ayres grove cn Mount St – lower corner	Concrete sidewalk
2	0.192	Buran Cl	Light concrete pavement car park
3	0.089	Buran Cl – second parking lot	Asphalt concrete – dark-aged
4	0.098	Parking lot in front of Police Station – Kelly Cl cn Buran Cl	Asphalt concrete – aged
5	0.084	Westfield compound close to Rashays, car park	Asphalt concrete – aged
5_soil	0.173	soil patch along Kelly Cl, on the right of car park of #5	Ochre soil
6	0.123	Coles car park, Westfield compound (north of Pascoe Walk)	Asphalt concrete – aged and soiled with airborne ochre soil
6_soil	0.226	Soil patch along the car park	Ochre soil
7	0.098	Pedestrian walk connecting Buran Cl to Pascoe walk	Grey concrete and soil & grass in the background
8	0.095	Library car park, close to Hobo sensor #2	Asphalt concrete – dark-aged
9	0.308	entry to Pascoe walk	Light concrete pavement
10	0.212	Pascoe walk	Grass – green, irrigated and in good health
11	0.141	Dawson Mall	Pavers (lighter pattern where measurement taken)
11b	0.086	Dawson Mall in front of station #4	Pavers (dark and light pattern)
12	0.103	Dawson mall	Pavers (dark and light pattern)
13	NA	NA	NA
14	0.089	Vegas Hotel car park close to EnergyBus	Asphalt concrete – dark-aged
15	0.087	Centrelink car park	Asphalt concrete – dark-aged
15.2	0.109	In front of 55 North PDE	Cement concrete sidewalk pavement
16	0.190	Transport rooftop car park	Cement concrete
17	NA	NA	NA
18	NA	NA	NA
19	0.106	Car park next to Caltex (within Westfield compound). Very cloudy	Asphalt concrete – aged
20	0.100	assumed equal to #4-19	Asphalt concrete – aged
21	0.100	assumed equal to #4-19	Asphalt concrete – aged
22	0.242	assumed equal to #23	Cement concrete
23	0.242	Westfield roof top car park	Cement concrete

5.3 Microclimate simulation model validation

The model validation was performed considering the period of the fieldwork activity, which covers the central hours of the day of 22nd Feb 2021, by comparing the results of the simulations (Mod in the charts) with the observed quantities (Obs in the charts). The comparison has been performed between computed results and a range of different measurement techniques: air temperatures measured by the sensors installed on the light poles at 3.5 m (Figure 30), air temperature measurements performed with the carts at the 23 locations of data collection (Figure 31), and surface temperatures as measured by the drone with infrared thermography.

The differences between the measured and modelled air temperatures do not exceed 1 °C for most of the day, and started to increase after 2.30 pm. This can be ascribed to the difference between the constant wind speed of 2 m/s used as an input forcing the model, which produces an underestimation of the ambient temperature in the morning when the actual wind speed is in the range 1.1-1.5 m/s at Kingswood and at 10 m in Mt Druitt (Figure 25). Then, for the same reason, the simulations overestimate the ambient temperatures after 1 pm, when the measured wind speed exceeds 2 m/s, with increasing differences for increasing wind speed. As mentioned in the methods section, the wind speed was input as a constant due to a model limitation. Further, the model was unstable at lower wind speeds.

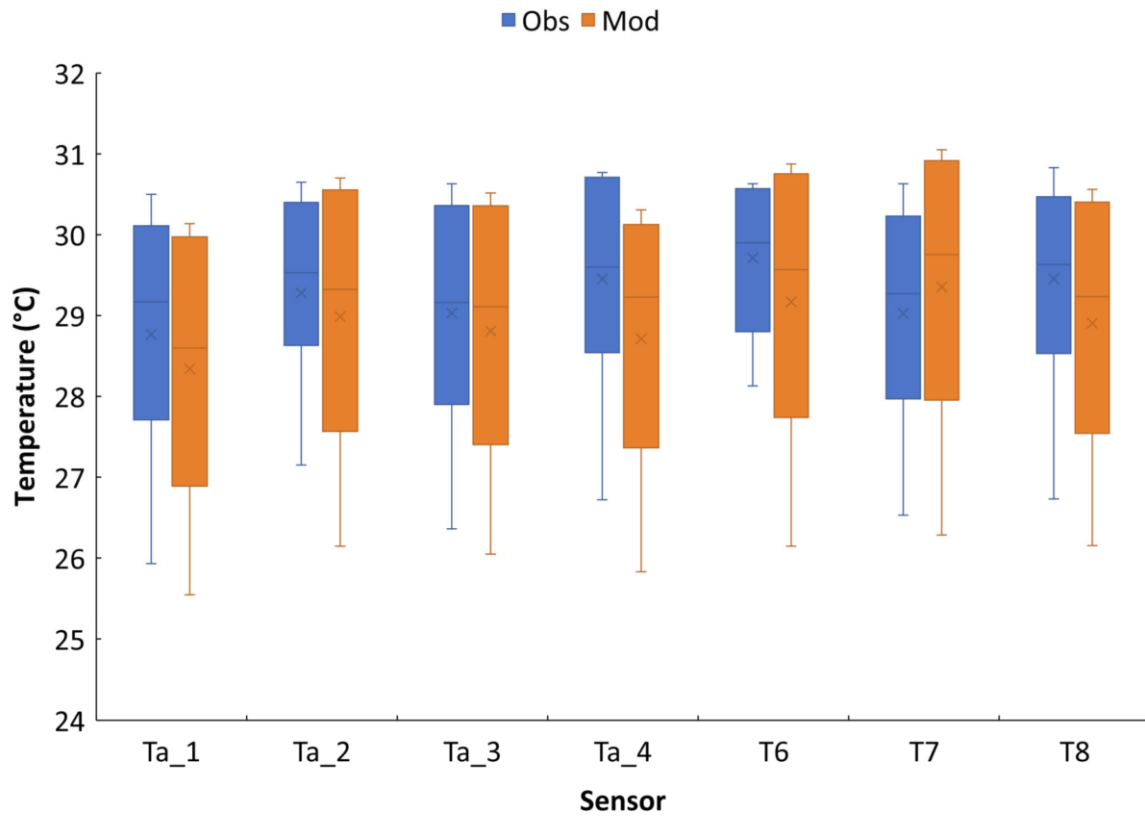


Figure 30. Boxplots showing a comparison between the measured (Obs) and simulated (Mod) air temperature at 3.5 m height for all the sensors installed on the light poles, for all hours of the campaign.

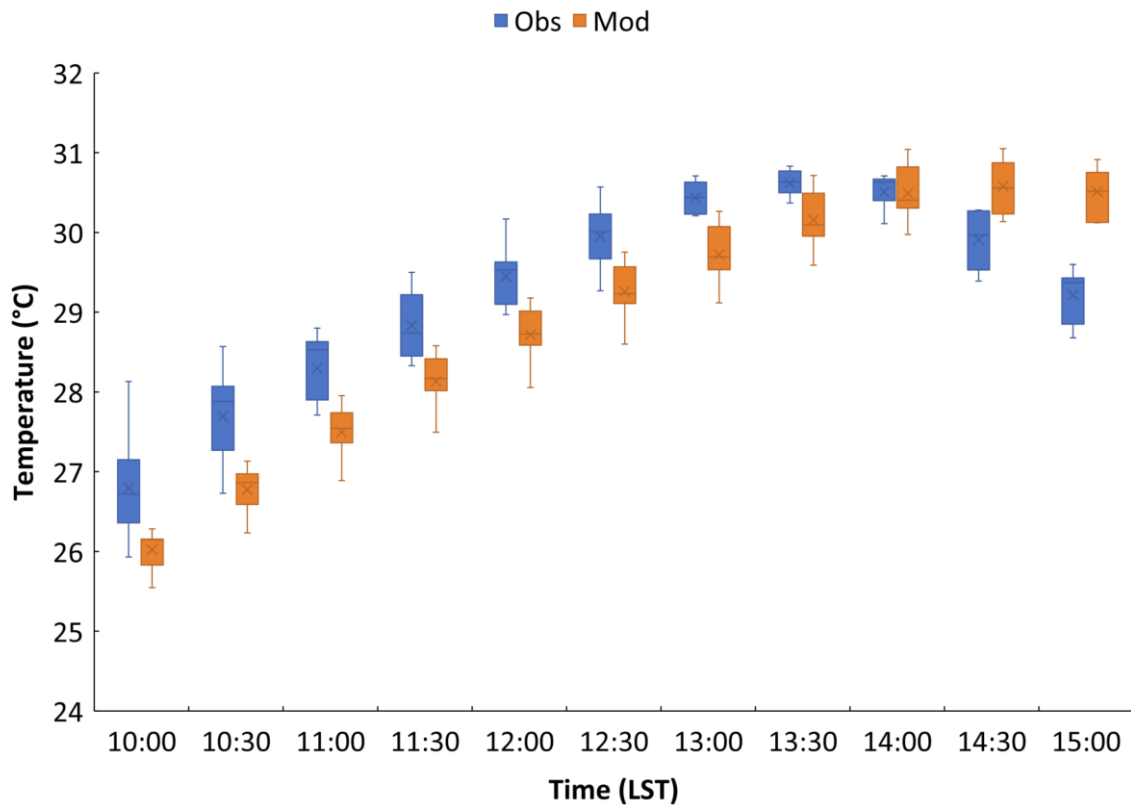


Figure 31. Boxplots showing a comparison between the measured (Obs) and simulated (Mod) air temperature at 1.4 m height for all the measurements performed by the carts at the different measurement points across the domain.

These differences between measured and modelled ambient temperatures are thus to be ascribed to the different wind speed, and they fall within the 1 °C deviation reported in the literature [7–9]. The comparison of the surface temperatures also shows a good agreement between measured and observed values, with car parks showing a surface temperature in the proximity of 45 °C as in the measurements, with variations depending on solar access and shading.

Therefore, we conclude that the model can represent the unmitigated scenario capturing all trends and spatial variability, with absolute differences Obs-Mod within 0.5-0.7 °C when the measured wind speed is 2 ± 0.5 m/s (Table 5). Some differences are unavoidable due to the uncertainty in the input of optical properties of roofs, foliage of trees and roughness of urban elements. Some of the differences at 1.4-1.5 m height can be ascribed to local conditions, with obstacles (e.g., parked cars or trees) leading to a different wind speed measured locally than the simulated one. The simulations, instead, overestimate the specific humidity by approximately 9% between 10.30 am and 1.30 pm, with a closer estimation after 2 pm. Therefore, further calibration would be required to use simulated humidity data.

Table 5. Observed values of air temperature (Tair) and wind speed (WS) at the EnergyBus location (at 1.5 m and 10 m) and quantities modelled in ENVI-met.

Time	Tair Obs 1.5 m (°C)	Tair Mod 1.5 m (°C)	Δ Tair (Obs – Mod) 1.5 m (°C)	Tair Obs 10 m (°C)	Tair Mod 10 m (°C)	Δ Tair (Obs – Mod) 10 m (°C)	WS Obs 10 m (m/s)	WS Kingswood (m/s)	WS Mod input (m/s)
10:30	28.31	28.01	0.30	26.93	26.23	0.70	1.26	1.15	2
11:00	28.44	28.98	-0.54	27.28	26.96	0.32	1.51	1.57	2
11:30	29.42	29.74	-0.32	27.95	27.58	0.37	1.48	1.64	2
12:00	30.02	30.41	-0.39	28.76	28.16	0.60	1.20	1.61	2
12:30	30.82	31.02	-0.20	29.15	28.72	0.43	1.69	1.84	2
13:00	30.75	31.56	-0.81	29.47	29.25	0.22	1.71	1.86	2
13:30	31.10	31.99	-0.89	29.84	29.69	0.15	1.93	1.92	2
14:00	30.96	32.2	-1.24	29.87	30.06	-0.19	2.72	1.90	2
14:30	30.28	32.33	-2.05	29.13	30.07	-0.94	3.36	3.39	2
15:00	29.50	32.14	-2.64	28.42	29.93	-1.51	3.53	3.75	2

5.4 Results of the mitigation scenarios

Once the model has been validated, the simulations were performed in the different scenarios previously discussed, and namely:

- Base case – unmitigated
- Unirrigated greenery – 10 unirrigated trees on Dawson Mall and 337 additional trees in other locations;
- Irrigated greenery – 10 passively irrigated trees on Dawson Mall and 337 additional trees in other locations;
- Cool materials – Albedo of roofs increased to 0.75 and albedo of car parks and pedestrian areas increased to 0.40;
- Combined – Combination of all the above mitigation strategies plus shading of car parks.

For all simulations, we extracted the results averaged for every grid cell of the domain, excluding the 30 m close to the boundary, which are typically not representative. Then, we computed the average of the ambient temperature at pedestrian height (1.4 m) over the entire domain.

The first hours of the simulation were discarded, as spin-up time, considering as valid the results after 6 am. The maximum reductions are achieved in the combined scenario and equal a peak air temperature reduction of 1.24 °C, followed by the cool materials scenario with a peak reduction of 1.17 °C, and then irrigated and unirrigated greenery scenarios with reductions of 0.76 °C and 0.71 °C, respectively (Figure 32 and Table 6). The maximum temperature reductions are computed at 5 and 6 pm, because heat mitigation technologies also delay and reduce heat absorption and storage in urban pavements, while without heat mitigation, absorbed and stored heat is then released by convection. These temperature reductions are in line with results previously achieved with heat mitigation on a small area [9,36], while peak air temperature reductions of 2.2-2.9 °C are possible only with a Sydney-wide application of heat mitigation [26,37], including the irrigation of greenery, which can be allowed by the synergy of green and blue infrastructure. Without the application of heat mitigation at the regional scale, an airflow of warm air decreases the mitigation potential, similarly to what happens when leaving the windows open with air conditioning in operation during a hot day. Greater ambient temperature reductions can be achieved with water misting [38] or other forms of evaporative cooling, which, however, increase the ambient humidity [39]. Water

misting also presents challenges in terms of maintenance and sanitation, and therefore it was not modelled in this study.

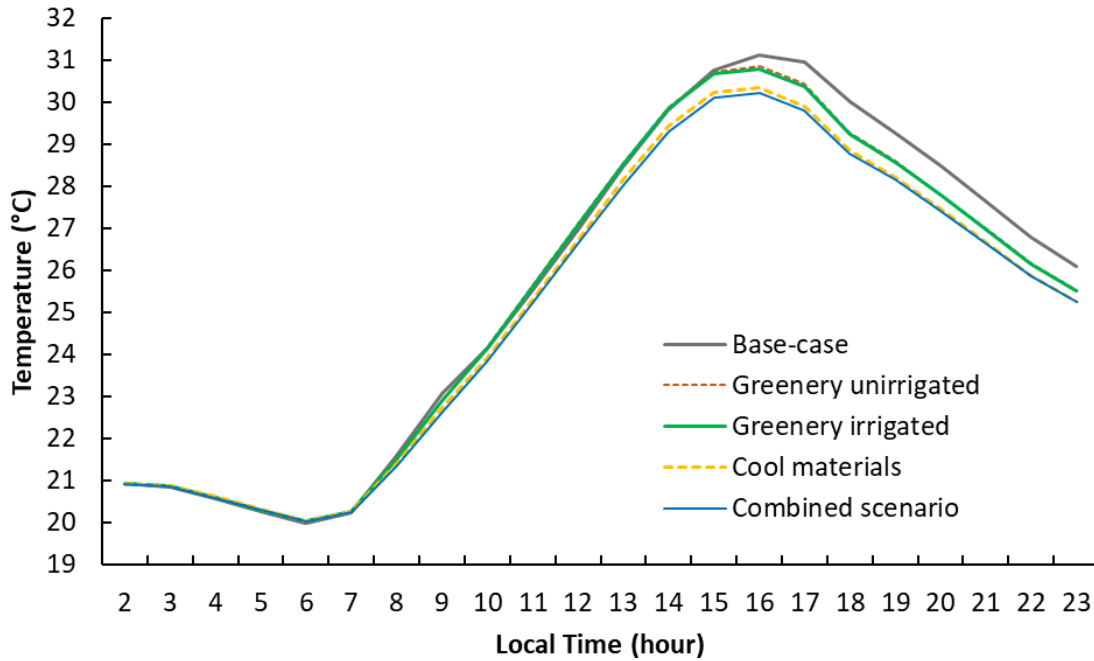


Figure 32. Hourly ambient temperature averaged over the whole simulation domain for the base case and heat mitigation scenarios. The first hours (before 6 am) are simulation spin up time.

Table 6. Ambient temperature in the base case (unmitigated) and temperature reduction in the mitigated scenarios at 1.4 m, averaged over the entire simulation domain (excluding the first 30 m along the boundary).

Time (hour)	Air temperature in the base case (°C)	Temperature reduction (base case – mitigation scenario) in °C			
		Greenery unirrigated	Greenery irrigated	Cool materials	Combined scenario
6	19.97	-0.06	-0.06	-0.07	-0.05
7	20.23	-0.04	-0.04	-0.02	0.00
8	21.58	0.08	0.08	0.19	0.24
9	23.07	0.16	0.17	0.35	0.43
10	24.15	-0.02	0.00	0.23	0.32
11	25.54	-0.09	-0.07	0.21	0.31
12	26.99	-0.12	-0.09	0.26	0.36
13	28.45	-0.11	-0.07	0.32	0.43
14	29.81	-0.07	-0.02	0.38	0.50
15	30.76	0.04	0.10	0.53	0.65
16	31.11	0.25	0.31	0.77	0.89
17	30.96	0.53	0.59	1.06	1.16
18	30.00	0.72	0.76	1.17	1.24
19	29.27	0.67	0.71	1.07	1.11
20	28.47	0.67	0.69	1.02	1.05
21	27.63	0.64	0.67	0.96	0.99
22	26.77	0.62	0.63	0.91	0.93
23	26.09	0.56	0.57	0.82	0.84

With the simulated hourly values of ambient temperature, we then computed the ratio of the mitigated to unmitigated temperature for each scenario (Table 7), which we used as a mitigation coefficient to correct the air temperature in the climate files for the building energy simulations and then for the assessment of electricity demand and heat related mortality.

While temperature reductions for the whole domain are in the range previously discussed (Table 6), even greater local temperature reductions are computed for the hotspots in Mt Druitt, such as Dawson Mall, the carparks between Dawson Mall and Centrelink, and the large carpark near the Westfield complex (Figure 32), even at 12

pm. Here we show the results at 12 pm for the base case and temperature differences between the base case and the mitigation scenarios, while the plots for all scenarios at 12 pm, 1 pm and 2 pm are offered in the Annex A.

Table 7. Mitigation coefficients computed in the different scenarios.

Period	Heat mitigation scenario			
	Greenery unirrigated	Greenery irrigated	Cool materials	Combined scenario
Morning (7-12)	1.0000	0.9995	0.9916	0.9886
Afternoon (13-16)	0.9992	0.9975	0.9836	0.9796
Evening (17-20)	0.9781	0.9768	0.9635	0.9616
Night (21-6)	0.9837	0.9833	0.9757	0.9749

More in detail, we computed peak reductions of 0.3 °C along Dawson Mall with the passively irrigated trees and 0.7-0.8 °C in the car parks behind the community centre or within the Westfield complex with cool materials and even 1.6 °C with the canopy shading the in the Westfield complex (Figures 33 and 34).

Dawson Mall proves particularly difficult to mitigate for two reasons: location and nature of the mitigation. Dawson Mall is located on the southern of the area of interest subject to mitigation, and it develops along a north-south axis. Consequently, Dawson Mall receives warm air from the south, from an unmitigated area. Moreover, trees or other alternative methods such as artificial canopies do improve human thermal comfort by reducing the solar radiation directly reaching people and by shading the street pavement and reducing the surface temperature, and along Dawson Mall, they can reduce the pavement temperature by more than 15 °C (Figure 35). However, both trees and canopies locally reduce the wind speed as determined with measurements in the field and wind tunnels [40], thus reducing the convective cooling. In this case, we computed a reduction in the wind speed from ~ 0.8 m/s (base case) to ~ 0.5 m/s along Dawson Mall (see Annex A). Cool materials along Dawson Mall deliver a reduction in surface temperature by 6-7 °C (the albedo increase is modest, to 0.40 for pavements to contain potential glare issues), so the two approaches are complementary.

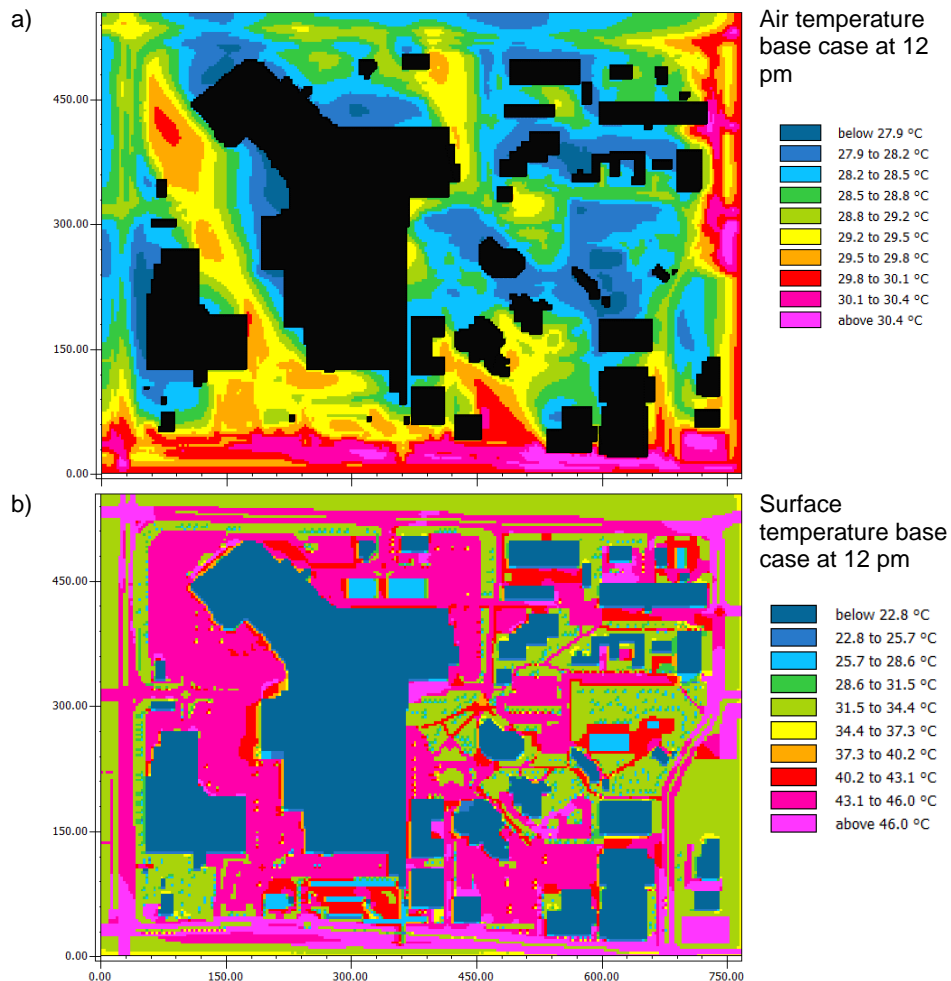


Figure 33. Air temperature (a) and surface temperature distribution (b) for the base case at 12 pm.

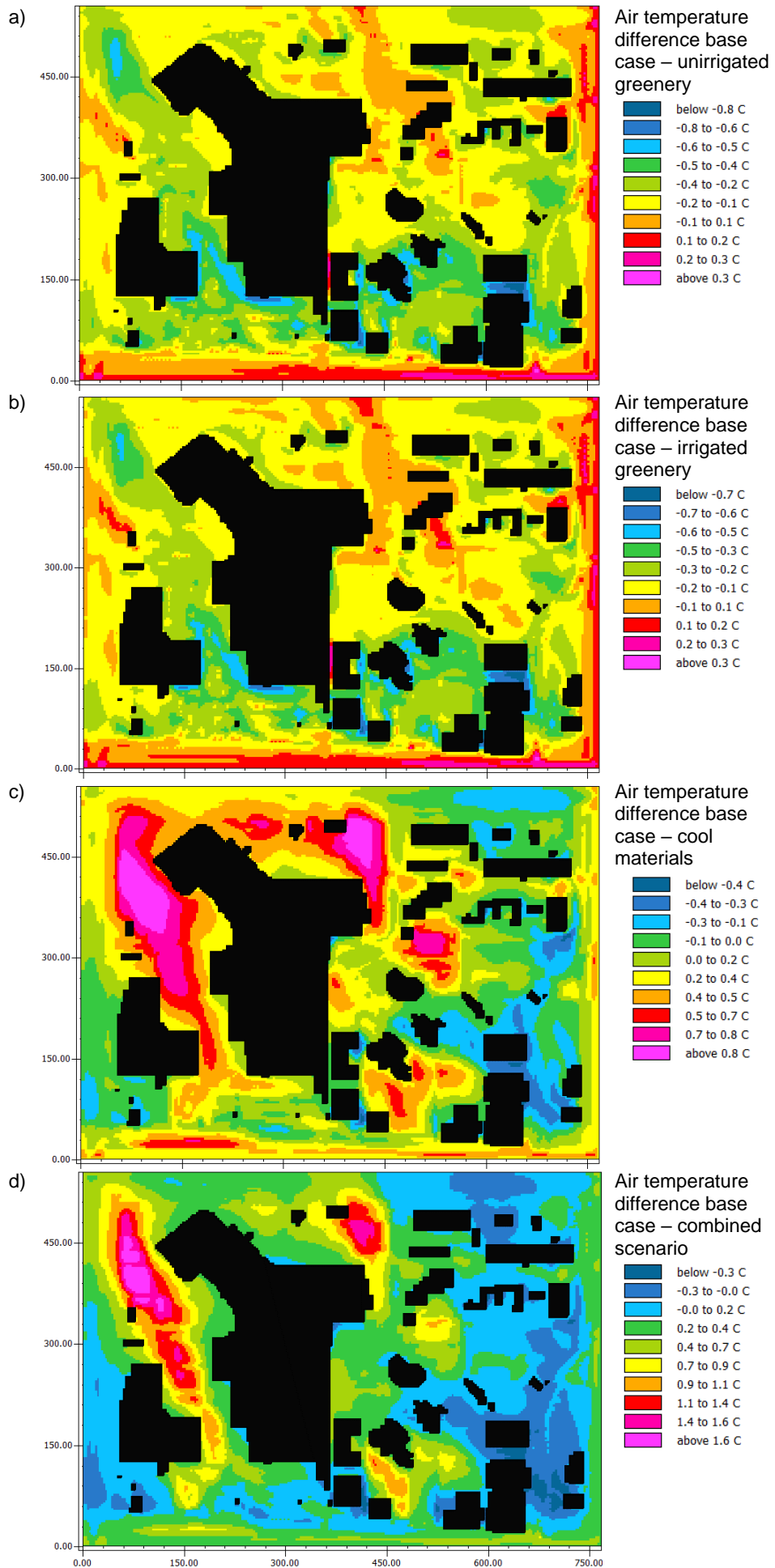


Figure 34. Air temperature reductions in the heat mitigation scenarios compared with the base case, at 12 pm.

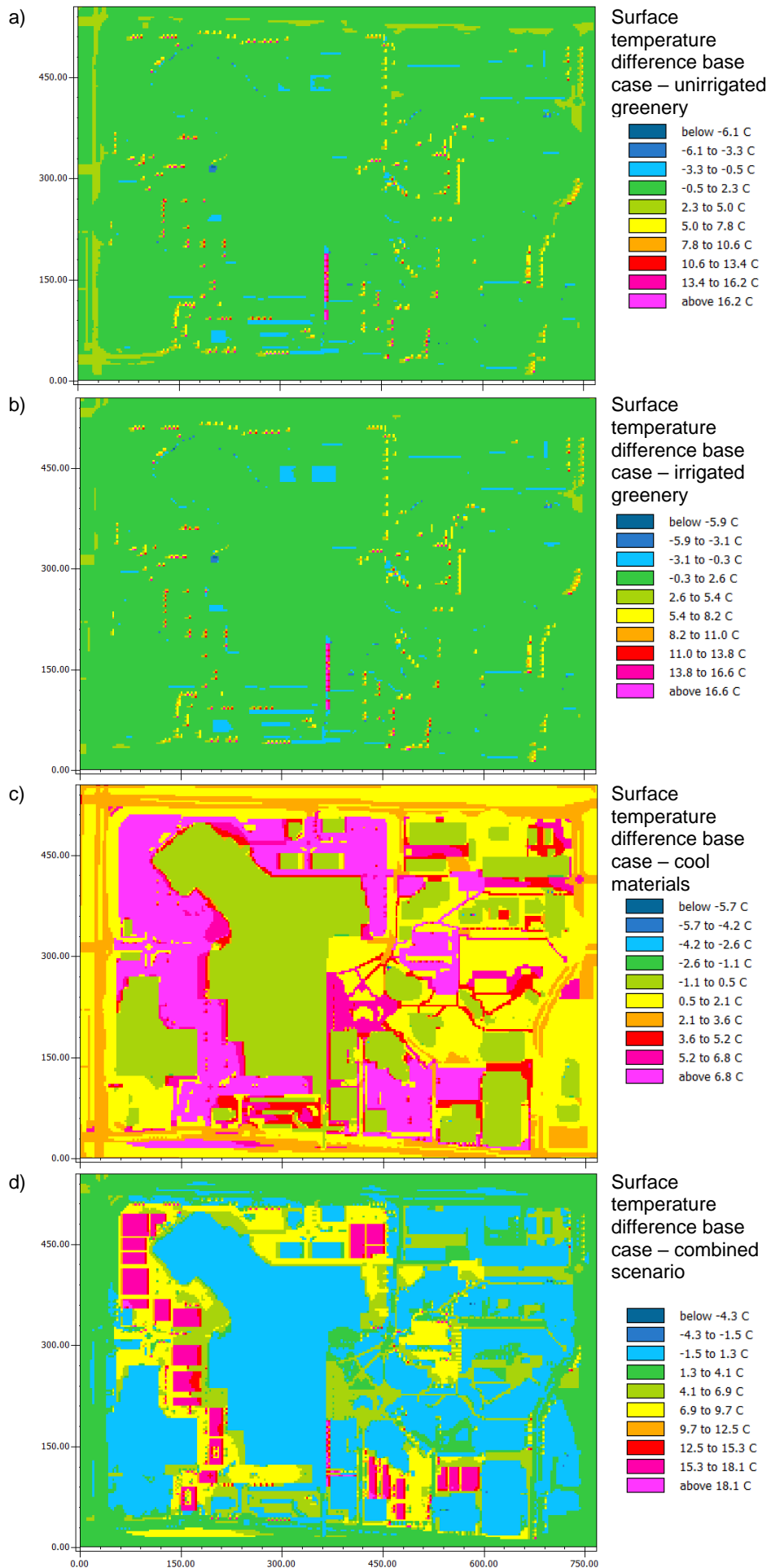


Figure 35. Surface temperature differences (base case minus mitigated scenario) in the heat mitigation scenarios, at 12 pm.

5.5 Results of Building Performance Simulations

The simulations of the selected buildings have been performed with weather data from Horsley Park, or Mt Druitt in the unmitigated scenario, or Mt Druitt in the combined mitigation scenario. In all cases, buildings have been modelled with a conventional roof with albedo 0.15 (even in the combined scenario, making the assumption that it's the only building in the area without a cool roof) or with a cool roof with albedo 0.75, in both cases with thermal emittance equal to 0.90 (for a metal roof it would be in the range 0.40-0.60 depending on ageing and coating [41]).

The absolute values of the cooling energy needs for all buildings are 20-40% higher in Mt Druitt (urban area) than at Horsley Park (equestrian centre, non-urban), depending on insulation level and internal heat loads, with relative differences that are consistent with the vast literature on building energy needs in urban areas vs adjacent non-urban areas [42]. This substantial difference against the temperature differences of 1.2 °C (on average) between the built environment of Mt Druitt (warmer) and the non-urban context of Horsley Park (cooler) is not surprising and is in line with the relevant literature [35,42]. In fact, even small and frequent trespasses of ambient temperature above the set point for cooling (i.e., the thermostat temperature above which the air conditioning system is activated) deliver cumulatively significant differences. Part of the increase in cooling energy needs, in this case, it is due to the higher humidity in Mt Druitt than at Horsley Park (normally urban areas are on average drier than non-urban areas [35], but this might be due to local conditions), causing higher latent heat loads.

The differences are smaller for buildings with high internal heat gains (i.e., heat released internally because of artificial lighting, high occupancy, cooking, or other human activities releasing heat) such as shopping malls, while the influence of the outdoor climate is maximum for buildings with low internal heat gains such as offices and residential buildings (Table 8).

Table 8. Cooling energy needs (cooling loads) in kWh/m² for the cooling period (15 Oct – 15 Apr) for the selected buildings in unmitigated and mitigated scenarios with a conventional roof or a cool roof.

Building (existing/new)	Stories	Roof insul.	Cooling energy needs (kWh/m ²)					
			Conventional roof (albedo = 0.15)			Cool roof (albedo = 0.75)		
			Horsley Park	MtDruitt Unmit	Mt Druitt Mit	Horsley Park	MtDruitt Unmit	Mt Druitt Mit
Office low rise (existing)	2	Low	45.3	58.0	53.7	36.7	48.2	44.3
Office low rise (new)	2	High	38.8	50.8	46.7	37.1	48.8	44.8
Shopping mall low-rise (existing)	2	Low	184.9	216.7	209.4	169.8	201.2	193.9
Shopping mall low-rise (new)	2	High	180.8	212.2	205.0	177.6	208.9	201.8
School (new)	3	High	53.9	74.5	68.9	52.0	72.3	66.7
Apartment low-rise (new)	3	High	27.9	39.5	34.7	26.0	37.2	32.5

A reflective roof can deliver cooling energy savings in all situations, with the greatest advantage for poorly insulated low-rise buildings (e.g., existing office buildings). Obviously, for a high-rise building, the roof has a strong influence on the heat balance of the last floor, and then it has a low impact on the thermal balance of the other floors (only indirectly on the penultimate floor). In this project, we compute cooling energy savings in the range between 1.5% (for a highly insulated shopping mall) and 18% for an uninsulated low-rise office building (Table 9), in all considered climate contexts (namely, out of the urban texture, and within Mt Druitt with or without heat mitigation). The computed savings are consistent with measured data presented in the literature on cool roofs savings [43,44].

While the insulation levels used for the new buildings are the Deemed to Satisfy provisions given by the National Construction Code (NCC 2019, Vol 1) for climate zone 6 (where Western Sydney is classified into), there is no rationale for high insulation levels for buildings with high internal heat gains in a hot climate. In fact, the NCC allows for the design of buildings with performance solutions while meeting the performance requirements expressed in the NCC, using one of the allowed verification methods. Therefore, even new buildings can be designed and constructed with lower and more appropriate insulation levels that allow for heat dissipation, when appropriate. In fact, a shopping mall with low roof insulation and a cool roof has cooling energy needs (201 kWh/m²) by approximately 4% lower than the same building with high roof insulation (209 kWh/m²), considering the unmitigated climate in Mt Druitt, for instance. For buildings with low internal heat gains (e.g., offices), the uninsulated and

insulated roof with a reflective coating have the same performance. In all cases, high insulation reduces the cooling energy needs only with a solar absorptive roof.

The most substantial cooling energy savings can be achieved with the combination of cool roofing and urban heat mitigation (i.e., unmitigated climate & conventional roof minus mitigated climate & cool roof), namely for building with a cool roof within an urban texture where all buildings have cool roofs and urban heat mitigation is implemented as in the most effective scenario (Table 10). In this case, cooling energy savings range between 10% and 23.7%, excluding the case of highly insulated shopping malls.

Table 9. Cooling energy savings (in terms of cooling loads) achievable with cool roofs expressed in relative terms (i.e., (conventional roof – cool roof)/conventional roof, expressed as %) or absolute (conventional minus cool roof, expressed in kWh/m²) for the cooling period (15 Oct – 15 Apr) for the selected buildings in unmitigated and mitigated scenarios with a conventional roof or a cool roof.

Cool roofs savings Building (existing/new)	Stories	Roof insul.	Relative (%)			Absolute (kWh/m ²)		
			Horsley Park	MtDruitt Unmit	Mt Druitt Mit	Horsley Park	MtDruitt Unmit	Mt Druitt Mit
Office low rise (existing)	2	Low	18.9%	17.0%	17.5%	8.5	9.8	9.4
Office low rise (new)	2	High	4.4%	3.9%	4.1%	1.7	2	1.9
Shopping mall low- rise (existing)	2	Low	8.1%	7.1%	7.4%	15.1	15.5	15.5
Shopping mall low- rise (new)	2	High	1.8%	1.5%	1.6%	3.2	3.3	3.2
School (new)	3	High	3.5%	2.9%	3.1%	1.9	2.2	2.2
Apartment low-rise (new)	3	High	6.9%	5.8%	6.4%	1.9	2.3	2.2

Table 10. Cooling energy savings (in terms of cooling loads) achievable with urban heat mitigation with a conventional roof (i.e., unmitigated minus mitigated climate with a conventional roof), a cool roof (i.e., unmitigated minus mitigated climate with a cool roof), or the combination of cool roof and heat mitigation (unmitigated climate & conventional roof minus mitigated climate & cool roof) for the cooling period (15 Oct – 15 Apr).

Mitigation savings Building (existing/new)	Stories	Roof insul.	Relative (%)			Absolute (kWh/m ²)		
			Mitig. (conv. Roof)	Mitig. (cool roof)	Cool roof & mitig.	Mitig. (conv. Roof)	Mitig. (cool roof)	Cool roof & mitig.
Office low rise (existing)	2	Low	7.5%	8.1%	23.7%	4.3	3.9	13.7
Office low rise (new)	2	High	8.2%	8.3%	11.9%	4.1	4.0	6.0
Shopping mall low- rise (existing)	2	Low	3.4%	3.6%	10.5%	7.3	7.3	22.7
Shopping mall low- rise (new)	2	High	3.4%	3.4%	4.9%	7.2	7.2	10.4
School (new)	3	High	7.5%	7.7%	10.4%	5.6	5.6	7.8
Apartment low-rise (new)	3	High	12.0%	12.5%	17.6%	4.7	4.7	6.9

5.6 Influence of microclimate on electricity demand

To compute the electricity demand per capita for all uses in the climate conditions of Mt Druitt, we first considered the semi-hourly temperature data from the BOM station in Horsley Park for the period 2000-2020. Then, we computed the semi-hourly temperature using the relation between the measured data in Mt Druitt and the observations in Horsley Park (Figure 19), and finally, we computed the temperature in the combined mitigation scenario with the mitigation coefficients (Table 7), as discussed in the methods section. In this case, we considered only the warm-hot period, from November to March, when air conditioning is in operation in commercial buildings.

By applying the electricity demand model developed with the period 2013-2017, we can study the electricity demand from 2000 to 2020 with climate as the only variable (i.e., as if there were the same number of buildings,

with the efficiency and same energy use patterns). Therefore, we see that over the last 21 years, the electricity demand has been constantly increasing due to the increase in ambient temperature (Table 7), which is the only variable in this case, as the electricity demand is modelled as a function of temperature and extra-terrestrial solar radiation, as presented in the methods section.

Obviously, there are fluctuations year by year due to interannual variability (e.g., hot and dry summer, followed by a rainy summer). However, the increasing trend is clear, and it is equal to approximately 0.2% per year, or 4% in 20 years, only due to the local climate change. Then, the computed per capita electricity demand is approximately 3% higher in Mt Druitt than at the non-urban location of Horsley Park. The best heat mitigation scenario (combined scenario) can then deliver a reduction in per capita electricity demand of 0.06 MWh or 1.5% of the unmitigated demand in Mt Druitt during the warm-hot months (Table 7). This might appear to be a small reduction, but the electricity demand here considered includes all uses in NSW, and it is not limited to building thermal uses (i.e., heating, ventilation and air conditioning). Thus, transport (e.g. trains and lifts), artificial lighting, cooking and industrial uses are included.

The yearly per capita electricity demand in NSW is approximately 8.5 MWh with a total annual in the state equal to 69.8 TWh in 2019-2020 (based on figures from the Australia Energy Regulator), with a steady decrease since 2005 due to increased energy efficiency, penetration of renewable energy and change in final uses. While the breakdown of energy consumption by sector is known, data by sector and energy source (i.e., electricity, fuel, natural gas, etc.) are not available; thus, only a bottom-up approach can be used to estimate an approximate relative weight. Over the course of the year, the electricity demand is minimum when the air temperature is of 18 °C (when the electricity demand in NSW is approximately 10.5 GW), which can offer an appraisal of the peak daily load in the intermediate season, while the absolute peak load is of approximately 14 GW, and the absolute base load (nighttime in the intermediate season) is of approximately 5.5 GW. Unfortunately, it is not possible to separate air conditioning uses from other uses in energy utility data. However, this offers an appraisal of the relevance of the weight of the non-thermal uses on the cumulative demand.

Table 11. Per capita electricity demand in MWh over the hot season (from November to March).

Year	Horsley Park (MWh)	Mt Druitt unmitigated (MWh)	Mt Druitt mitigated combined (MWh)	Unmitigated – Mitigated (MWh)	Unmitigated - Mitigated (%)
2000	3.59	3.69	3.63	0.06	1.7%
2001	3.75	3.86	3.81	0.06	1.5%
2002	3.73	3.84	3.78	0.06	1.5%
2003	3.73	3.84	3.78	0.06	1.5%
2004	3.78	3.89	3.83	0.06	1.5%
2005	3.75	3.86	3.80	0.06	1.5%
2006	3.78	3.89	3.83	0.06	1.5%
2007	3.73	3.84	3.78	0.06	1.5%
2008	3.64	3.74	3.69	0.05	1.3%
2009	3.85	3.96	3.90	0.06	1.6%
2010	3.78	3.90	3.84	0.06	1.5%
2011	3.77	3.88	3.82	0.06	1.5%
2012	3.67	3.77	3.71	0.05	1.4%
2013	3.77	3.89	3.83	0.06	1.5%
2014	3.76	3.87	3.82	0.06	1.5%
2015	3.77	3.89	3.83	0.06	1.5%
2016	3.86	3.98	3.91	0.06	1.6%
2017	3.93	4.06	3.99	0.07	1.7%
2018	3.85	3.97	3.91	0.06	1.6%
2019	3.91	4.03	3.97	0.07	1.7%
2020	3.78	3.90	3.84	0.06	1.5%
<i>Average</i>	<i>3.77</i>	<i>3.88</i>	<i>3.82</i>	<i>0.06</i>	<i>1.5%</i>

5.7 Influence of microclimate on the risk of heat-related mortality

The risk of heat-related mortality has been computed with the selected model (developed with Sydney-wide epidemiological data [20,45]) using temperature data from Horsley Park or Mt Druitt in the unmitigated scenario, or Mt Druitt in the combined mitigation scenario (Figure 36). As discussed in the methods section, here we use this regression only as a risk estimation, while an appropriate appraisal of the heat-related mortality in Mt Druitt would require local epidemiological data. Moreover, the statistical information at the suburb scale might be affected by considerable uncertainty.

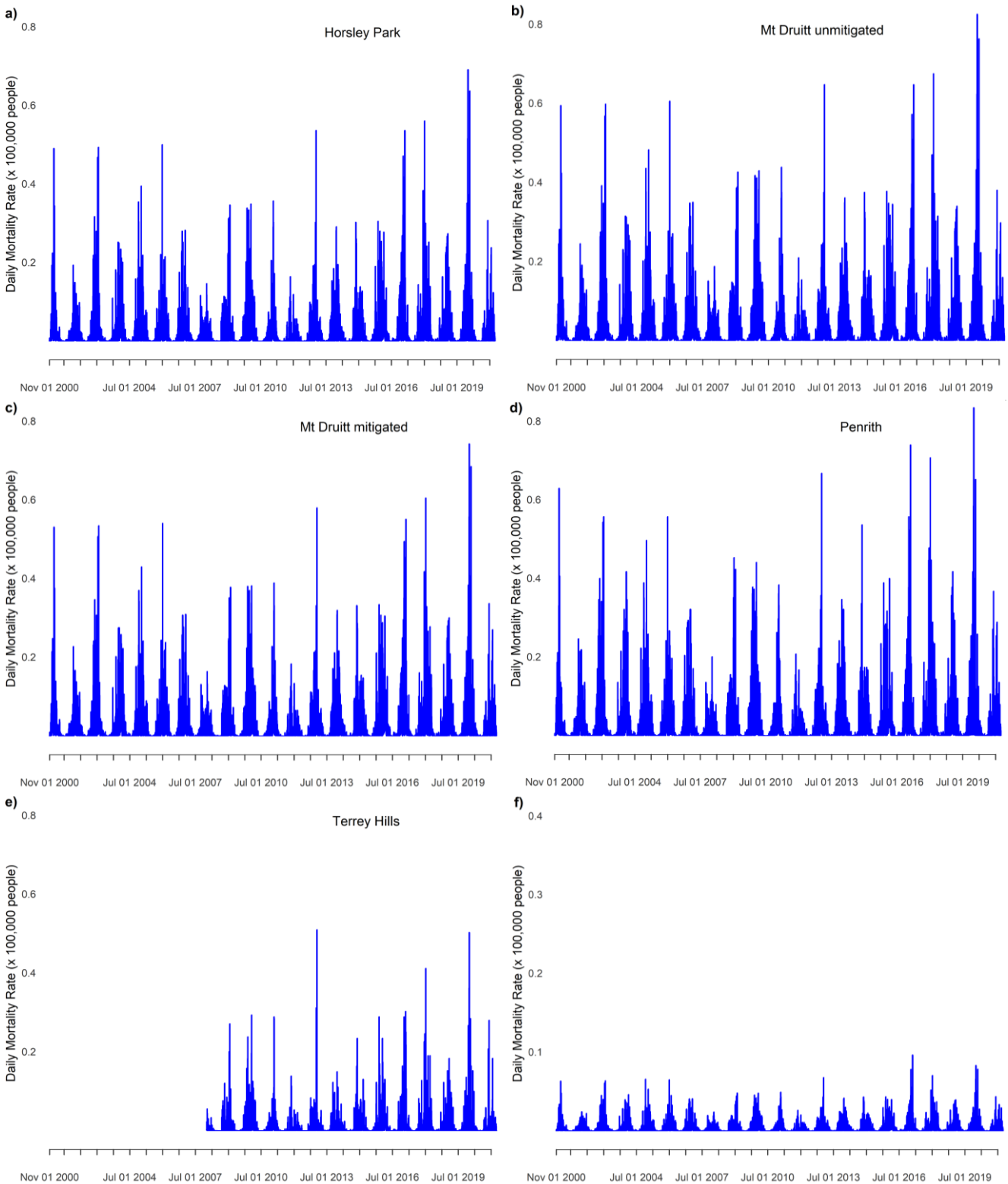


Figure 36. Daily heat-related mortality rate computed as a function of daily maximum ambient temperature (no temperature data are available before 2008 in Terrey Hills).

Here, we show that the computed daily mortality rate risk is considerably higher in the unmitigated scenario in Mt Druitt than in Horsley Park, and it approaches the values computed for Penrith, where the computed daily mortality per 100,000 people is greater by ~ 0.3 than in Terrey Hills (Northern Beaches). The peak values are computed for hot spells when the daily maximum temperature reaches its peak. Heat mitigation can reduce the peak daily mortality rate risk by approximately 0.09 deaths per 100,000 people (Figure 36 f). Considering a long period, we observe that the risk increased in recent years with the increased frequency of extremely high ambient temperatures. However, to appraise the patterns and seasonal dynamics, it is easier to focus on a single summer, such as 2016-2017 (Figure 37).

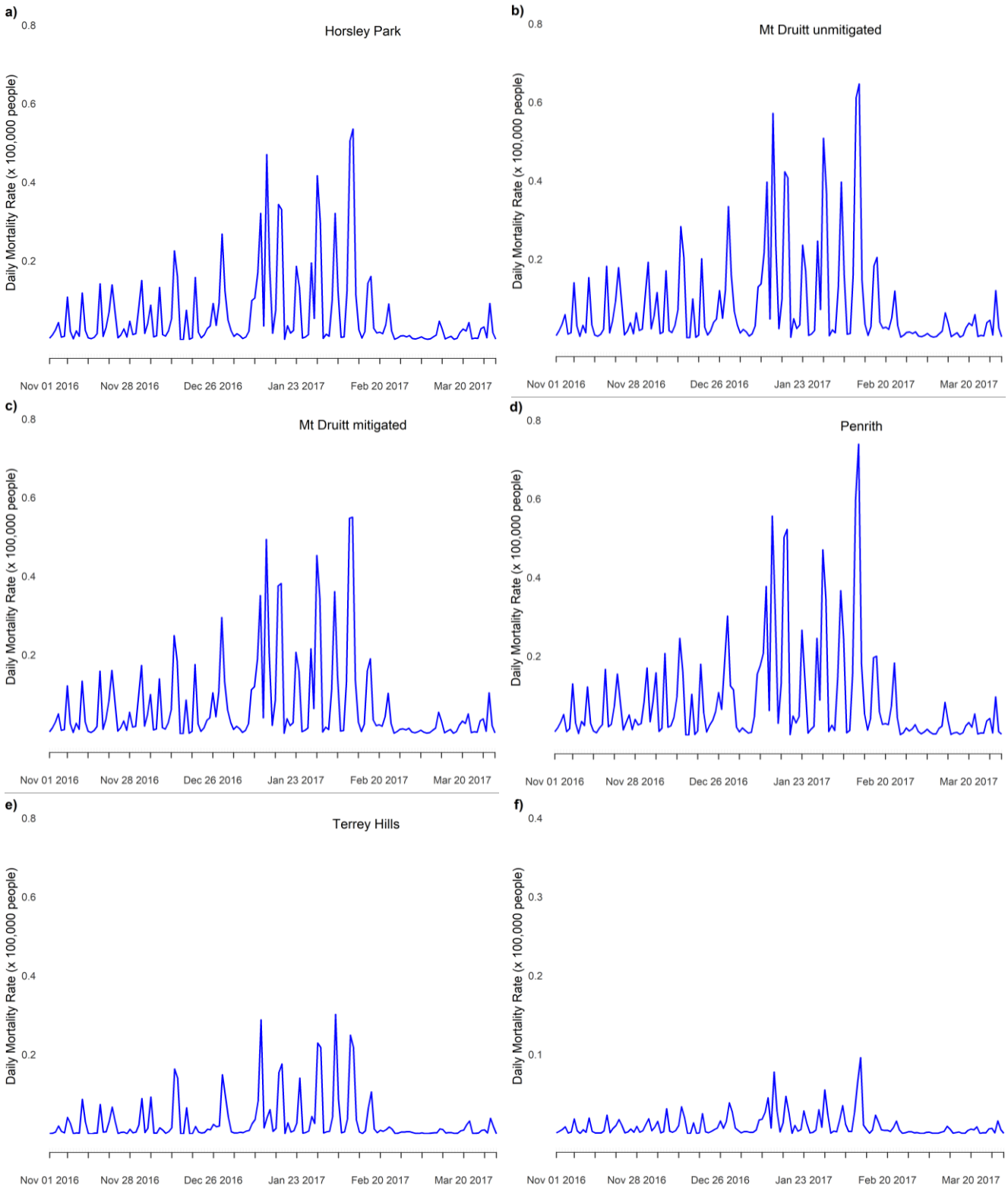


Figure 37. Daily heat-related mortality rate computed as a function of daily maximum ambient temperature for the period November 2016 – March 2017.

In this case, we can note that the risk of heat-related mortality starts to manifest already in November, and while in coastal suburbs such as the Northern Beaches council area (where Terrey Hills is located) are exposed to negligible risk after the first half of February, the risk is greatly reduced but still not negligible in Mt Druitt and Penrith.

Since the relation between daily maximum ambient temperature and heat-related mortality is exponential, even modest reductions in heat exposure can deliver a reduction in the heat-related mortality risk. As stated in the methods section and here discussed, the results presented are an estimation of the risk based on a correlation between daily maximum temperature and Sydney-wide heat-related mortality. A complete epidemiologic analysis with data from Mt Druitt and suburbs in the proximity would offer further insight since the socio-economic context in Mt Druitt presents peculiarities with respect to the average of the Greater Sydney area.

6. Conclusions and Recommendations

Climate change and urbanization are causing an increase in ambient temperature across Greater Sydney, with the strongest effects felt in Western Sydney. Heatwaves are becoming more frequent and intense, and the period interested by hot spell is lasting longer every year.

Here, we analysed the local climate in the suburb of Mount Druitt, which is a socio-economically disadvantaged area, with a special focus on Dawson Mall, a popular open-air shopping mall, which will be interested by an urban revitalisation project supported by Blacktown City Council.

To determine the most effective interventions for reducing ambient temperatures, improving thermal comfort and reducing the cooling energy needs in buildings, we first characterised the local climate in Mt Druitt. We mapped the hot spot in the area, established a network of temperature and humidity sensors which collected data for more than one year, and performed a fieldwork campaign on a clear sky day, with air temperature, humidity, and wind speed measurements at 23 locations, accompanied by a drone flight measuring the surface temperatures, and albedo measurements of street pavements.

The long-term measurements show that the average of the air temperatures measured in Mt Druitt in peak conditions is 1.2-1.7 °C hotter than the values recorded at the Bureau of Meteorology's station in Horsley Park, which is approximately 10 km south of Mt Druitt, in a non-urban area at the same distance from the coast. This is an expected difference in the ambient temperature between an urban and non-urban adjacent area.

The drone-taken infrared images have shown that several car parks reached surface temperatures exceeding 55 °C, where the albedo is 9%, while cement concrete rooftop car parks displayed an albedo of approximately 20-24%, instead.

Upon consultation with Blacktown City Council and the design team, with the measured data, we calibrated a microclimate model to assess five design scenarios:

- Base case – unmitigated
- Unirrigated greenery – 10 unirrigated trees on Dawson Mall and 337 additional trees in other locations
- Irrigated greenery – 10 passively irrigated trees on Dawson Mall and 337 additional trees in other locations
- Cool materials – Albedo of roofs increased to 0.75 and albedo of car parks and pedestrian areas increased to 0.40
- Combined – Combination of all the above mitigation strategies plus shading of car parks.

The maximum reductions are achieved in the combined scenario and equal a peak air temperature reduction of 1.24 °C, followed by the cool materials scenario with a peak reduction of 1.17 °C, and then irrigated and unirrigated greenery scenarios with reductions of 0.76 °C and 0.71 °C.

These temperature reductions are in line with results previously achieved with heat mitigation on a small area, while peak air temperature reductions of 2.2-2.9 °C are possible only with a Sydney-wide application of heat mitigation, including the irrigation of greenery, which can be allowed by the synergy of green and blue infrastructure.

Trees or other alternative methods such as artificial canopies do improve human thermal comfort by reducing the solar radiation directly reaching people and by shading the street pavement, thus reducing its surface temperature. Along Dawson Mall, trees can reduce the pavement temperature by more than 15 °C.

Then, with data from Horsley Park, and in the unmitigated and mitigated combined scenario in Mt Druitt, we modelled poorly insulated and insulated buildings of different types: low-rise office, low-rise shopping mall, a school, and an apartment building.

The cooling energy needs for all simulated buildings is 20-40% higher in Mt Druitt (urban area) than at Horsley Park (equestrian centre, non-urban), depending on insulation level and internal heat loads, with relative differences that are consistent with the vast literature on building energy needs in urban areas. This documents an energy penalty for all urban buildings in Mt Druitt.

The differences are smaller for buildings with high internal heat gains (i.e., heat released internally because of artificial lighting, high occupancy, cooking, or other human activities releasing heat) such as shopping malls, while the influence of the outdoor climate is maximum for buildings with low internal heat gains such as offices and residential buildings (Table 8).

A reflective roof (albedo = 0.75) instead of a conventional roof (albedo = 0.15) can deliver cooling energy savings in all situations, with the greatest advantage for poorly insulated low-rise buildings (e.g., existing office buildings). Here, we computed cooling energy savings up to 18% for an uninsulated low-rise office building. High roof insulation (as per current building code levels) of a shopping mall was not beneficial, instead, because it reduces heat dissipation, and a shopping mall modelled with a cool roof without insulation had cooling energy needs by 4% lower than with high roof insulation.

Cooling energy savings in the range between 10% and 24% can be achieved with the combination of cool roofing and urban heat mitigation. The electricity demand over the hot period (November-March) for all uses can be reduced by 1.5% with urban heat mitigation. It is to be noted that the modelled electricity demand includes transport and all other uses. Finally, heat mitigation can reduce the risk of heat-related mortality, which still remains high in Western Sydney, and significantly higher than in coastal suburbs.

The project findings lead to the following recommendations:

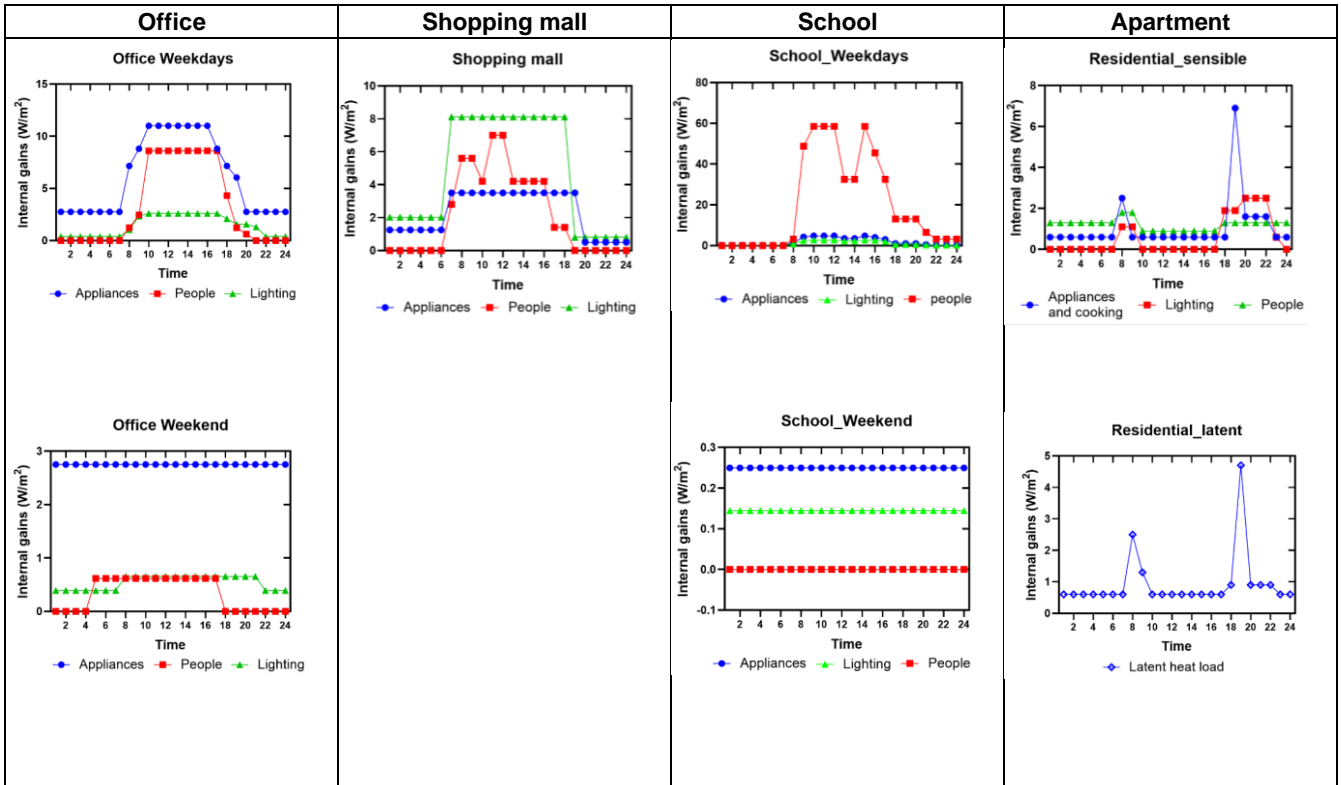
- Heat mitigation should be implemented in the most comprehensive way, with a combination of heat mitigation technologies, as in the combined scenario.
- Heat mitigation of a single hot spot is helpful to improve the local thermal comfort, but in the case of Dawson Mall an advective inflow of hot air due to the north-south axis of the pedestrian mall would reduce the air temperature mitigation.
- Heat mitigation should be implemented at the regional scale, i.e., Sydney-wide, to achieve reductions in the ambient temperature exceeding 2 °C, thus contrasting the effects of urbanization. A single council cannot alone achieve this level of urban heat mitigation.
- In addition to urban heat mitigation, an improvement of the building performance is also necessary to reduce the cooling energy demand of buildings in the context of global and regional warming.
- Hyper insulation is not the most appropriate strategy, and performance solutions – which are in compliance with the National Construction Code – should be pursued to reduce the cooling energy needs of buildings in Mt Druitt.
- Reflective roofing is an effective intervention that can deliver benefits at building and urban scale, acting in synergy with other heat-mitigation strategies.
- Reflective roofs and cool pavements are the single most effective strategy for reducing air temperature, and can work in positive synergy with greenery, which provides the greatest improvements on-site improvements in local thermal comfort by offering shading.
- No single heat mitigation strategy is sufficient if not in synergy with other approaches, implemented with a holistic vision.

Further research and monitoring should consider:

- Monitoring the effectiveness and performance of interventions in Mt Druitt, also exploiting the network of sensors established in this project.
- The development of synergies between heat-mitigation strategies.
- The development of synergies between blue and green infrastructure to keep evapotranspirative cooling operational, and greenery in a healthy status by exploiting the storage of stormwater.

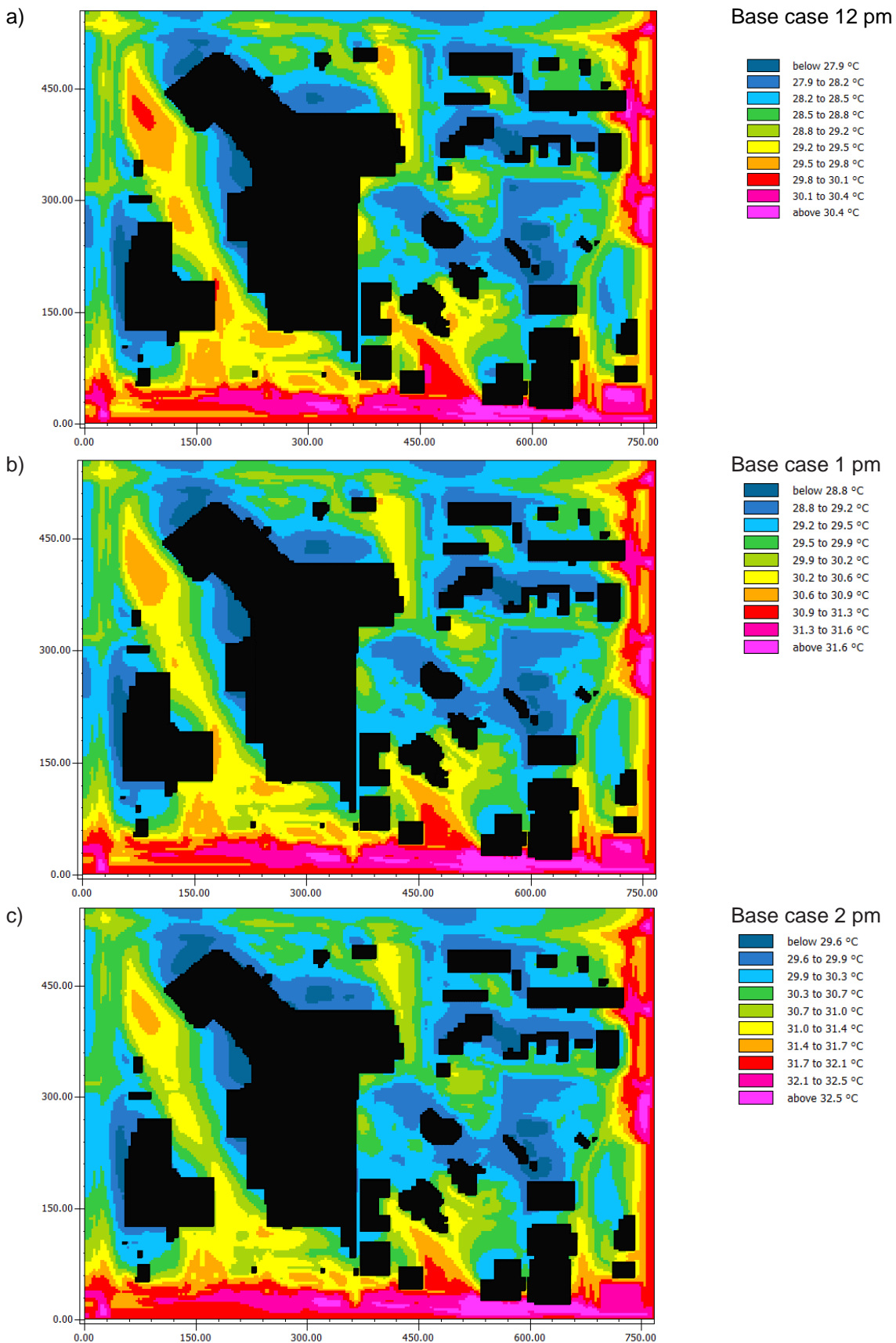
Annex A – Building parameters for energy simulations

Building Type	Office		Shopping mall		School	Apartment	
	Existing	New	Existing	New	New	New	
Floor area (m ²)	1200		1100		1100	624	
Aspect ratio	1:1		2:1		2:1	1:4.3	
Window to Wall Ratio (WWR)	0.6		0.3		0.32	0.24	
Year Built	1990	2018	1990	2018	1990	1990	
Number of stories	2		2	2	3	3	
Building height (m)	7.2		13.8	13.8	12.6	8.4	
Lighting internal gains (W/m ²) <i>(radiant fraction 0.42)</i>	Hourly Max	2.61		8.12		2.76	2.5
	Hourly Mean	1.45		4.77		1.13	0.6
	Hourly Min	0.39		0.81		0.15	0
Equipment internal gains (W/m ²)	Hourly Max	11		3.5		4.75	
	Hourly Mean	6.16		2.31		1.86	
	Hourly Min	2.75		0.5		0.25	
Occupancy density (person/m ²)	0.1		0.2		0.5	0.04	
Roof R-value (m ² ·K/W)	0.26	3.2	0.5	3.2	3.2	3.2	
Wall R-value (m ² ·K/W)	1	1	1	1	1	1	
Window U-value (W/m ² K)	2.4	2.4	4.2	4.2	2.4	5.6	
Window SHGC (summer)	0.25 (same for all buildings)						
Roof reflectance	0.15 conventional roof 0.75 cool roof						
Roof thermal emittance	0.90						
Wall solar reflectance	0.15						
Wall thermal emittance	0.90						
Ventilation op. hours (l/s. p)	7.5 (same for all buildings)						
Infiltration (op. hours) (ac/h)	1 (same for all buildings)						
Infiltration (non-op. hours) (ac/h)	1.5						
Heating setpoint (°C)	20 (same for all buildings)						
Heating setback (°C)	NA (system off out of working ours for commercial buildings, following NCC)						
Cooling setpoint (°C)	25 (same for all buildings)						
Cooling setback (°C)	NA (system off out of working ours for commercial buildings, following NCC)						

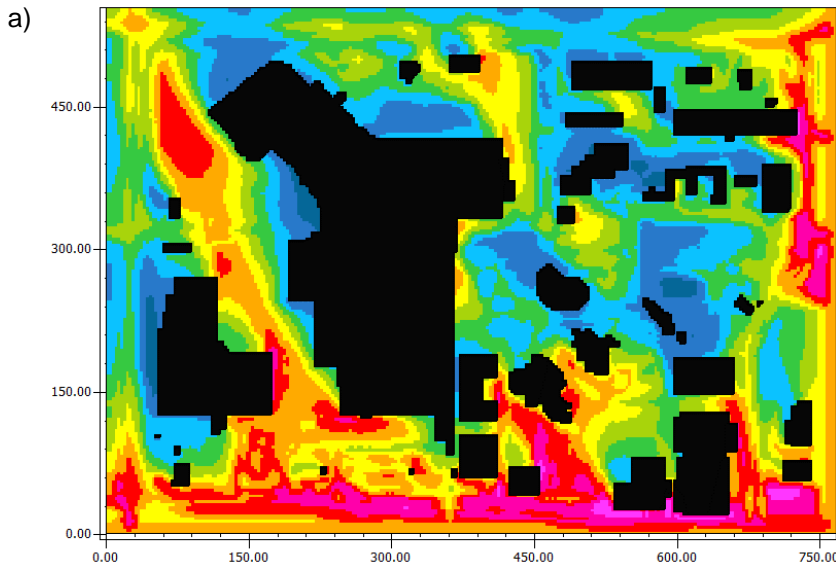


Annex B – Maps output of microclimate simulations

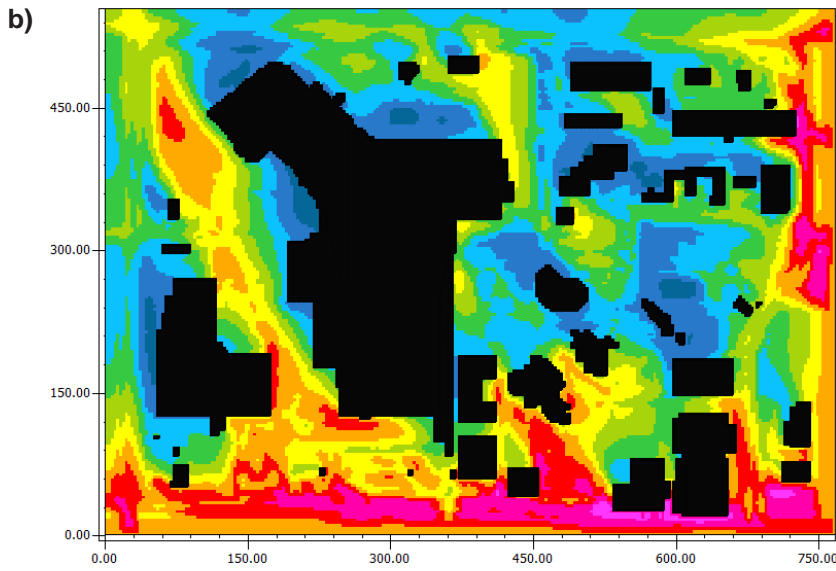
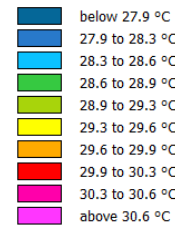
Air temperature distribution



Greenery – unirrigated

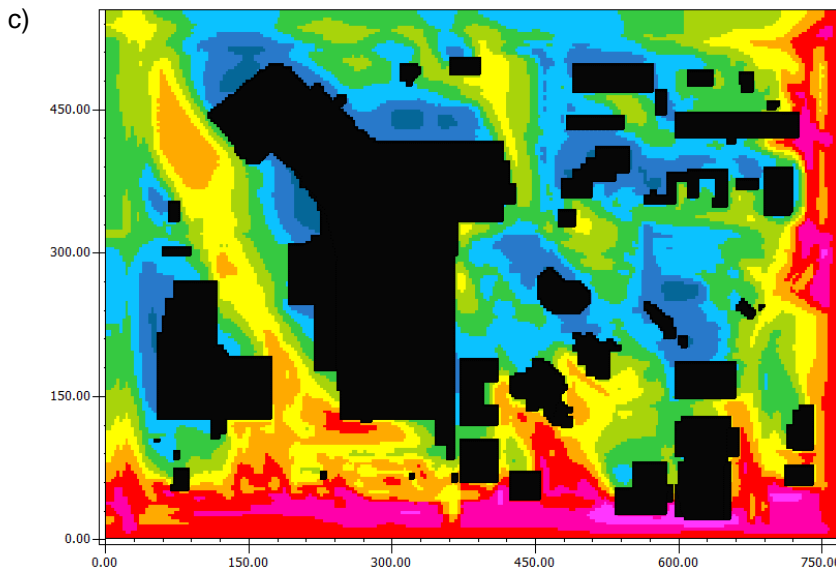
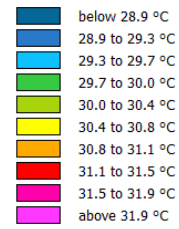


10+337 Unirrigated trees 12 pm



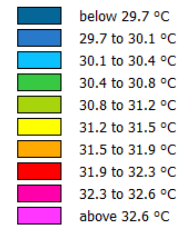
Unirrigated greenery

1 pm

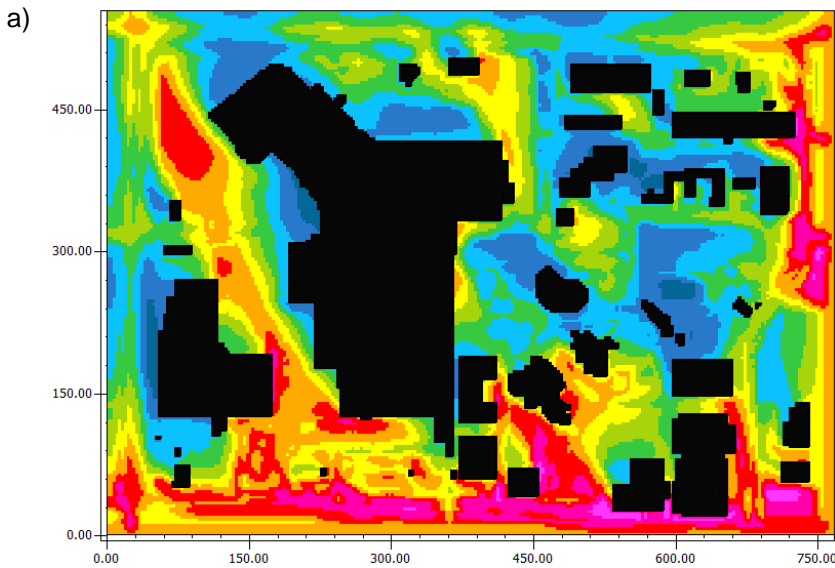


Unirrigated greenery

2 pm

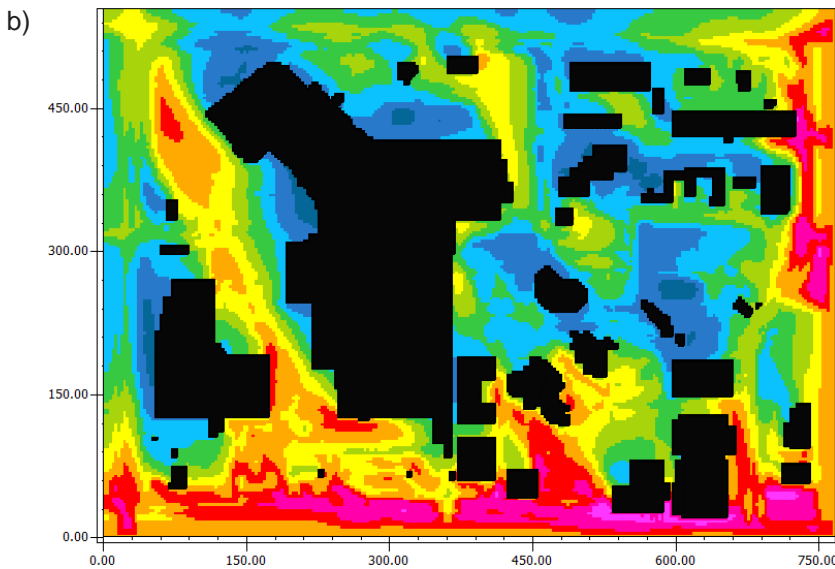
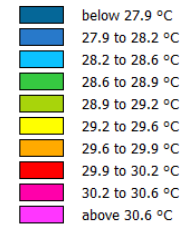


Greenery – Passively irrigated trees on Dawson Mall



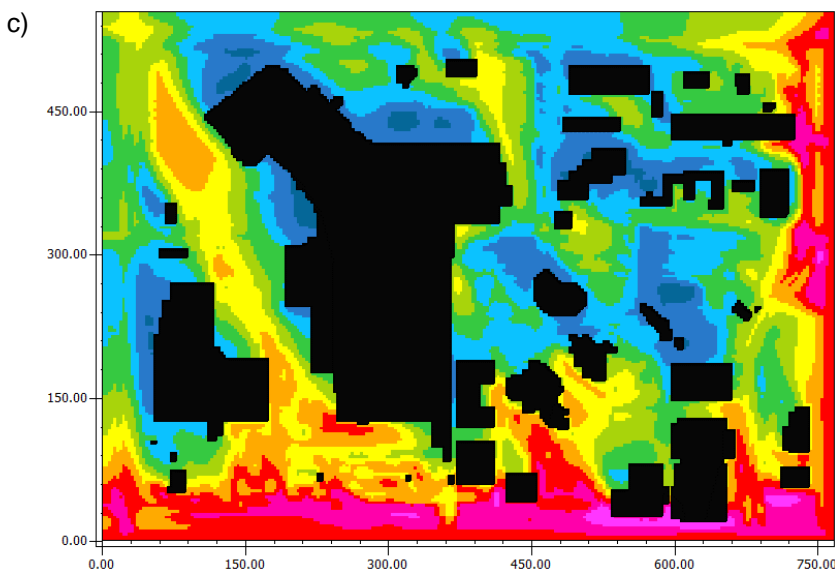
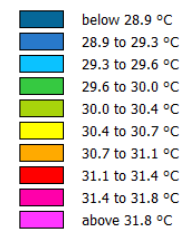
Irrigated trees on Dawson Mall

12 pm



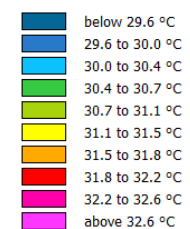
Irrigated trees on Dawson Mall

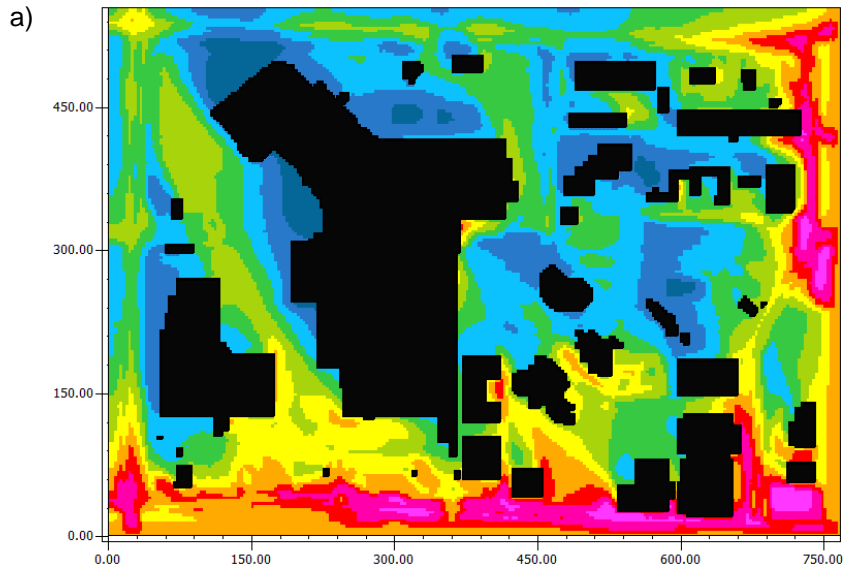
1 pm



Irrigated trees on Dawson Mall

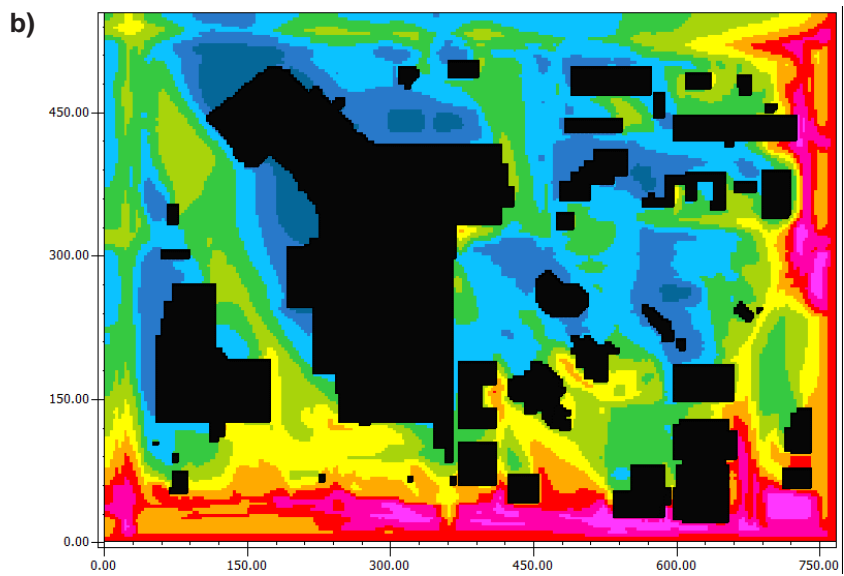
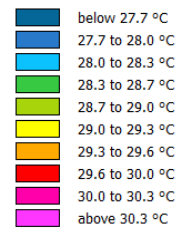
2 pm





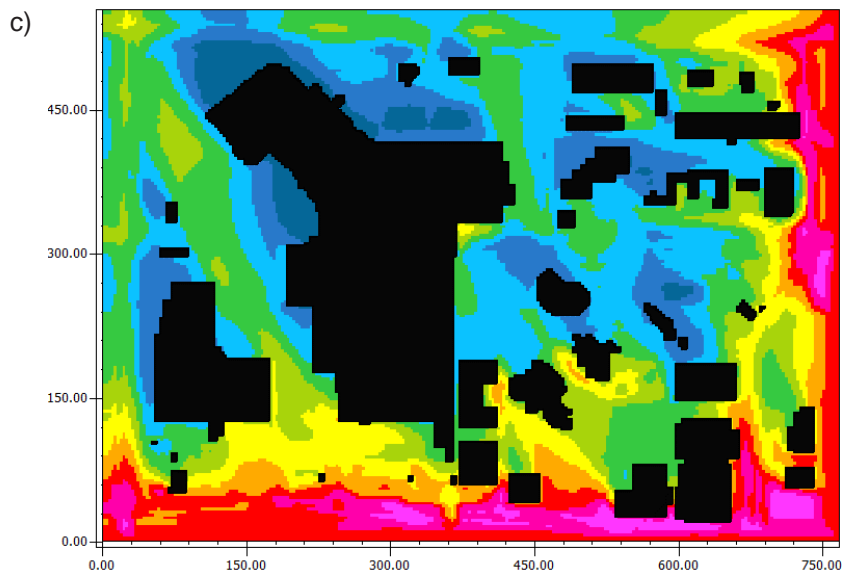
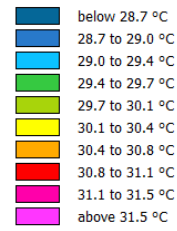
Cool materials

12 pm



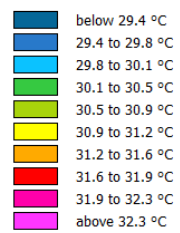
Cool materials

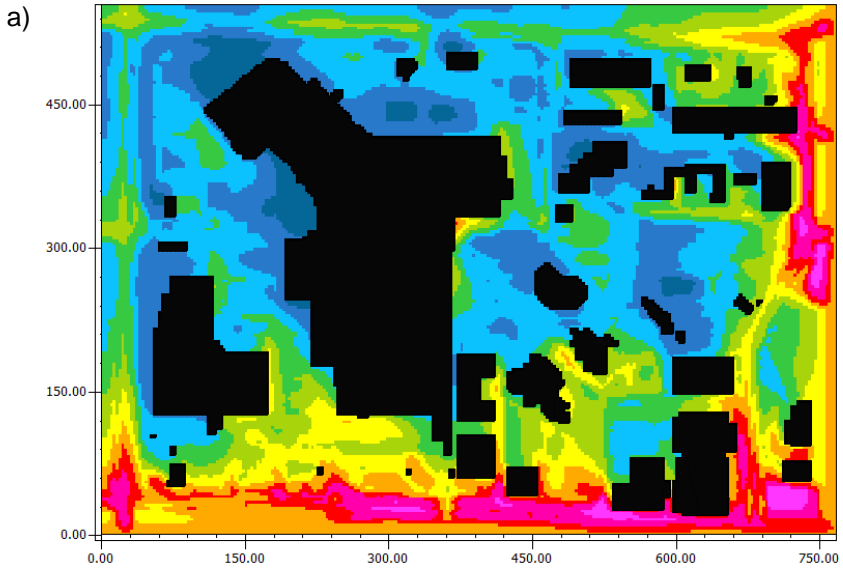
1 pm



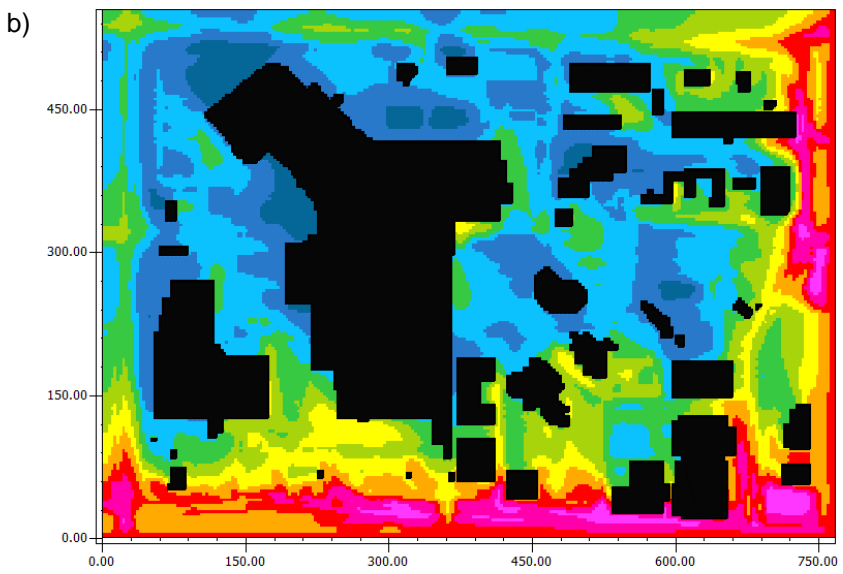
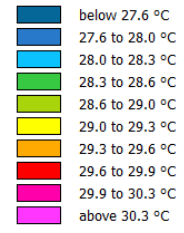
Cool materials

2 pm

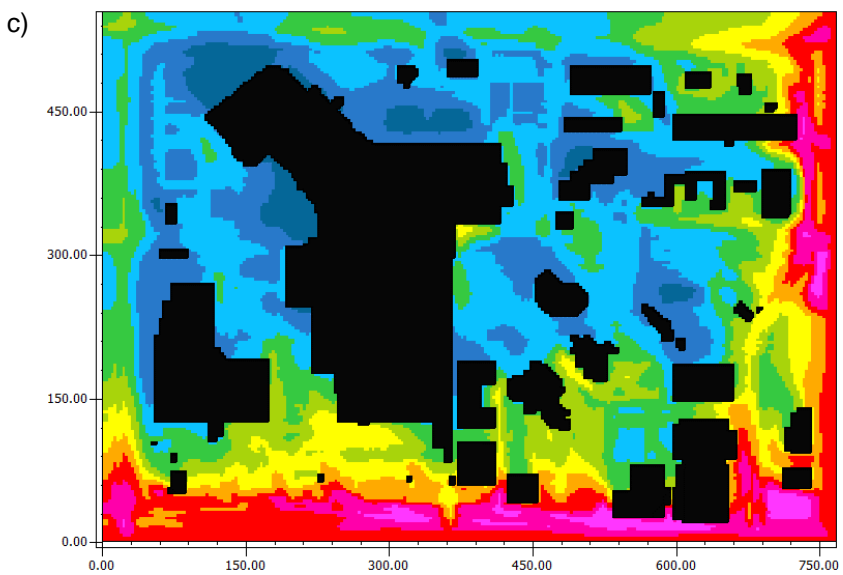
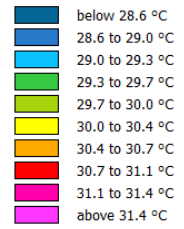




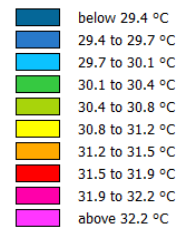
Combined scenario
12 pm



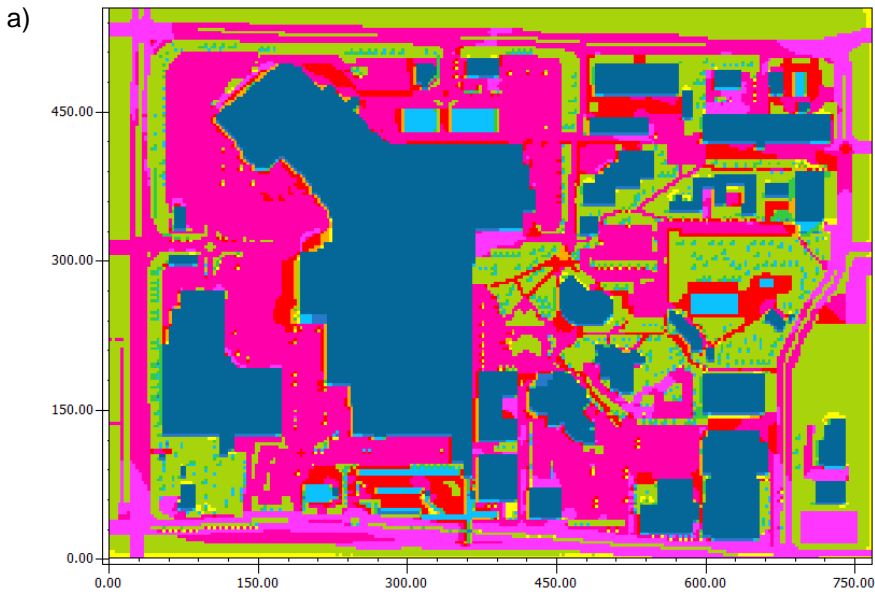
Combined scenario
1 pm



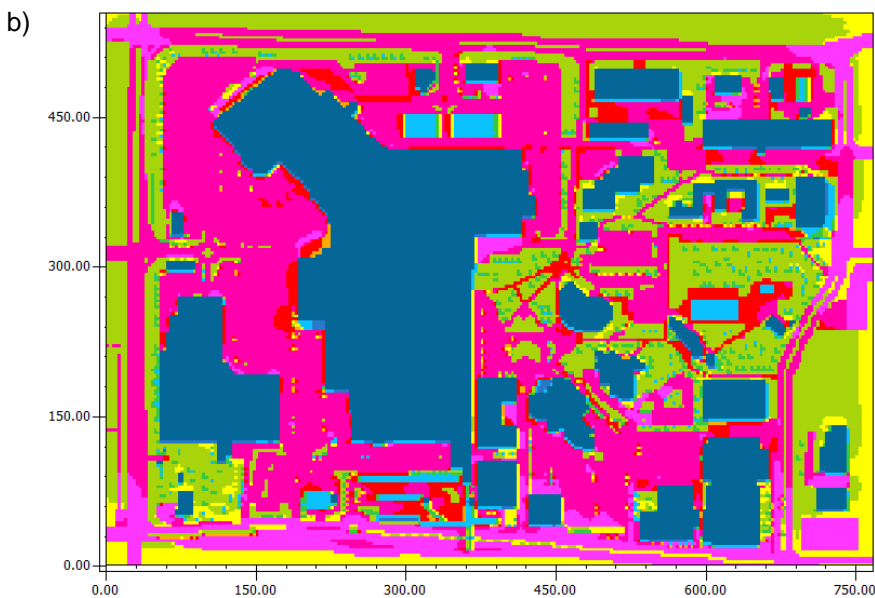
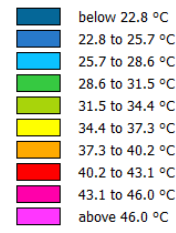
Combined scenario
2 pm



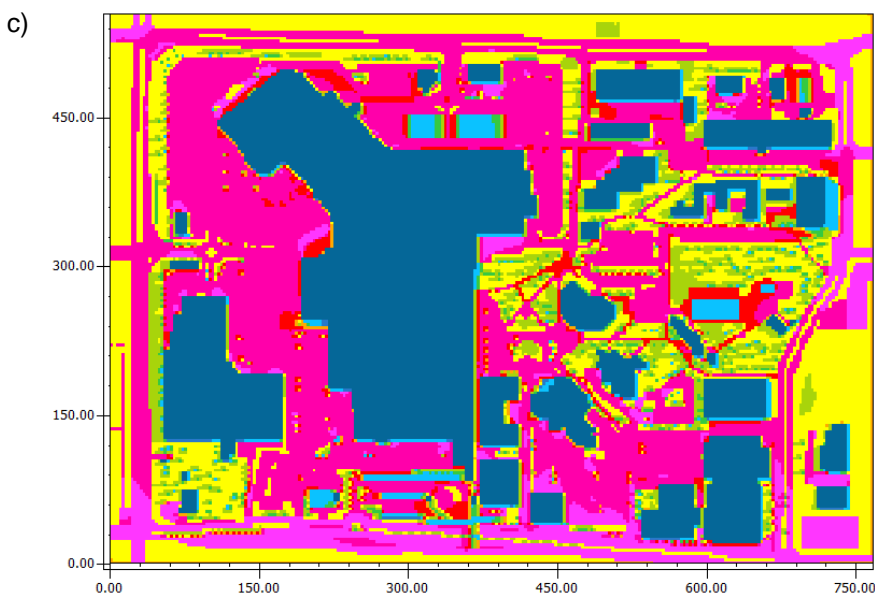
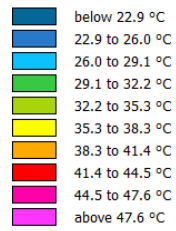
Surface temperature distribution



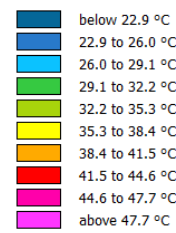
Base case 12 pm



Base case 1 pm



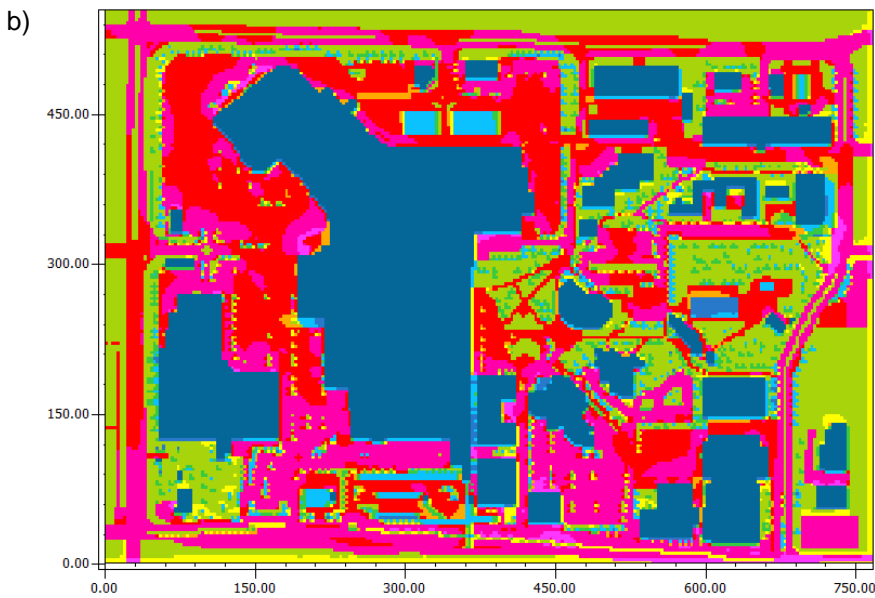
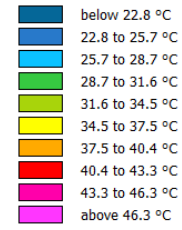
Base case 2 pm



Greenery – unirrigated

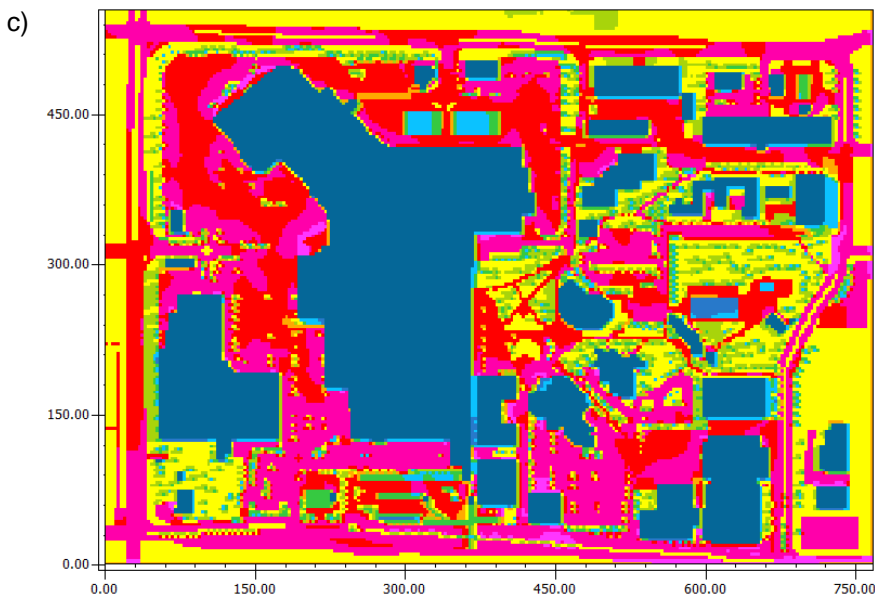
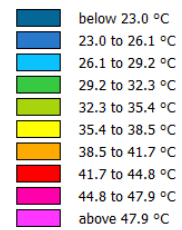


10+337 Unirrigated trees 12 pm



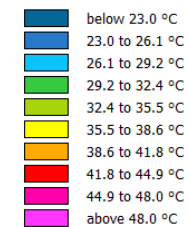
Unirrigated greenery

1 pm



Unirrigated greenery

2 pm

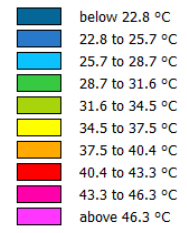


Greenery – Passively irrigated trees on Dawson Mall



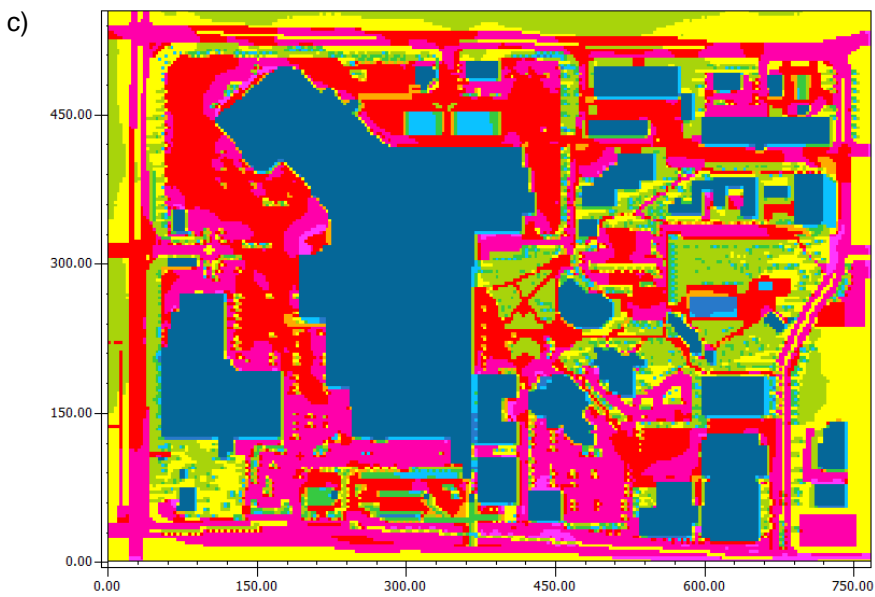
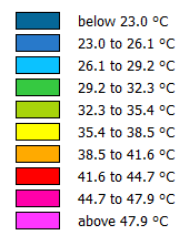
Irrigated trees on Dawson Mall

12 pm



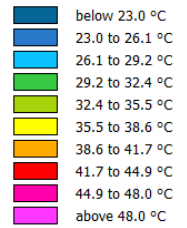
Irrigated trees on Dawson Mall

1 pm

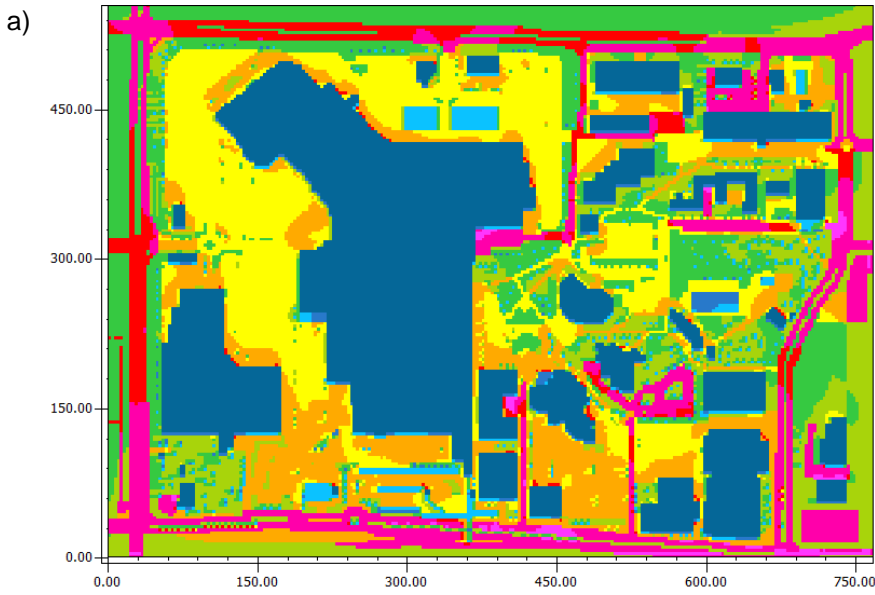


Irrigated trees on Dawson Mall

2 pm

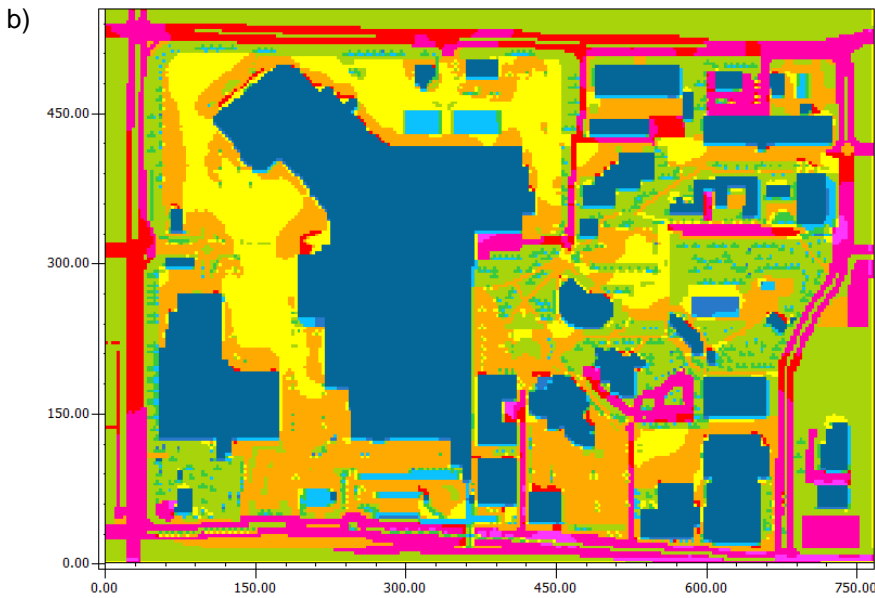
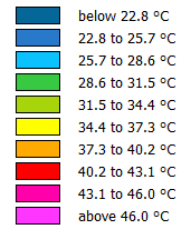


Cool materials



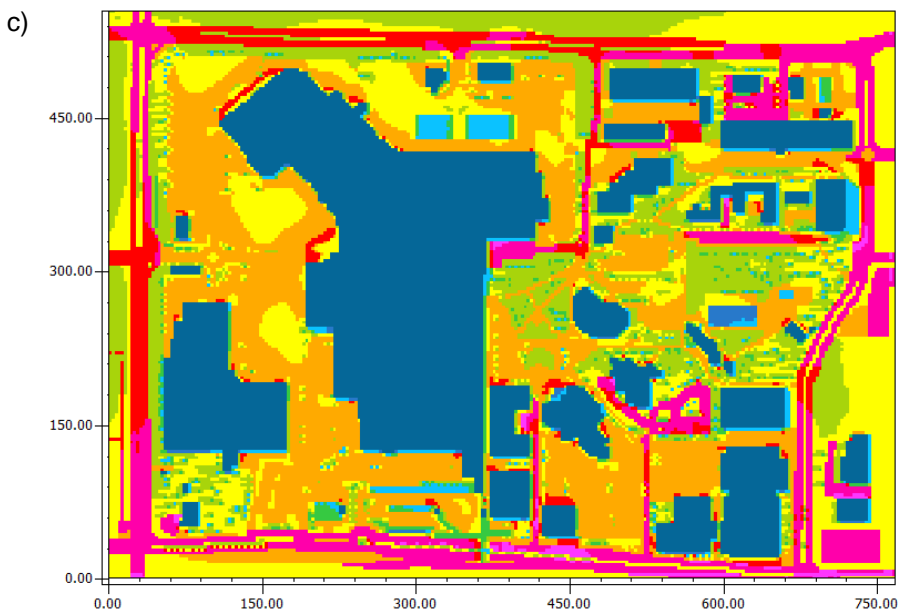
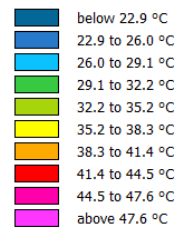
Cool materials

12 pm



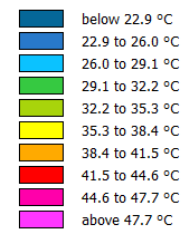
Cool materials

1 pm



Cool materials

2 pm

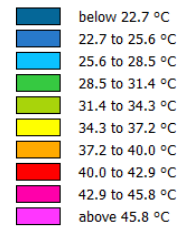


Combined scenario



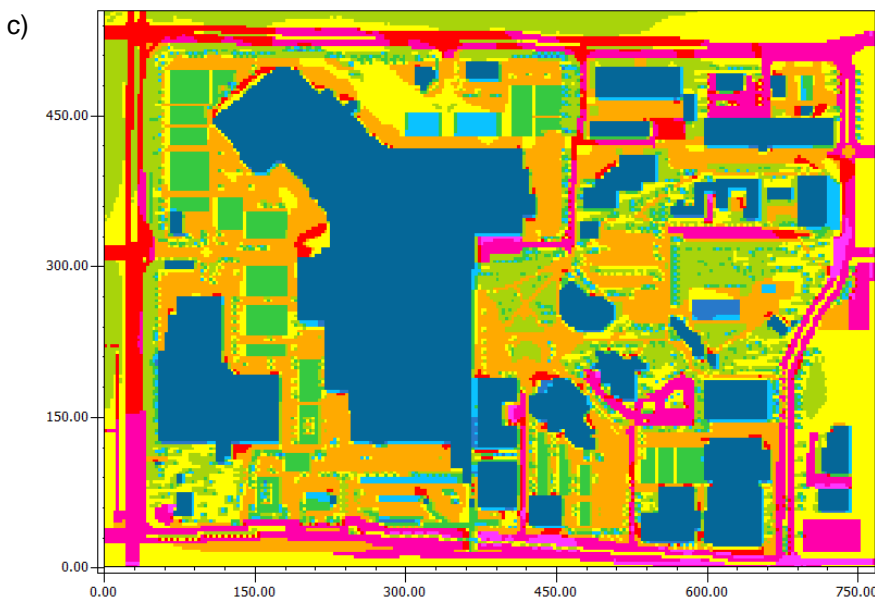
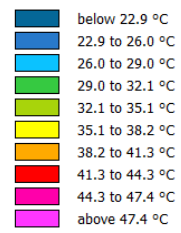
Combined scenario

12 pm



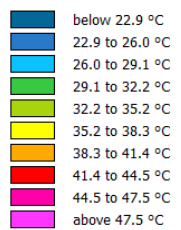
Combined scenario

1 pm



Combined scenario

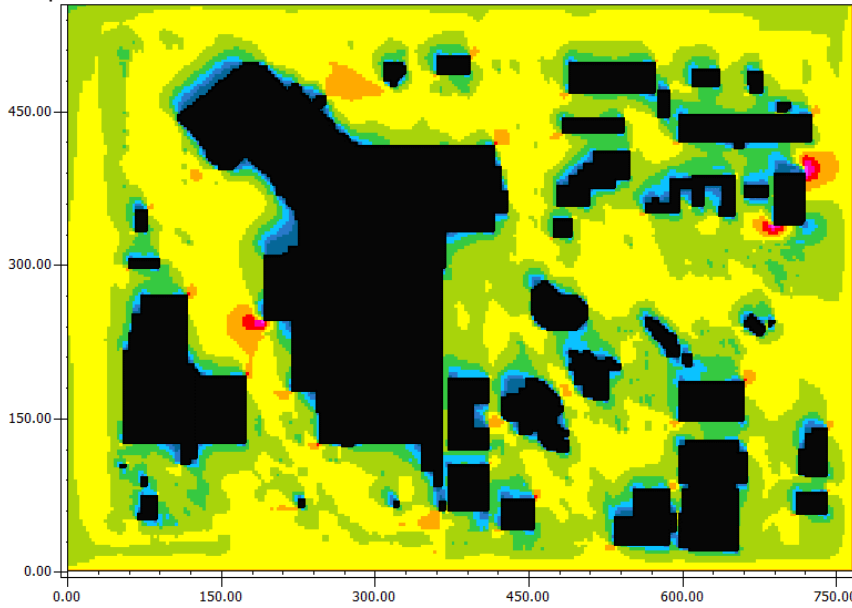
2 pm



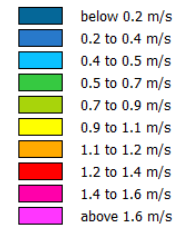
Wind speed distribution

Wind speed – base case

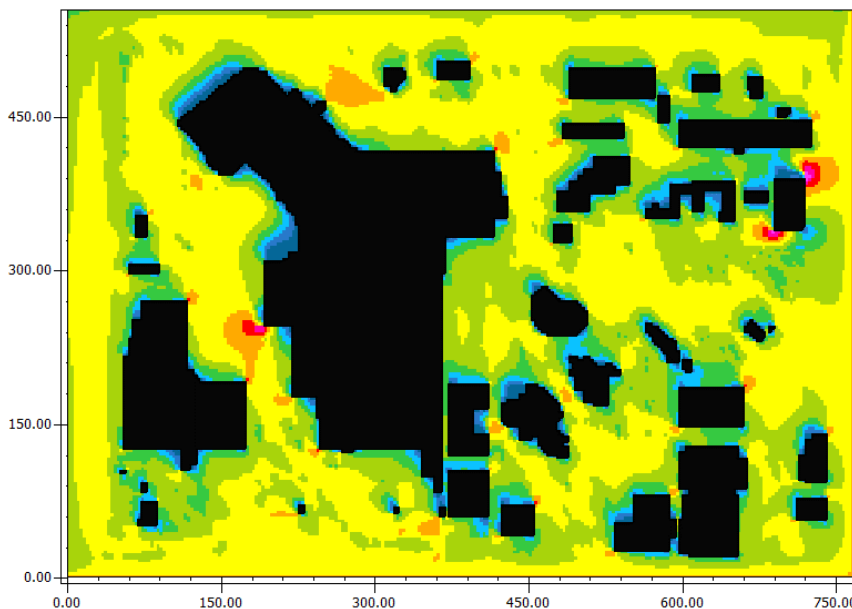
a)



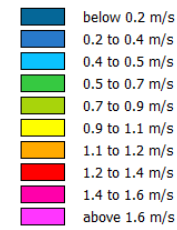
Base case 12 pm



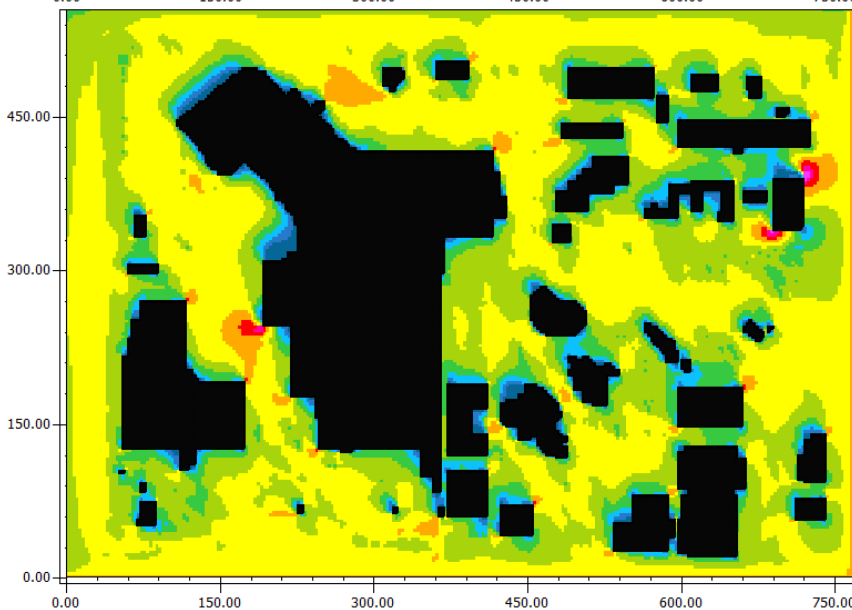
b)



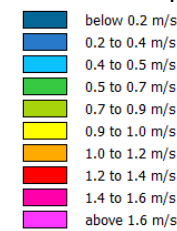
Base case 1 pm



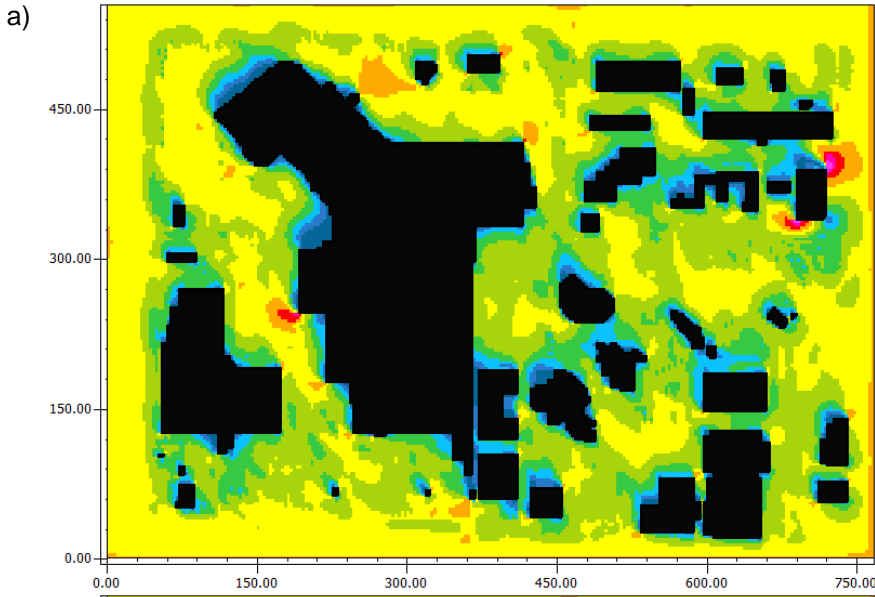
c)



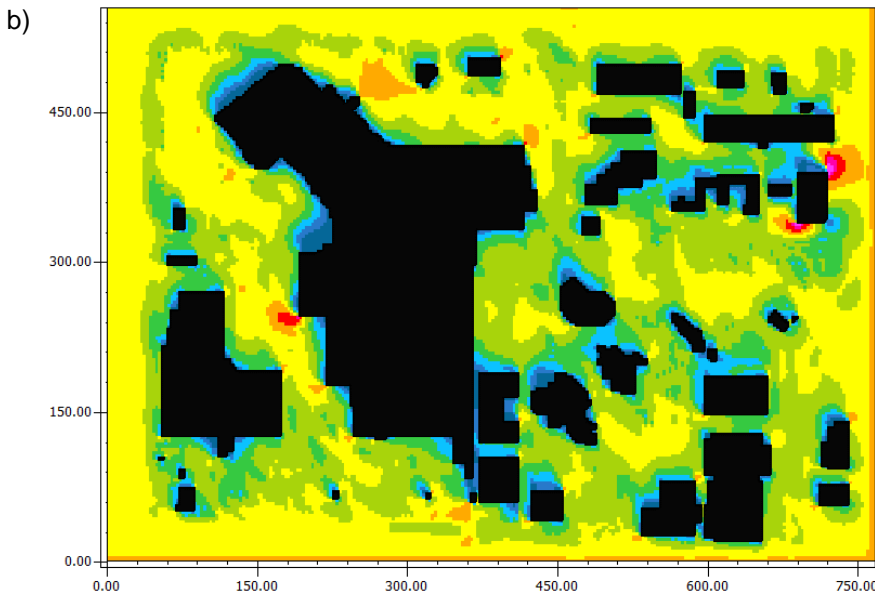
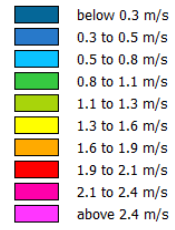
Base case 2 pm



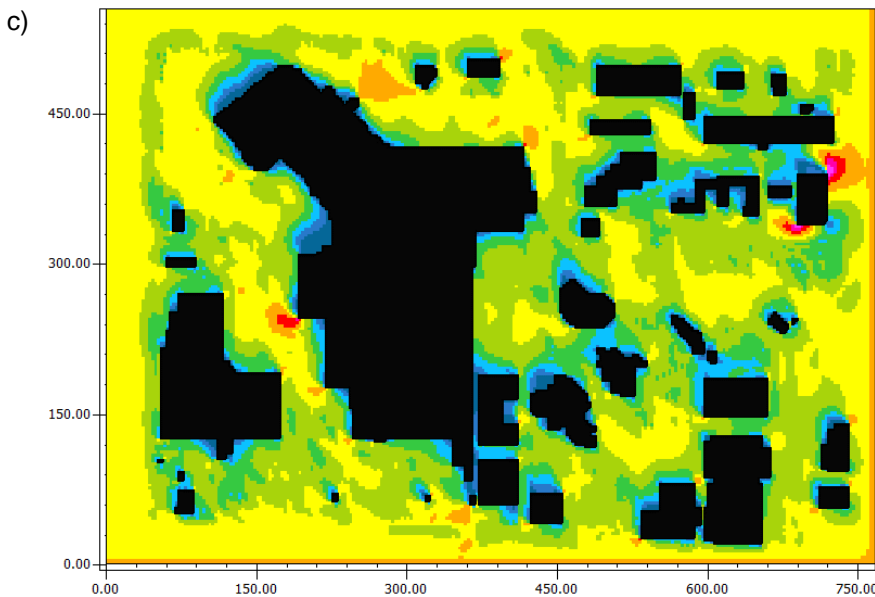
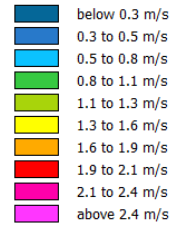
Greenery – unirrigated



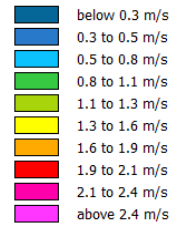
10+337 Unirrigated trees 12 pm



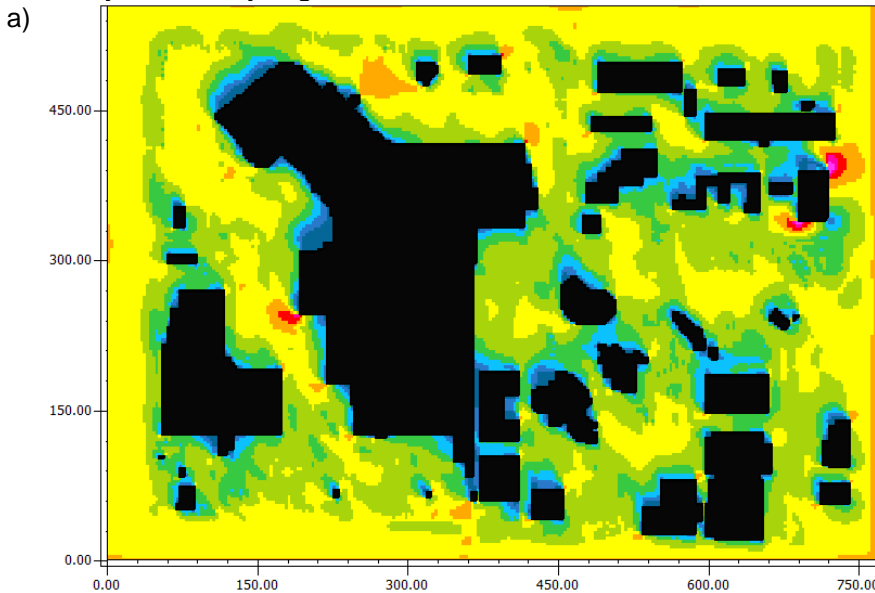
Unirrigated greenery 1 pm



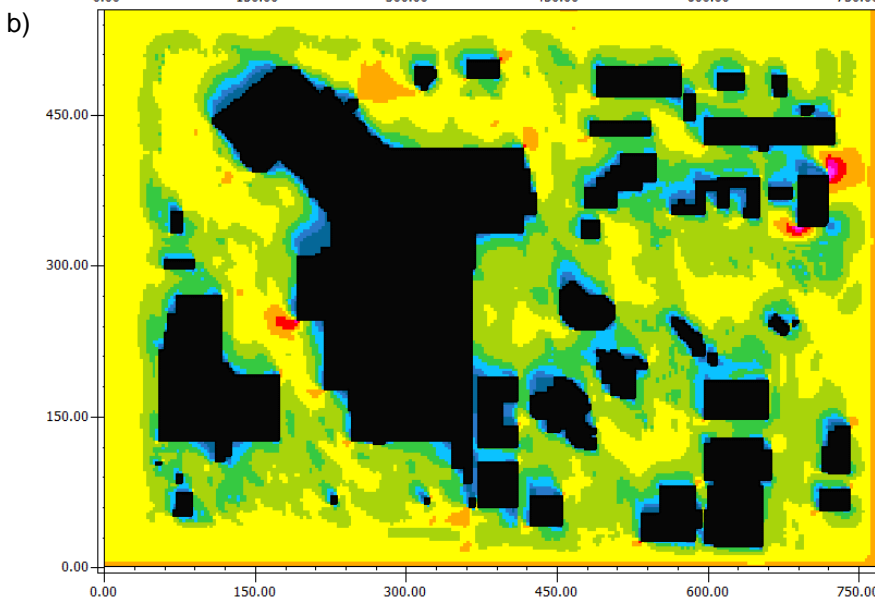
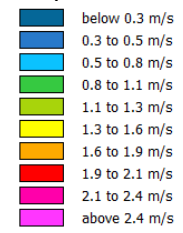
Unirrigated greenery 2 pm



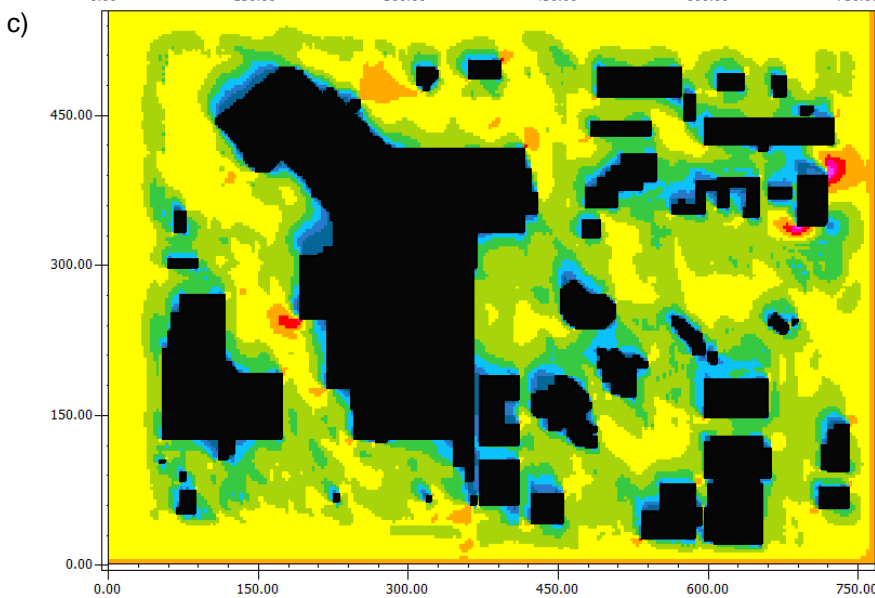
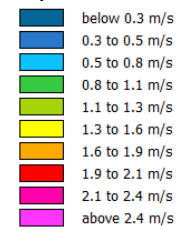
Greenery – Passively irrigated trees on Dawson Mall



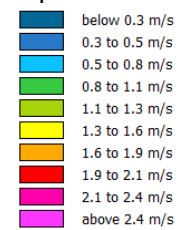
Irrigated trees on Dawson Mall
12 pm



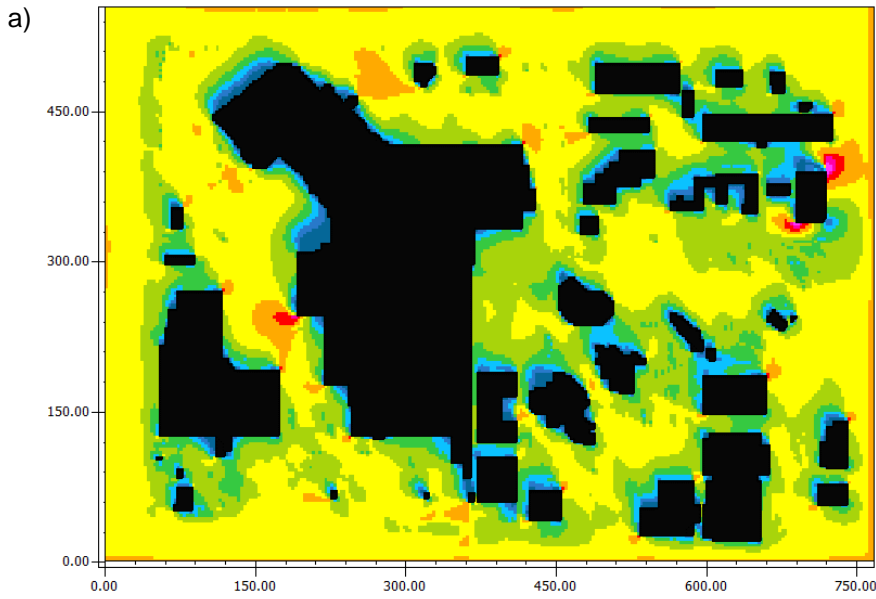
Irrigated trees on Dawson Mall
1 pm



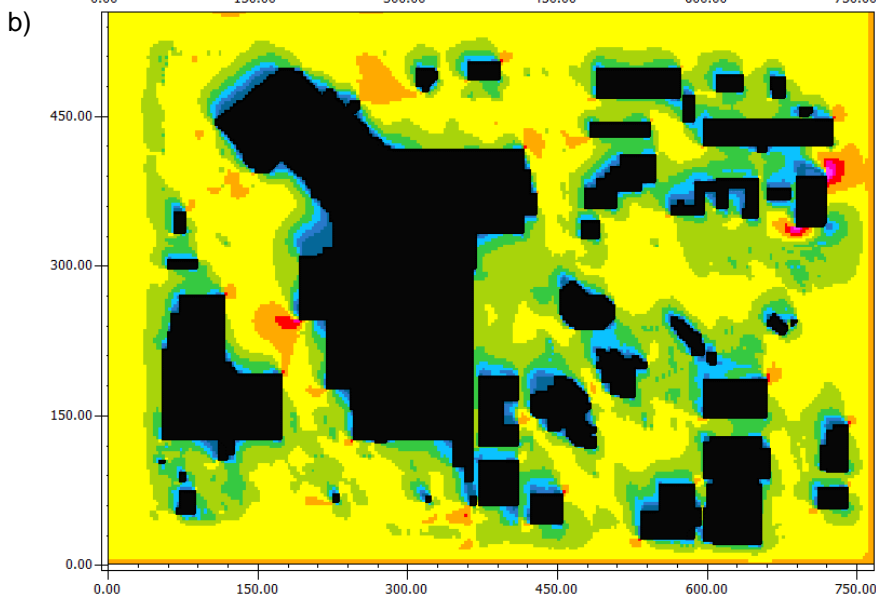
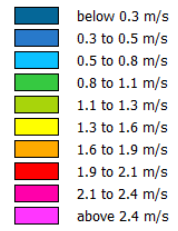
Irrigated trees on Dawson Mall
2 pm



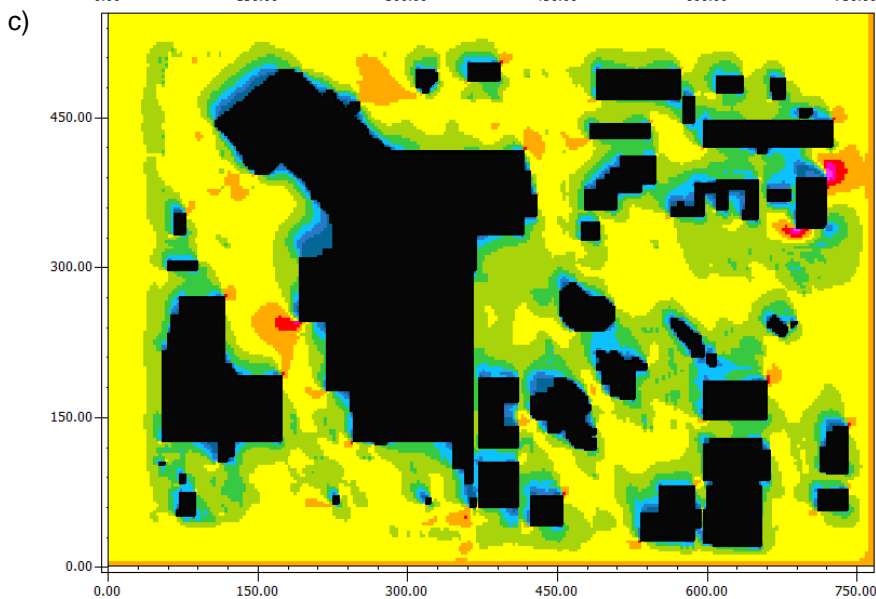
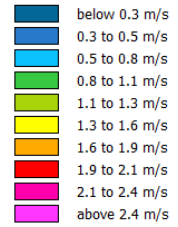
Cool materials



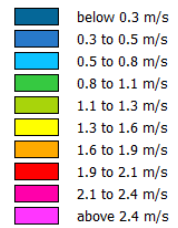
Cool materials
12 pm



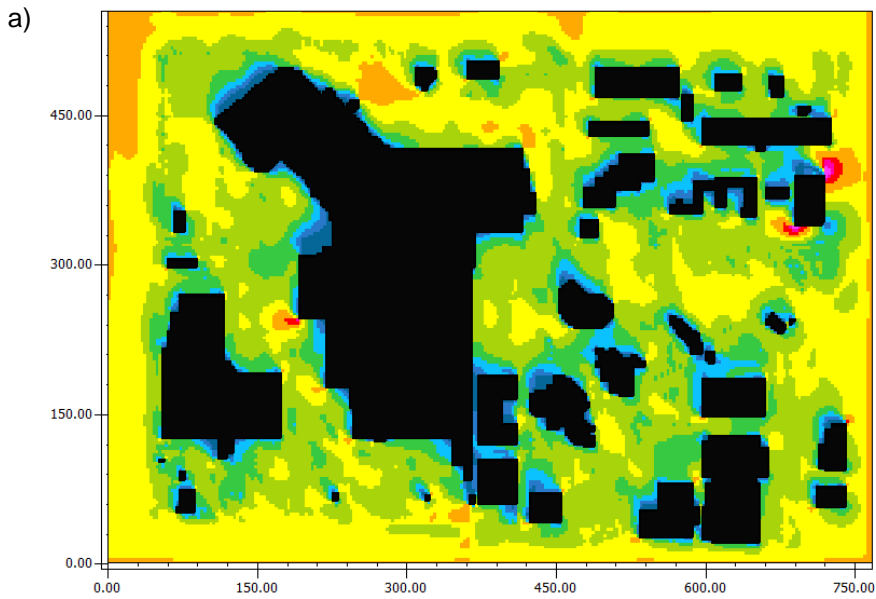
Cool materials
1 pm



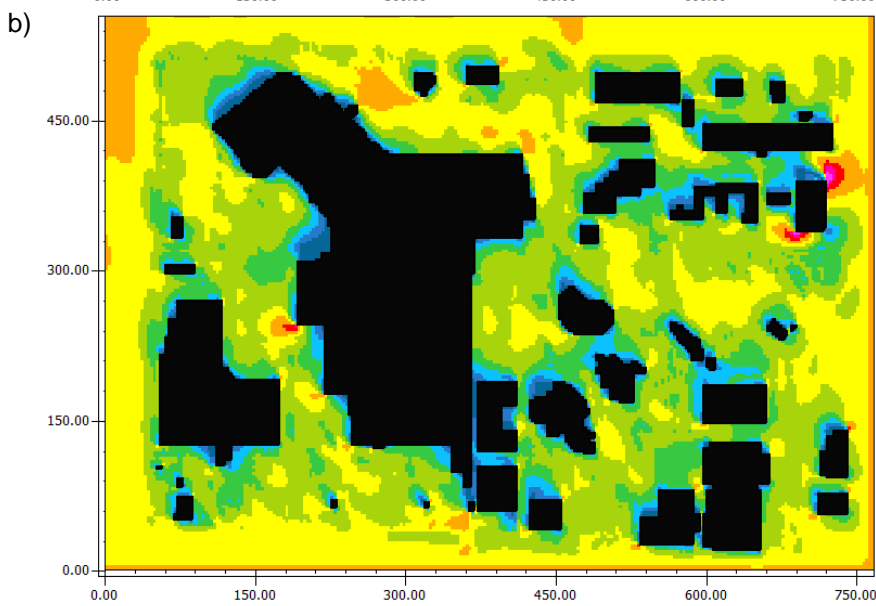
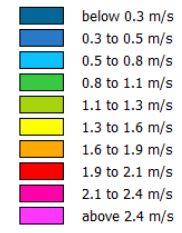
Cool materials
2 pm



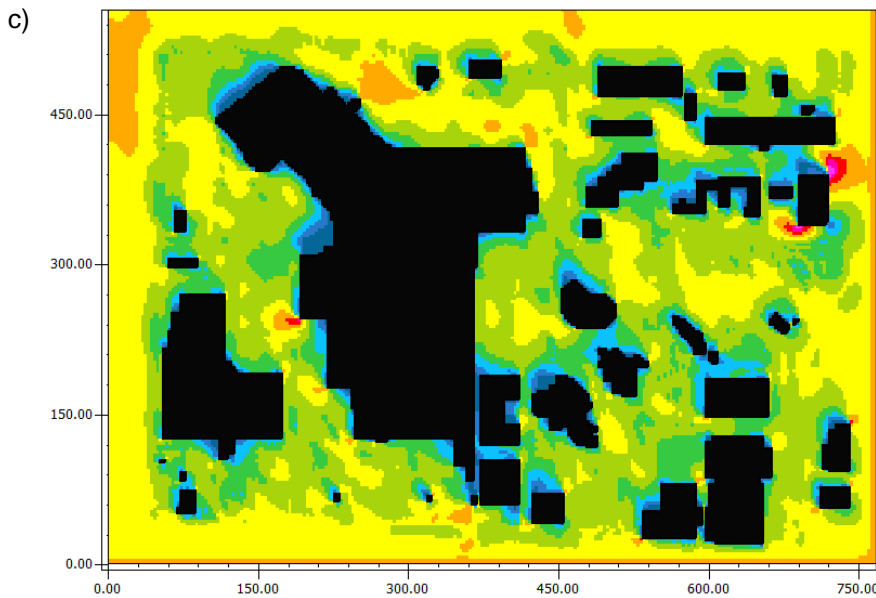
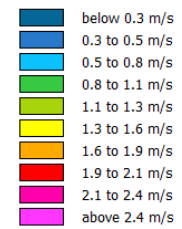
Combined scenario



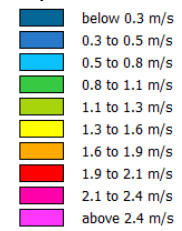
Combined scenario
12 pm



Combined scenario
1 pm



Combined scenario
2 pm



References

- [1] Australian Bureau of Meteorology, Climate Data, (2017). <http://www.bom.gov.au/climate/data/> (accessed August 24, 2017).
- [2] J. Estévez, P. Gavilán, J.V. Giráldez, Guidelines on validation procedures for meteorological data from automatic weather stations, *Journal of Hydrology*. 402 (2011) 144–154. <https://doi.org/10.1016/j.jhydrol.2011.02.031>.
- [3] G.J. Levermore, J.B. Parkinson, Analyses and algorithms for new Test Reference Years and Design Summer Years for the UK, *Building Service Engineering Research and Technology*. 27 (2006) 311–325. <https://doi.org/10.1177/0143624406071037>.
- [4] R. Paolini, A. Zani, M. MeshkinKiya, V.L. Castaldo, A.L. Pisello, F. Antretter, T. Poli, F. Cotana, The hygrothermal performance of residential buildings at urban and rural sites: Sensible and latent energy loads and indoor environmental conditions, *Energy and Buildings*. (2016). <https://doi.org/10.1016/j.enbuild.2016.11.018>.
- [5] M. Bruse, H. Fleer, Simulating surface–plant–air interactions inside urban environments with a three dimensional numerical model, *Environmental Modelling & Software*. 13 (1998) 373–384. [https://doi.org/10.1016/S1364-8152\(98\)00042-5](https://doi.org/10.1016/S1364-8152(98)00042-5).
- [6] X. Yang, L. Zhao, M. Bruse, Q. Meng, Evaluation of a microclimate model for predicting the thermal behavior of different ground surfaces, *Building and Environment*. 60 (2013) 93–104. <https://doi.org/10.1016/j.buildenv.2012.11.008>.
- [7] A. Middel, K. Hüb, A.J. Brazel, C.A. Martin, S. Guhathakurta, Impact of urban form and design on mid-afternoon microclimate in Phoenix Local Climate Zones, *Landscape and Urban Planning*. 122 (2014) 16–28. <https://doi.org/10.1016/J.LANDURBPLAN.2013.11.004>.
- [8] F. Salata, I. Golasi, R. de Lieto Vollaro, A. de Lieto Vollaro, Urban microclimate and outdoor thermal comfort. A proper procedure to fit ENVI-met simulation outputs to experimental data, *Sustainable Cities and Society*. 26 (2016) 318–343. <https://doi.org/10.1016/j.scs.2016.07.005>.
- [9] S. Haddad, G. Ulpiani, R. Paolini, A. Synnefa, M. Santamouris, Experimental and Theoretical analysis of the urban overheating and its mitigation potential in a hot arid city–Alice Springs, *Architectural Science Review*. (2019). <https://doi.org/10.1080/00038628.2019.1674128>.
- [10] ISO, ISO 13788. Hygrothermal performance of building components and building elements - Internal surface temperature to avoid critical surface humidity and interstitial condensation - Calculation methods, (2012).
- [11] US Department of Energy, EnergyPlus, EnergyPlus Engineering Reference: The Reference to EnergyPlus Calculations, 2016. <https://doi.org/citeulike-article-id:10579266>.
- [12] Australian Building Codes Board, National Construction Code, (2019). <http://www.abcb.gov.au>.
- [13] University of Colorado, NASA, Solar Radiation and Climate Experiment (SORCE), (2017). <http://lasp.colorado.edu/home/sorce/> (accessed June 26, 2017).
- [14] I. Reda, A. Andreas, Solar position algorithm for solar radiation applications, *Solar Energy*. 76 (2004) 577–589. <https://doi.org/10.1016/j.solener.2003.12.003>.
- [15] Geoscience Australia, National Exposure Information System (NEXIS) Building Exposure Local Government Area (LGA) aggregated metadata (v7.2016), (2016).
- [16] M. Santamouris, A. Synnefa, R. Paolini, S. Haddad, G. Ulpiani, S. Garshasbi, M. Sadeghi, K. Vasilakopoulou, F. Fiorito, A strategic study on the role of water in mitigating urban heat in Western Sydney, Sydney, Australia, 2017.

- [17] B.E. Psiloglou, C. Giannakopoulos, S. Majithia, M. Petrakis, Factors affecting electricity demand in Athens, Greece and London, UK: A comparative assessment, *Energy*. 34 (2009) 1855–1863. <https://doi.org/10.1016/j.energy.2009.07.033>.
- [18] H. Son, C. Kim, Short-term forecasting of electricity demand for the residential sector using weather and social variables, *Resources, Conservation and Recycling*. 123 (2017) 200–207. <https://doi.org/10.1016/j.resconrec.2016.01.016>.
- [19] M. Santamouris, Cooling the buildings – past, present and future, *Energy and Buildings*. 128 (2016) 617–638. <https://doi.org/10.1016/j.enbuild.2016.07.034>.
- [20] S.N. Gosling, G.R. McGregor, A. Páldy, Climate change and heat-related mortality in six cities part 1: model construction and validation., *International Journal of Biometeorology*. 51 (2007) 525–40. <https://doi.org/10.1007/s00484-007-0092-9>.
- [21] J.C. Semenza, C.H. Rubin, K.H. Falter, J.D. Selanikio, W.D. Flanders, H.L. Howe, J.L. Wilhelm, Heat-Related Deaths during the July 1995 Heat Wave in Chicago, *New England Journal of Medicine*. 335 (1996) 84–90. <https://doi.org/10.1056/NEJM199607113350203>.
- [22] J.C. Semenza, J.E. McCullough, W.D. Flanders, M.A. McGeehin, J.R. Lumpkin, Excess hospital admissions during the July 1995 heat wave in Chicago, *American Journal of Preventive Medicine*. 16 (1999) 269–277. [https://doi.org/10.1016/S0749-3797\(99\)00025-2](https://doi.org/10.1016/S0749-3797(99)00025-2).
- [23] K. Yenneti, L. Ding, D. Prasad, G. Ulpiani, R. Paolini, S. Haddad, M. Santamouris, Urban Overheating and Cooling Potential in Australia: An Evidence-Based Review, *Climate*. 8 (2020) 126. <https://doi.org/10.3390/cli8110126>.
- [24] M. Santamouris, L. Ding, F. Fiorito, P. Oldfield, P. Osmond, R. Paolini, D. Prasad, A. Synnefa, Passive and active cooling for the outdoor built environment – Analysis and assessment of the cooling potential of mitigation technologies using performance data from 220 large scale projects, *Solar Energy*. 154 (2017) 14–33. <https://doi.org/10.1016/j.solener.2016.12.006>.
- [25] M. Santamouris, R. Paolini, S. Haddad, A. Synnefa, S. Garshasbi, G. Hatvani-Kovacs, K. Gobakis, K. Yenneti, K. Vasilakopoulou, J. Feng, K. Gao, G. Papangelis, A. Dandou, G. Methymaki, P. Portalakis, M. Tombrou, Heat mitigation technologies can improve sustainability in cities. An holistic experimental and numerical impact assessment of urban overheating and related heat mitigation strategies on energy consumption, indoor comfort, vulnerability and heat-related m, *Energy and Buildings*. 217 (2020) 110002. <https://doi.org/10.1016/j.enbuild.2020.110002>.
- [26] S. Garshasbi, S. Haddad, R. Paolini, M. Santamouris, G. Papangelis, A. Dandou, G. Methymaki, P. Portalakis, M. Tombrou, Urban mitigation and building adaptation to minimize the future cooling energy needs, *Solar Energy*. 204 (2020) 708–719. <https://doi.org/10.1016/j.solener.2020.04.089>.
- [27] E. Carnielo, M. Zinzi, Optical and thermal characterisation of cool asphalts to mitigate urban temperatures and building cooling demand, *Building and Environment*. 60 (2013) 56–65. <https://doi.org/10.1016/j.buildenv.2012.11.004>.
- [28] F. Rosso, A.L. Pisello, F. Cotana, M. Ferrero, On the thermal and visual pedestrians' perception about cool natural stones for urban paving: A field survey in summer conditions, *Building and Environment*. 107 (2016) 198–214. <https://doi.org/10.1016/j.buildenv.2016.07.028>.
- [29] R. Paolini, G. Terraneo, C. Ferrari, M. Sleiman, A. Muscio, P. Metrangolo, T. Poli, H. Destailats, M. Zinzi, R. Levinson, Effects of soiling and weathering on the albedo of building envelope materials: Lessons learned from natural exposure in two European cities and tuning of a laboratory simulation practice, *Solar Energy Materials and Solar Cells*. 205 (2020) 110264. <https://doi.org/10.1016/j.solmat.2019.110264>.
- [30] R. Paolini, A.G.A.G. Mainini, T. Poli, L. Vercesi, Assessment of Thermal Stress in a Street Canyon in Pedestrian Area with or without Canopy Shading, *Energy Procedia*. 48 (2014) 1570–1575. <https://doi.org/10.1016/j.egypro.2014.02.177>.
- [31] R. Levinson, H. Pan, G. Ban-Weiss, P. Rosado, R. Paolini, H. Akbari, Potential benefits of solar reflective car shells: Cooler cabins, fuel savings and emission reductions, *Applied Energy*. 88 (2011) 4343–4357. <https://doi.org/10.1016/j.apenergy.2011.05.006>.

- [32] M. Santamouris, Analyzing the heat island magnitude and characteristics in one hundred Asian and Australian cities and regions, *Science of The Total Environment*. 512 (2015) 582–598. <https://doi.org/10.1016/j.scitotenv.2015.01.060>.
- [33] T.R. Oke, The energetic basis of the urban heat island, *Quarterly Journal of the Royal Meteorological Society*. 108 (1982) 1–24. <https://doi.org/10.1002/qj.49710845502>.
- [34] T.R. Oke, *Boundary Layer Climates*, Methuen and Co., New York, 1987.
- [35] R. Paolini, A. Zani, M. MeshkinKiya, V.L.V.L.V.L. Castaldo, A.L.A.L. Pisello, F. Antretter, T. Poli, F. Cotana, The hygrothermal performance of residential buildings at urban and rural sites: Sensible and latent energy loads and indoor environmental conditions, *Energy and Buildings*. 152 (2017) 792–803. <https://doi.org/10.1016/j.enbuild.2016.11.018>.
- [36] S. Haddad, R. Paolini, G. Ulpiani, A. Synnefa, G. Hatvani-Kovacs, S. Garshasbi, J. Fox, K. Vasilakopoulou, L. Nield, M. Santamouris, Holistic approach to assess co-benefits of local climate mitigation in a hot humid region of Australia, *Scientific Reports*. 10 (2020) 14216. <https://doi.org/10.1038/s41598-020-71148-x>.
- [37] M. Santamouris, R. Paolini, S. Haddad, A. Synnefa, S. Garshasbi, G. Hatvani-Kovacs, K. Gobakis, K. Yenneti, K. Vasilakopoulou, J. Feng, K. Gao, G. Papangelis, A. Dandou, G. Methymaki, P. Portalakis, M. Tombrou, Heat Mitigation Technologies Can Improve Sustainability In Cities An Holistic Experimental And Numerical Impact Assessment Of Urban Overheating And Related Heat Mitigation Strategies On Energy Consumption, Indoor Comfort, Vulnerability And Heat-Related Mo, *Energy and Buildings*. 217 (2020) 110002. <https://doi.org/10.1016/j.enbuild.2020.110002>.
- [38] G. Ulpiani, Water mist spray for outdoor cooling: A systematic review of technologies, methods and impacts, *Applied Energy*. 254 (2019) 113647. <https://doi.org/10.1016/J.APENERGY.2019.113647>.
- [39] Y. Wang, Y. Li, S. di Sabatino, A. Martilli, P.W. Chan, Effects of anthropogenic heat due to air-conditioning systems on an extreme high temperature event in Hong Kong, *Environmental Research Letters*. 13 (2018) 034015. <https://doi.org/10.1088/1748-9326/aaa848>.
- [40] R. Buccolieri, C. Gromke, S. di Sabatino, B. Ruck, Aerodynamic effects of trees on pollutant concentration in street canyons, *Science of The Total Environment*. 407 (2009) 5247–5256. <https://doi.org/10.1016/J.SCITOTENV.2009.06.016>.
- [41] A. Green, L. Ledo Gomis, R. Paolini, S. Haddad, G. Kokogiannakis, P. Cooper, Z. Ma, B. Kosasih, M. Santamouris, Above-roof air temperature effects on HVAC and cool roof performance: Experiments and development of a predictive model, *Energy and Buildings*. 222 (2020) 110071. <https://doi.org/10.1016/j.enbuild.2020.110071>.
- [42] M. Santamouris, On the energy impact of urban heat island and global warming on buildings, *Energy and Buildings*. 82 (2014) 100–113. <https://doi.org/10.1016/j.enbuild.2014.07.022>.
- [43] H. Akbari, R. Levinson, L. Rainer, Monitoring the energy-use effects of cool roofs on California commercial buildings, *Energy and Buildings*. 37 (2005) 1007–1016. <https://doi.org/10.1016/j.enbuild.2004.11.013>.
- [44] P.J. Rosado, D. Faulkner, D.P. Sullivan, R. Levinson, Measured temperature reductions and energy savings from a cool tile roof on a central California home, *Energy and Buildings*. (2014). <https://doi.org/10.1016/j.enbuild.2014.04.024>.
- [45] S.N. Gosling, G.R. McGregor, J.A. Lowe, Climate change and heat-related mortality in six cities Part 2: climate model evaluation and projected impacts from changes in the mean and variability of temperature with climate change., *International Journal of Biometeorology*. 53 (2009) 31–51. <https://doi.org/10.1007/s00484-008-0189-9>.

